



**Generation and Migration of Oil from Perhydrous
Longyear Coal**

by

Ikechukwu Mokogwu (BSc. Hons)

**A thesis submitted as part of the requirements for the
Degree of Master of Science (by Research)
in**

Petroleum and Environmental Process Engineering

University of Nottingham

September 2011

ACKNOWLEDGEMENT

I would like to express my unreserved appreciation to my project supervisor; Dr. David Large for his patience and careful guidance throughout the course of this research. Special thanks to Dr. Clement Uguna who painstakingly guided me through all the experimental procedures. Dr. Will Meredith, Archibald Vikki and Chris Marshall were also extremely helpful during this period.

Gratitude goes to my brothers and parents, Mr. and Mrs. Mokogwu for their financial and moral support.

Finally, I would like to thank all my friends; Eghosa, Dami, Stella, Akin, Bolaji, Samuel, Tobi and the Pastors and members of Harvest Chapel Nottingham for their encouragement and support.

ABSTRACT

Hydrous pyrolysis of immature Longyear coal samples was done to assess the source of bitumen found in the coal, the petroleum generation potential and the possibility of liquid hydrocarbon migration within the coal. Hydrous pyrolysis results obtained showed an impressive average bitumen yield of 320 mg/g TOC which increases towards the upper portion of the seam. This increase coincides with an increase in original hydrogen content and hydrogen index of the samples indicating an improvement in oil generation potential of the kerogen up-seam.

The hopane ratios indicated thermal maturity which was consistent in both the initial coal and generated bitumen. High proportion of C₂₉ steranes was observed in initial extracts and generated bitumen indicating high plant input in the original organic matter. The uniformity of the source and maturity parameters in the bitumen extract and pyrolysis bitumen yield indicates that the bitumen located in-situ was generated by the coal.

The Longyear seam showed an unusual high loss of lower molecular weight hydrocarbons towards the upper portion of the seam as shown by the decrease of the aliphatic fractions of the initial coal bitumen. This loss was marked by an exceptional increase in Pr/nC₁₇ and Ph/nC₁₈ ratios towards the upper portion of the seam. Having established uniform thermal maturity and source input at all portions of the seam, the most probable explanation for this loss is that liquid hydrocarbon migration has occurred within the Longyear seam. The generative capacity of the Longyear coal and the observed migration profile makes the Longyear seam significant as a source rock in the Arctic basin and as a source of oil via retorting.

TABLE OF CONTENT

ACKNOWLEDGEMENT	i
ABSTRACT	ii
LIST OF FIGURES	vi
LIST OF TABLES	vii
1 INTRODUCTION	
1.1 Background	1
1.2 Aims of study	3
1.3 Objectives	3
2 LITERATURE REVIEW	
2.1 Coal Formation	4
2.2 Petroleum generation and migration from coal	6
2.3 Coal as a source rock for oil	9
2.4 Characterising Oil prone coals	9
2.4.1 Coal petrography and coal macerals	10
2.4.1.1 The vitrinite group	11
2.4.1.2 The liptinite group	11
2.4.1.3 The inertinite group	12
2.4.2 Coal maturity and maturity parameters	13
2.4.2.1 Vitrinite reflectance (VR/R ₀) and Hydrogen index	13
2.4.3 Biological markers	14
2.4.3.1 Hopanes	15
2.4.3.2 Steranes	16
2.4.3.3 Isoprenoids and <i>n</i> -alkanes	18

2.5	Geography of the study area	19
2.6	Geological setting of the investigated region	20
2.7	The Longyear seam	24

3 EXPERIMENTAL TECHNIQUES AND METHODS

3.1	Experimental techniques	26
3.1.1	Gas Chromatography (GC)	26
3.1.2	Gas chromatography-mass spectrometry (GC-MS)	27
3.1.3	Hydrous pyrolysis technique	28
3.2	Experimental methods	29
3.2.1	Samples studied	29
3.2.2	Vitrinite reflectance and maceral composition determination	30
3.2.3	Elemental analysis of the samples	31
3.2.4	Hydrous Pyrolysis	31
3.2.5	Recovery and analysis of generated gas	33
3.2.6	Recovery generated bitumen	33
3.2.7	Separation of bitumen into fractions	34
3.2.8	Gas chromatography mass spectrometry (GC-MS) analysis of aliphatic fractions	34

4 RESULTS AND DISCUSSION

4.1	Elemental composition of Longyear coal	36
4.2	Gas yields	41
4.3	Bitumen yields	43
4.4	Bitumen composition	48

4.5	Biological marker distribution in the aliphatic fraction of Longyear Coals	50
5 CONCLUSIONS AND FUTURE WORK		
5.1	Conclusion	58
5.2	Future work	59
REFERENCES		60
APPENDICES		
Appendix A	Figures	68
Appendix B	Calculations	88

LIST OF FIGURES

Figure 2.1:	Hopanes and associated stereoisomers	16
Figure 2.2:	Steranes and associated stereoisomers	17
Figure 2.3:	Pristane structure	18
Figure 2.4:	Phytane structure	18
Figure 2.5:	The Svalbard archipelago	20
Figure 2.6:	Topographic Map of Svalbard	21
Figure 2.7:	The geologic map of Spitsbergen central basin	22
Figure 2.8:	The stratigraphic units of the central basin	23
Figure 2.9:	The stratigraphic generalised column of the central basin	24
Figure 2.10:	The lithologic section of the Basilikaelva section of the Firkanten formation showing the Todalen member	25
Figure 3.1:	Schematic diagram of a gas chromatograph	26
Figure 3.2:	Schematic diagram of the gas chromatograph-mass spectrometer	27
Figure 3.3:	Experimental configurations for the pyrolysis experiments	28
Figure 3.4:	A typical hydrous pyrolysis experimental setup	29
Figure 3.5:	The Parr 4740 series hastalloy cylindrical reactor vessel	32
Figure 3.6:	Pressure gauge showing the inlet/outlet and valve	32
Figure 3.7:	Soxhlet extraction setup	34
Figure 4.1:	Hydrogen content of initial Longyear samples at different depths showing the perhydrous line	36
Figure 4.2:	The vitrinite reflectance and hydrogen content profiles of the Longyear seam	37

Figure 4.3:	Hydrogen content of the Longyear coal samples showing a decrease in hydrogen content with hydrocarbon generation	39
Figure 4.4:	Changes in the TOC content change with depth of Longyear coals at various stages of maturity	40
Figure 4.5:	TOC content change with depth of the Longyear coals at various stages of simulated maturity	40
Figure 4.6:	Total gas yields of the Longyear seam at various depths	42
Figure 4.7:	Changes in generated gas yields with depth of the Longyear seam	42
Figure 4.8:	C ₁ -C ₄ gas fractions of the Longyear coals at different depths	43
Figure 4.9:	Bitumen yields from extracted Longyear coal samples at different sample sizes	44
Figure 4.10:	Changes in bitumen yield with seam depth	44
Figure 4.11:	Hydrous pyrolysis yields from Longyear coals samples at various Depths	45
Figure 4.12:	Comparism between HI and bitumen yield of the Longyear coal samples	47
Figure 4.13:	Percentage composition of each fraction in extracted bitumen at various depths	48
Figure 4.14:	Change in aliphatic yields from initial coal extracts with depth of the seam	49
Figure 4.15:	Percentage composition of each fraction in generated bitumen at various depths	50
Figure 4.16:	Tri-plot of the C ₂₇ , C ₂₈ and C ₂₉ steranes	52
Figure 4.17:	Pr/nC ₁₇ trend with depth in the aliphatic fraction of initial coal bitumen Extract	57

LIST OF TABLES

Table 2.1:	Summary of maceral groups and subgroups	12
Table 2.2:	Several hopane ratios and their interpretations	16
Table 2.3:	Several sterane ratios and their interpretations	17
Table 2.4:	Isoprenoid ratios and interpretations	19
Table 3.1:	Sample numbering and representation with seam depth	29
Table 3.2:	The initial geochemical characteristics of Longyear coal	30
Table 4.1:	Hydrogen content of Longyear coal at various stages of Experimentation	38
Table 4.2:	Total bitumen yield of each sample	46
Table 4.3:	Percentage composition of fractions in initial the coal bitumen at various depths	48
Table 4.4:	Relevant sterane ratios at various depths of the Longyear seam	51
Table 4.5:	Total sterane concentrations of the Longyear seam at various depths	51
Table 4.6:	Relevant hopane ratios at various depths of the Longyear seam	54
Table 4.7:	Relevant <i>n</i> -alkane ratios	55
Table 4.8:	Relevant isoprenoid and isoprenoid/ <i>n</i> -alkane ratios	56

CHAPTER ONE

INTRODUCTION

1.1 Background

Abundant perhydrous (~6 wt% H) coal deposits are located within Spitsbergen, in the high latitude Svalbard archipelago of Norway. These coal deposits are very rich in terrestrially derived organic matter and are believed to be oil prone (Cmiel and Fabianska, 2004; Orheim et al., 2007). The oil content of these coals has the potential to enhance their value both directly as a source for oil via retorting and indirectly as a petroleum source rock in the Arctic basin. As little is known about the oils present in these coals, this project will determine:

1. The origin of the oil present in the coals
2. Whether the oil has migrated within the coal sequence

The first is essential as it has not been proven that the oil comes from the coal. The second question is also essential as migration within the coal could give a misleading impression of the oil potential of the coals.

The interest in coal as a hydrocarbon source has been renewed in the wake of a steady increase in global energy demands. Soaring oil prices have re-established the need for more rigorous oil prospecting, new field development and proper characterisation of existing hydrocarbon reserves. As these energy concerns continue to grow, the need for the efficient utilisation of alternative fossil fuel sources such as coal is also being brought into focus. The relevance of coal as a natural resource goes beyond its energy generating capability. In recent times, scientists have developed a very strong scientific opinion on coal and its ability to generate and expel liquid hydrocarbons in geologic basins. This has resulted in coal deposits being classified based on their calorific value, oil generation and hydrocarbon source rock potential. However, greater research emphasis is now being laid on the source rock potential of coals. This is because of the discovery of several large coal-sourced oil deposits around the world (Klerk, 2009; Powell et al., 1991).

Previous investigative studies have yielded positive results in the area the source rock capabilities of coal and several coal sourced oil deposits have been recognised (Larter, 1995). The most significant coal-sourced oil deposits are found in the Grippsland and Cooper basins in Australia, the Beaufort-Mackenzie basin in Canada, the Turpan basin in China and the Taranaki basin in New Zealand (Czochanska et al., 1988; Issler and

Snowdon, 1990; Moore et al., 1992; Vincent et al., 1985). Nevertheless, these discoveries have not put to rest the prolonged scientific debate that coal can serve as a source rock for liquid hydrocarbons. The factors that determine the formation and existence of oil prone coals are yet to be clearly understood. The isolated patterns of these discoveries and the heterogeneous nature of coal deposits have not favoured the argument that coal can act as a source rock for liquid hydrocarbons. Hence, several workers still maintain the opinion that coal could at best still be a source of gaseous hydrocarbons (van Krevelen, 1982).

The perhydrous and oil prone nature of the Svalbard coal deposits offers a unique prospect for investigating and understanding the conditions and controls responsible for the formation of oil prone coals. Better understanding of these controls can be attained by examining the nature and composition of the oil found within these coal deposits. However, the primary challenge will be to determine whether the oil present in the Svalbard coal was originally derived in-situ or has migrated into the coal sequence from a nearby organic sedimentary sequence. This could be ascertained by biomarker analysis and by simulating the oil generation process in coal using the hydrous pyrolysis technique (Carr et al., 2009; Lewan, 1997). Although pyrolysis could be hydrous or anhydrous (absence of water), adopting the hydrous pyrolysis technique will be more suitable for this study because of its ability to generate higher yields of oil and bitumen for analysis. Comparing biological marker compositions in the oil extracted from the coal before hydrous pyrolysis with the oil obtained from hydrous pyrolysis will be definitive in determining the source and depositional environment of the oil present in the coal.

The understanding of these controls often finds relevance in oil exploration and in characterising the nature and quantity of oil in reservoirs that are sourced from coals. Geologists have the task of making exploration decisions based on whether or not oil has been generated from coal in a basin. A thorough understanding of oil migration patterns will help to open up new plays and reduce exploration cost as the risk of drilling dry wells could be reduced. The nature and composition of the oils if ascertained will play a key role in business decision making and production economics. Oil rich bituminous coals are also a strong target for coal liquefaction (Klerk, 2009).

1.2 Aim of study

To ascertain if the bitumen present in the Svalbard coal was generated by the coal and to investigate the possibility of migration of such oils within the sequence.

1.3 Objectives

- To evaluate the source of the oil present in the coal and to identify any changes in its nature of using biomarker analysis.
- To determine the amount of bitumen or oil that can be generated from Svalbard coal using hydrous pyrolysis and soxhlet extraction.
- To measure the changes in bitumen composition, concentration and nature from the bottom to the top of the coal seam.
- To assess oil migration by noting the changes in bitumen volume, composition and identifying changes in relevant biomarker concentrations within the aliphatic fractions of the extracted bitumen.

CHAPTER TWO

LITERATURE REVIEW

The factors responsible for the formation of oil prone coals will be better understood if several fundamental concepts are established. These concepts include; coal formation, its petrographic properties and organic constituents. The most widely accepted parameters that serve as pointers to oil proneness also need to be defined. General considerations on petroleum generation and the possibility of oil migration within a coal sequence will be accessed. The geology and geography of the study region will be reviewed in order to determine what role these have played in the origin of perhydrous coals in the region.

2.1 Coal Formation

The word coal is derived from the Greek word "col" and represents a readily combustible rock containing more than 50 weight % and more than 70 volume % of carbonaceous material (Tatsch, 1980). Coal is an organically formed sedimentary rock, composed mainly of decayed and lithified plant remains. It is derived from the rapid accumulation and burial of land derived (terrestrial) plant materials in a specialised depositional environment known as a sedimentary basin (Morris, 1998). Most coals are formed under non-marine conditions and result from the accumulation of freshwater or lacustrine sediments. The original sediment formed by this process is a damp, spongy material called peat. This later becomes dried, compressed and modified both in composition and texture due to the overburden pressure associated with burial (Ward, 1984). Different kinds of peat originate as a result of varying original material and burial conditions. This eventually leads to the formation of different kinds of coals. The formation of peat is governed by certain controls. These controls are a combination of geologic, geographic, biochemical and geochemical aspects (Tissot and Welte, 1984).

Peat formation is facilitated by the presence and rapid accumulation of large amounts of plant materials. This sort of accumulation depends on the efficiency of photosynthesis (Ward, 1984). Plant productivity on land became possible for the first time after the evolution of higher plants during the Devonian period (350-401 million years ago). This allowed the production of the necessary biomass for the formation of peat which flourished during the Carboniferous period (Ward, 1984). Teichmüller and Teichmüller (1982) are of the opinion that the conditions necessary for the formation of thick peat deposits and invariably coal seams are:

- A slow, steady and continuous rise of the groundwater table i.e. subsidence,
- Adequate protection of the swamp area (by sand bars, spits etc.) against major floods by sea and flood waters from rivers, and
- A low energy relief which would restrict the supply of river sediments which could hinder the peat formation process.

Previous studies by Dallmann (1993) revealed that these kinds of conditions operated in the early Svalbard basin. However, coal seam formation generally depends on the palaeogeographical and structural interactions within the sedimentary region (Teichmüller and Teichmüller, 1982). Although the tectonic setting is similar to that for the formation of petroleum, the source lithofacies involved differ (Teichmüller, 1989; Ward, 1984).

Mechanical breakage, biochemical and geochemical processes are initiated soon after the accumulation of dead plant remains. Biochemical changes take place at the surface under oxidizing conditions but as burial depth increases, the presence of stagnant water causes reducing conditions to prevail (Ward, 1984). At this point, the PH ranges from neutral to slightly acidic and the acidity increases with burial depth (Teichmüller and Teichmüller, 1979). The degree of acidity also depends on the original plant material. The acidity of peat plays an important role in determining the rate of bacterial activity as highly acidic conditions hinder the activity of bacteria (Teichmüller and Teichmüller, 1982). Although Teichmüller and Teichmüller (1982) argue that microbial activities play a prominent role in the initial stage of peat formation only, the ultimate peat characteristic is determined by the type and composition of the parent organic material known as kerogen (Tissot and Welte, 1984). In a situation where the peat is derived from abundant hydrogen-rich land-plant debris, such peat will mature to coals that will have the capacity to generate liquid hydrocarbons. This is believed to be the case of the Svalbard coals and some Australian coals (Larter, 1995).

A combination of geochemical and geologic processes eventually pave the way for coalification which is the physical and chemical conversion of peat into various types of coal due to the action of temperature, pressure, time and biochemical interactions (Orem and Finkelman, 2003). The degree of coalification is proportional to the intensity of the above mentioned factors. The common terms peat, brown coal, bituminous coal and anthracite represent various levels of the coalification series (Teichmüller and Teichmüller, 1979; Thomas, 1992). These stages of coalification are referred to as levels of rank which serve as an indication of the progression of peat all the way to anthracite coal (Tissot and Welte, 1984). Increasing rank (i.e. from peat to anthracite) is characterised by a decrease in moisture content and an increase in calorific value (Teichmüller and Teichmüller, 1982). According to Hunt (1979), the process of

maturation is what converts the immature organic matter in source rocks to oil and gas and for coals, this would occur during the initial stages of coalification (Hunt, 1991; Larter, 2011). Thermal maturity of a coal or any source rock depends on the interplay of the previously mentioned factors. This will eventually affect their ability to generate and expel liquid hydrocarbons.

2.2 Petroleum generation and migration from coal

The processes that yielded hydrocarbons within the Svalbard coals have not been previously defined. However, these processes would not differ greatly from the ideas already expressed by several scientists that petroleum generation from a source rock is as a result of kerogen maturation. Kerogen which is the naturally occurring, dense, insoluble organic matter composition of a source rock is the vital raw material for hydrocarbon generation (Vandenbroucke and Largeau, 2007). Kerogen represents the most abundant strain of organic matter on the earth and is the major component of coals, shales and source rocks. The possibility and ease with which an organic matter rich sedimentary rock will expel liquid hydrocarbons is dependent on the original constituents of the kerogen (Van Krevelen, 1984). Conventional organic constituents of kerogen are woody plant material (terrestrial origin) and algae (marine origin). Kerogens are described as Type I when they contain mainly algal constituents and Type III when they have a greater proportion of woody plant materials. Type II kerogens fall in between the woody and algal composition having a mixture of the terrestrial and marine (Vandenbroucke and Largeau, 2007). Coal is typically characterised as a type III kerogen.

Hydrocarbon generation in coal occurs as a result of thermal decomposition of kerogen. The chemical and physical changes which occur in coal as a result of increasing temperature and pressure with burial lead to coalification and increase in coal rank (Ward, 1984). Geochemical changes such as the increase in carbon and relative decrease in elemental oxygen and hydrogen also take place (Tissot and Welte, 1984). The result of these changes is an increase in aromaticity, elimination of functional groups and decrease in the chain-like structures on coal. These considerations signify a loss in carbon, oxygen and also hydrogen resulting in the release of hydrogen and oxygen rich carbon containing molecules (Tissot and Welte, 1984). This process typically gives rise to low molecular weight volatiles and mainly gases which are widely regarded as the actual hydrocarbon generating capacity of coals (Hunt, 1991; Isaksen et al., 1998; Larter, 1995; Sykes and Snowdon, 2002). However, Tissot (1969) is of the opinion that higher molecular weight hydrocarbons and oils are also generated during this process.

These findings are backed up with examples of liquid hydrocarbon accumulations that linked to coal as reported by (Czochanska et al., 1988; Issler and Snowdon, 1990; Moore et al., 1992; Vincent et al., 1985).

Oil and gas accumulations are mainly located in relatively coarse-grained permeable and porous sedimentary rocks which contain very a little amount of organic matter (Hunt et al., 1967). It is highly unlikely that the huge volumes of petroleum found in these rocks have originated in them from organic matter which would leave no trace or remains. Hence it can be concluded that the point of petroleum origin is not identical with the site where it is located in economically exploitable quantities. Under geologic conditions and geochromatographic effects, generated oil has the tendency to move horizontally or vertically through the coal sequence and accumulate in pools (Huang, 1999).

Petroleum migration can be defined as the movement of hydrocarbons generated by a source rock in a thermal maturation process from the parent to the carrier strata (Zhao and Cheng, 1998). The initial movement (typically up to a maximum of a few hundred metres) of newly generated hydrocarbons out of the source rock which is synonymous with expulsion is termed primary migration. Further movement of hydrocarbons into a more permeable porous rock unit, or basin of accumulation is termed secondary migration (Huang, 1999; Tissot, 1988). Secondary migration eventually leads to the separation of oil and gas in selected parts of these rocks (Hunt, 1979). In several cases, liquid and gaseous hydrocarbons could migrate through fine-grained sedimentary rocks like mudstones or a coal sequence. Such a case has been reported in the Gulf of Mexico where petroleum migrates vertically through a mudstone sequence assisted by very high pressure (Larter, 2011). This could also be the case in Svalbard because of the unusually high concentrations of bitumen found in the coals. Three major viewpoints have dominated the research of petroleum migration from coal:

- The initial view is that oil from coal cannot migrate out of the coal matrix. Migration would occur only when the generated oil is cracked into smaller hydrocarbon gas molecules (Durand, 1983; van Krevelen, 1982).
- Migration of oil can only occur under a combination of very stringent conditions. The coal pore structure and the maceral composition being the most important conditions (England, 1993; Powell, 1986).
- Coals expel oil readily even with greater ease than mudstones (Huang, 1999; Huc and Hunt, 1980).

Petroleum migration is actually the most important factor in determining whether and to what extent a coal sequence has given rise to liquid hydrocarbons (Wilkins and George, 2002). The viewpoint of several workers is that there are some major controlling factors

responsible for the migration of oil from coal (Huc and Hunt, 1980; Hunt, 1979; Killips et al., 1998; Zhao and Cheng, 1998). These factors are broadly classified into the distribution characteristics of the coal pore and the external tectonic stresses (Zhao and Cheng, 1998). The distribution characteristics relate directly to the coal structure and porosity which is as a result of the maceral composition and maceral associations. Despite the heterogeneity and complexity of coal macerals, coals generally exhibit a porous microstructure. This microstructure has a significant influence on the migration of liquid hydrocarbons from coal (Given, 1984). Coals have a molecular sieve-like structure which limits the free movement of liquid hydrocarbons (Radke et al., 1984). Hence, it is unlikely that the larger hydrocarbon molecules would be able to drift significant distances from their source of generation. The hydrocarbons are stored up within the coal structure until some level of cracking occurs and smaller (usually methane) molecules can readily migrate through the tiny pores. Littke et al. (1990) suggested that coal exhibits weak microporosity with an increase in burial depth and invariably, as the coal rank increases, the porosity disappears. Should the coal sequence exhibits a macroporous structure; hydrocarbons are easily expelled and migrate from the coal core (Littke et al., 1990; Zhao and Cheng, 1998). Higher molecular weight hydrocarbons are most often trapped within the structure or released last under intense stress. Because of this ability of coal to withhold generated hydrocarbons, the oil from coal is quite often light oil.

Hunt (1991) suggested that tectonic compressive shear stresses which result from overburden acts as an external force for the migration and expulsion of hydrocarbons from coal. These stresses drive hydrocarbons from the porous structure in the direction of weaker stresses to carrier strata. The greater the shear stress, the more the tendency for the hydrocarbons to migrate (Zhao and Cheng, 1998). Although there are reported evidences of such stresses in the Svalbard region, there are no documented evidences of oil migration from coal in this region (Dallmann et al., 1988). This may be due to the general limitations of most migration mechanisms, which is the relative ratio of oil to water in a sedimentary basin during hydrocarbon generation and primary migration. In as much as the mechanism for the separation of generated oil from formation water is not fully understood, the ratio of oil to water should not be ignored in petroleum migration models (Hunt, 1991).

When compared to mudstones, oil migration from coal leaves a greater geochromatographic effect on the strata and surrounding beds than mudstones. This means that there is an apparent change in the chemical and physical properties of the hydrocarbons as they migrate (Zhao and Cheng, 1998). This geochromatographic effect shows a direct relationship with the pore distribution characteristics, pore intensity, the molecular size and the organic abundance of the source rock. Hence, identifying these

changes in residual oil or bitumen property in coals and other source rocks is vital for unlocking the questions of migration.

2.3 Coal as a source rock for oil

A petroleum source rock is defined as an organic matter rich sedimentary rock that in its natural state will generate and expel sufficient hydrocarbons to form a commercial accumulation of oil or gas (Hunt, 1979). Source rocks act as the centre for petroleum generation from insoluble organic matter known as kerogen. Larter (2011) explained that a source rock is a fine-grained sediment with abundant organic matter that could generate liquid or gaseous hydrocarbons on thermal modification in a sedimentary basin. Classic source rocks, usually limestones or shales display similar characteristics, containing at least 0.5% total organic carbon (TOC) and about 1% organic matter (Schlumberger, 2011). Based on this definition of a source rock, coal immediately qualifies to be considered as a source rock because of its organic matter rich nature. However, source rock classification is not exactly straightforward and in a strict sense, other factors such as expulsion and migration need to be considered (Fleet and Scott, 1994). Coal also presents a very complex petrography which makes it challenging to determine exactly which coal sequence will act as a source rock. In various studies conducted by Boreham and Powell (1991), Diessel (1992), Durand (1983), Hunt (1991) and Petersen (2002), these challenges have been reviewed and attempts have been made to discuss the geochemical and petrological issues relating to the nature, and identification of coal source rocks and the issue of migration (Fleet and Scott, 1994).

2.4 Characterising Oil prone coals

Early characterisation efforts have been based on coal petrology and maceral composition. However, the complete reliance on maceral composition for the classification of coals as oil prone has proven to be unreliable (Petersen, 2002). This has led several scientists to adopt other microscopic and geochemical parameters that can be used to characterise coals based on their source rock potential (Horsfield et al., 1988; Murchison, 1991). These parameters include the Hydrogen index (HI), Vitrinite Reflectance (VR denoted by R_0) and Hydrogen/Carbon (H/C) ratios which can be obtained by various experimental techniques. Coal petrography along with some other relevant experimental and classification techniques that will be applied in this study are discussed in the sections below:

2.4.1 Coal petrography and coal macerals

The oil prone nature of coals is attributed to the composition of the original materials found in them (Wilkins et al., 2002). Teichmüller and Teichmüller (1982) defined coal facies as the primary genetic types of coal, which are dependent on the environment under which peats originate. Petrography in a broader sense refers to the systematic description of a coal sample in hand specimen and under thin section while coal macerals are the basic organic constituents of coals which can be recognised at the microscopic level (Kearey, 1996). The petrography of Svalbard coals make them unique and oil prone (Orheim et al., 2007). From a petrology viewpoint, coal genesis is discussed based on the genesis of coal macerals, microlithotypes and lithotypes. While coal macerals are the most uniform microscopic constituents of coal, microlithotypes are typical maceral associations that can be recognized under the microscope, and lithotypes are layers of coal seams which can be distinguished with the naked eye (Teichmüller, 1989).

Coal macerals can be compared with minerals in rocks but differ from minerals in that minerals have a well-defined chemical composition and are most often crystalline whereas coal macerals vary greatly in their chemical composition as well as physical properties. Teichmüller (1989) observed that apart from the parent plant materials and climate, the degree and length of burial (which signifies rank) of these materials is pivotal for the microscopic appearance of macerals. As rank increases, macerals vary and their physical, chemical and technological properties are altered. Coal technologists have established the presence of a clear relation between the reflectance of a coal maceral and the coal rank (Stach, 1982). Invariably, the carbon or volatile matter yield of coal can be estimated by measuring its reflectance on a polished surface.

Coal structure and reflectance under incident light are the main parameters used to differentiate macerals and maceral groups under the microscope. Three main maceral groups have been identified in coals. These maceral groups can be subdivided to contain macerals, submacerals and maceral variety for a simpler and more practical classification (Teichmüller and Teichmüller, 1982). Each maceral group contains a series of macerals that are quite similar in origin and mode of conservation. The maceral groups are to some extent characterised based on their chemical composition and linked directly to the elemental composition of hydrogen, oxygen and carbon (Scott, 2002). However, Stach (1982) suggested that macerals belonging to the same maceral group differ from each other in morphology and structure rather than in reflectance. This means that there is only a relatively small difference in the elementary composition, volatile-matter yield and technological properties of macerals belonging to the same group. The three maceral groups are:

2.4.1.1 The vitrinite group

Vitrinites are by far the most frequent, complex and abundant maceral group occurring in bituminous coals (Scott, 2002). They are also the most important in source rock studies because of their abundance, differences in their reflectance which is due to varying original plant materials and the degree of preservation which serves as a pointer to hydrogen-richness and paleo-environment of deposition. When compared with other macerals, they have an intermediate reflectance which is lowest in high volatile coals and increases with rank. Orheim et al. (2007) has established that vitrinites are the most abundant macerals in the Svalbard coals. Teichmüller (1989) noted that vitrinites arise from lignin and cellulose of plant cell wall and also from tannings which permeate cell walls and fill cell lumens. Beyond containing true plant material, this group also contains detrital materials and chemical precipitates. For coal petrologists, the main morphological distinction between the members of this group is made between the cell wall (telinites), gels (gellinites/collinites) and the detrital material (detrinites). The circumstances under which the vitrinites originate make them very popular among terrigenous organic matter like coals, marls and carbonaceous shales (Scott, 2002). Hydrogen rich (perhydrous) vitrinites like detrovitrinites are regarded as oil prone and are very important in source rock studies. The most abundant vitrinite maceral in the Longyear coal is detrovitrinite (Orheim et al., 2007). Table 2.1 shows a summary of the maceral groups and relevant submacerals in these groups.

2.4.1.2 The liptinite group

They are often referred to as the exinite group and comprise of the spononite, cutinite, resinite, alginate and liptodetrinite macerals. Liptinites originate from hydrogen-rich plant organs as well as from decomposition products and algal and bacterial substances (Teichmüller, 1989). Crelling (1987) stated that the most outstanding petrographic property of the liptinite group is that they have a reflectance that is lower than that of the vitrinites and inertinites in the same coal sample. In low rank coals, liptinites are distinguished from vitrinites by higher hydrogen content. Liptinite macerals show a high sensitivity to progressive coalification and on carbonisation they yield high volumes of tar and gas (Stach, 1982). The liptinites are the least abundant, lightest and most volatile macerals. Their hydrogen rich nature makes them important as oil prone macerals despite their limited distribution (Hunt, 1991; Scott, 2002). Orheim et al. (2007) reported an extremely low percentage (2-3%) of liptinites in the Svalbard coals which usually existed as spononites, liptodetrinite and cutinite.

Group maceral	Maceral	Submaceral*
Vitrinite	Telinite	Telinite 1
		Telinite 2
	Collinite	Telocollinite
		Gelocollinite
		Desmocollinite Corpocollinite
Liptinite	Detrovitrinite	
	Sporinite	
Inertinite	Cutinite	
	Resinite	
	Alginate	
	Liptodetrinite	
	Micrinite	
	Micrinite	
	Semifusinite	
	Fusinite	Pyrofusinite Degradofusinite
	Sclerotinite	Fungosclerotinite
	Inertodetrinite	

Table 2.1. Summary of maceral groups and subgroups

* Incomplete and can be expanded

2.4.1.3 The inertinite group

Inertinite is obtained from the word "inert" which means that they are typically unreactive in their behaviour. They are quite unimportant with regards to their oil proneness but are relevant in classifying coals in a general sense and are present in Svalbard coals. This group comprises of macerals derived from plant relics similar to the vitrinites (Melendez, 2001). The distinguishing properties of inertinites include high reflectance, little or no fluorescence, high carbon and low hydrogen contents and low aromatization (Scott, 2002). Inertinite was initially used to refer to the maceral behaviour in coals of coking rank in which much of the inertinite did not soften (react) during carbonization unlike vitrinites and liptinites (Teichmüller, 1989). However, Diessel (1983) has been able to show that certain inertinites from Gondwana coals are partially reactive. Stach (1982) also observed that the maceral micrinite is not inert and in fact, differs in its origin from the rest of the inertinites. Nevertheless, micrinite is still grouped under the inertinite group which is a very diverse group, and its exact nature is still a subject controversy (Crelling et al., 1988; Diessel, 1983; Scott, 2002). Micrinite is

reported to be distributed in all the seam sections of the Svalbard coals. However, they do not play any role in classifying these coals as oil prone. Cmiel and Fabianska (2004) reported an abundance of fusinites and semifusinites in Longyear coals.

2.4.2 Coal maturity and maturity parameters

Thermal maturity is a measure of the degree to which the metamorphism of organic matter has progressed with time (Crelling, 2008). During the process of coal maturation, mobile products such as gas or crude oil are expelled from the coal lattice with subsequent aromatisation and condensation of the solid residual product (coal) taking place (Van Krevelen, 1984). Petroleum generation from coal organic matter begins under the pressure, temperature and time conditions when the coals pass through the sub-bituminous stage and end when the coals have reached a medium-bituminous rank. The degree of bituminisation is synonymous with the maturity of the crude oil generated by the coal and this serves as the basis for measuring the maturity at which coals can expel crude oil (Teichmüller, 1989). Understanding the process of maturity of coals is important in characterising oil prone coals and this degree of maturation can be measured by different parameters. These parameters include vitrinite reflectance (VR), hydrogen index (HI) and biological markers.

2.4.2.1 Vitrinite reflectance (VR/R₀) and Hydrogen index

Petersen et al. (2009) defined the vitrinite reflectance as a measure of the amount white light that will be reflected off the surface of the prepared vitrinite maceral. The reflectance measurement is usually done on the vitrinite maceral. This is because the vitrinites show a moderately consistent increase in reflectance with increasing rank (Crelling et al., 1988). This makes vitrinite reflectance an invaluable tool in assessing the level of thermal maturity of sediments. Thermal maturity has been established as the route to petroleum generation and vitrinite reflectance serves as a correlating tool for determining the maturity at which source rocks will generate and expel oil (Killops et al., 2002; Killops et al., 1998). Vitrinite Reflectance ranges of 0.5-0.6% R₀ to 1.3-1.35% have been suggested as the maturity threshold for which coals will generate oil (Hunt, 1991). Orheim et al. (2007) reported R₀ values averaging 0.71% for the Longyear seam indicating that they are in a maturity range for petroleum generation. However, a major limitation of this technique was observed by (Teichmüller and Teichmüller, 1967). They noted certain important jumps or disconformities in VR ranges with increase in rank. The first jump is between the 0.6-0.7% range and the second is between the 1.30-

1.40% ranges. These, were referred to as the first and second coalification jumps respectively. Orheim et al. (2007) noted a striking coalification jump from the lower to the upper section of the Longyear seam. A suppression of vitrinite reflectance by adsorption of hydrogen rich components by vitrinites has also been reported by (Diessel and Gammidge, 1998). The effect of this suppression is the reduction of R_0 values in very hydrogen rich coals. Vitrinite reflectance measurements have been applied over the years by coal petrologists in determining the maturity and rank of coals. Presently, the VR tool is used to trace the organic matter metamorphism from kerogen to hydrocarbons which would occur within certain VR ranges. Such ranges have been suggested by (Hunt, 1991; Isaksen et al., 1998; Petersen, 2002).

Hydrogen index (HI) is a measure of the ratio of the density of hydrogen in a material to its density in water while the hydrogen, carbon (H/C) ratio simply looks at the ratio of elemental hydrogen and carbon present in the coal sample. The hydrogen index of a source rock is measured using rock-eval pyrolysis. Hydrogen index varies with the maturity of a coal sample and several studies have suggested that there is increase in HI with thermal maturity up to a maximum (HI_{max}) value (Behar et al., 1995; Cooles et al., 1986; Pepper and Corvi, 1995; Sykes and Snowdon, 2002; Verheyen et al., 1984). Petersen and Nytoft (2006) have been able to show how a combination of VR and HI parameters can be used to determine maturity range for oil generation some other key relationships. Petersen (2006) explained the existence of a direct relationship between VR and HI at certain maturity ranges and eventually reported that oil prone coals fall within a HI range of 150-370mg HC/g TOC and a VR range of 0.6-0.95% R_0 while gas prone coals are typically found below these HI and VR ranges.

2.4.3 Biological markers

Biological markers are useful in reconstructing the ecology of peat-forming environments. In a geologic setting, they represent the remains of ancient organic matter-forming materials (Curtis et al., 2004; Peters et al., 2007). The information held in these relics aid in the differentiation, characterisation and assessment of depositional environments, age and maturity of sediments. In the discipline of organic geochemistry, the application of biological marker compounds for the correlation of sediments and petroleum accumulations has been firmly established (Jiamo et al., 1990; Moore, 1969). They are also very useful in distinguishing ancient non-marine and marine source rocks. Biological marker compounds bring insight into the history of oil formation and accumulation within a sedimentary system (Brassell et al., 1986).

Brassell et al. (1986) stressed that identifying coal sourced oils within a basin is achieved by correlating the inherent properties of the oil with that of the surrounding organic sedimentary sequences using biological markers. Oil source correlation within a basin will not be to coal in a strict sense but to sequences bearing terrigenous organic matter. However, biomarker information alone may be somewhat ambiguous since they may have been derived from terrigenous organic matter that has been deposited in a lacustrine or marine environment (Fleet and Scott, 1994). In summary, Ji-Yang et al. (1982) established that biological marker measurements can be used to access:

- a. The maturity of organic matter rich sediments and oils
- b. The extent of migration of an individual pool of oil
- c. The correlation of source rocks and oils.

A wide range of biological markers are available for achieving these measurements. However, for the purpose of this study, greater emphasis will be laid on the hopanes, steranes and acyclic isoprenoid biomarkers.

2.4.3.1 Hopanes

Hopanes are pentacyclic triterpenoids (six isoprene units) that contain between 27 – 30 carbon atoms. Although they can be found in both prokaryotic and eukaryotic organisms, they are most commonly derived from the cell membranes of prokaryotes (phototropic cyanobacteria and heterotrophic bacteria). The widespread distribution of hopanes in sedimentary organic matter is attributed to their prokaryote antecedent (Nytoft and Bojesen-Koefoed, 2001). Hopanes are characterised by several maturity-sensitive stereoisomers with $\beta\beta$ configurations easily converting to $\alpha\beta$ and $\beta\alpha$ under heightened stress (Chandru et al., 2008). Hopanes are widely used in providing maturity estimates in petroleum provinces as well as assessing paleoenvironments. Their high resistance to biodegradation also makes them very useful in assessing the biodegradation rates in highly degradable oil (Peters et al., 2007). Hopanes ratios are partly relied on to provide oil-source and oil-oil correlations (Moldowan et al., 1991). Several hopane ratios are vital in interpreting source and maturity of oils. These maturity ratios are obtained from C₂₉ to C₃₅ stereoisomers on the chromatograms m/z 191. Table 2.2 shows some the relevant hopane ratios and interpretations.

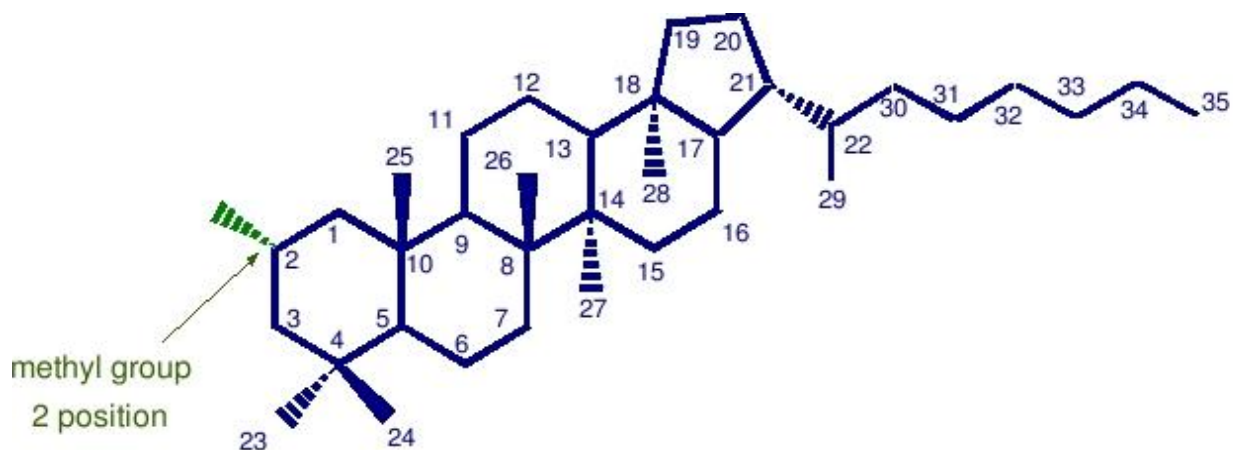


Fig. 2.1. Hopanes and associated stereoisomers

Information	Parameter	Comments
Source	C_{35}/C_{34} hopanes	Crude oils from coal/resin show lower C_{35}/C_{34} ratio (<0.6).
Maturity	$31S/(31S+31R)$ and $32S/(32S+32R)$	Increases from 0-0.6% (0.6% is considered point of equilibrium maturity). 0.57-0.62 = Equilibrium 0.50-0.54 = Immature/barely entering oil generation phase 0.57-0.62 = Attaining or surpassing the main phase of oil generation. (Moldowan et al., 1991)
Biodegradation	C_{25} -norhopanes	When C_{25} -norhopanes are absent, microbial attack favours C_{35} to C_{27} compounds (Peters et al., 2007).

Table 2.2. Several hopane ratios and their interpretations.

2.4.3.2 Steranes

Steranes are part of a class of compounds called steroids. They are derived from sterols in cell membranes of eukaryotes, mainly higher plants and algae (Huang and Meinshein, 1979). Although they are less abundant and prominent than hopanes in coals, they are very useful in interpreting paleoenvironments and maturity of oils. Higher land plants typically synthesize C_{29} sterols making them the most common Steranes present in coals and terrigenous organic matter (Jiamo et al., 1990). C_{27} steranes originate mainly from

marine planktons and are vital constituents of marine sediments. C₂₈ steranes are also characteristic of marine sediments.

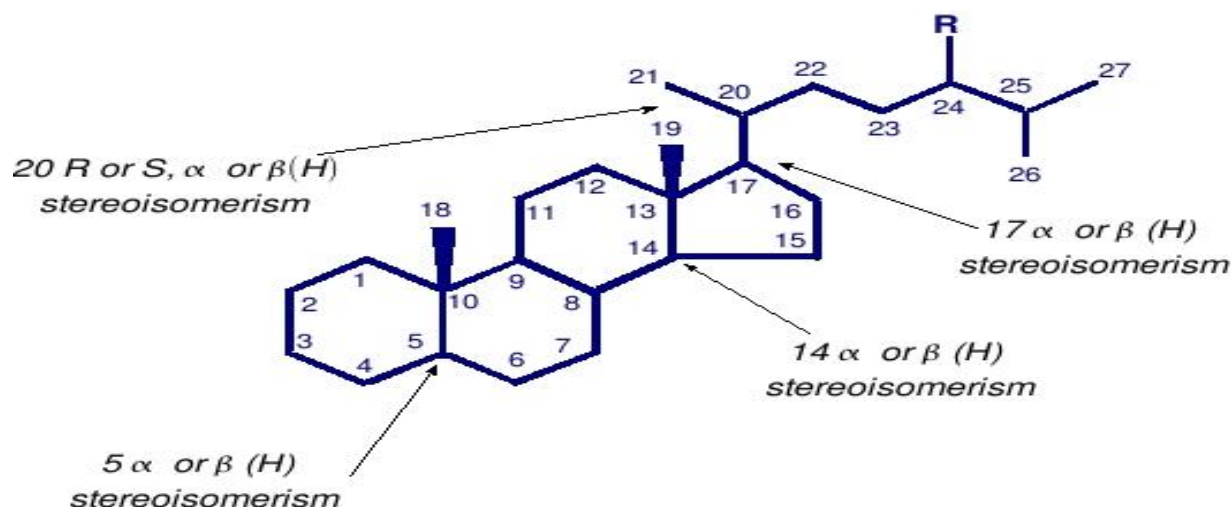


Fig. 2.2. Steranes and associated stereoisomers

Steranes exist in various diastereometric configurations which are affected largely by thermal maturity (Seifert, 1978). The more thermodynamically stable Steranes occur with increasing maturity. Table 2.3 shows some the relevant sterane ratios that are vital in interpreting source and maturity of oils. Such ratios can be obtained from C₂₇ to C₂₉ stereoisomers on the m/z 217 chromatogram.

Information	Parameter	Comments
Source	C ₂₉ steranes	Higher plant input to source rock. High C ₂₉ steranes relative to C ₂₇ – C ₂₉ steranes.
Age	C ₂₉ Monoaromatic steranes	High in oils derived from sources older than 350 million years.
Maturity	$\frac{29\alpha\alpha\alpha S}{29\alpha\alpha\alpha S + 29\alpha\alpha\alpha R}$ and $\frac{29\alpha\beta\beta R + S}{(29\alpha\beta\beta R + S) + (29\alpha\alpha\alpha S + 29\alpha\alpha\alpha R)}$	Increases from 0-0.5 (0.5 is considered point of equilibrium maturity). Parameter increases with thermal maturity (Moldowan et al., 1991)

Table 2.3. Several sterane ratios and their interpretations.

2.4.3.3 Isoprenoids and *n*-alkanes

Isoprenoids are derived from isoprene units located within the wax component of most plants. Isoprene constitutes the fundamental unit of isoprenoids consisting of five (5) carbon atoms (Burnham et al., 1982). Isoprenoids are typically stronger than biologically assembled proteins and polysaccharides because of the existence of a covalent C-C bond between the isoprene units. This makes them vital tools in assessing the rate of biodegradation in oils (Chandru et al., 2008). Naturally occurring Isoprenoids typically have chain lengths ranging from C₁₀ to C₂₀ with alternating sites of functionality and unsaturation as well as a different linking approach for the isoprene units (tail to tail, tail to head and head to head). Acyclic Isoprenoids are straight chained aliphatic compounds commonly found in the wax components of land plants. Pristanes and phytanes are the frequently reported acyclic Isoprenoids found in coals (Leythaeuser and Schwarzkopf, 1985).

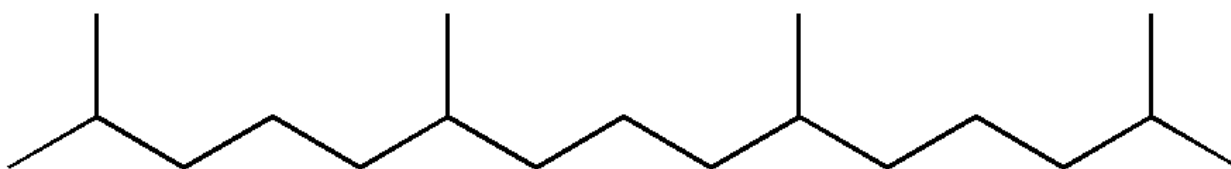


Fig. 2.3. Pristane structure

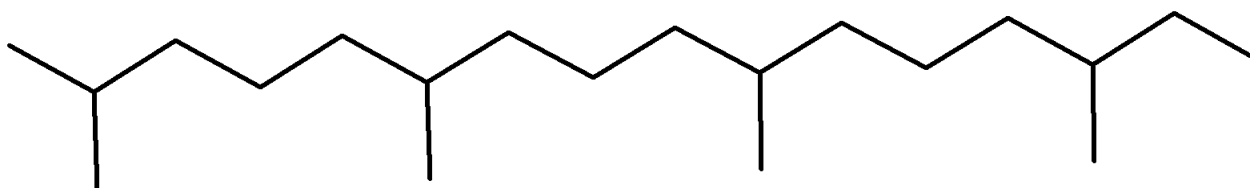


Fig. 2.4. Phytane structure

Pristanes and phytanes are believed to have originated from the decarboxylation (forming pristane) and dehydration (forming phytane) of phytol. Coals generally display a higher preference for pristanes than for phytanes (Hedberg, 1968). This forms the basis for one of the vital ratios (pristane/phytane) used in source and paleoenvironmental interpretation. Table 2.4 shows some important isoprenoid ratios

and their relevance. These ratios are obtained from the C₁₅ – C₃₁ *n*-alkane compounds on the chromatogram m/z 71.

Information	Parameter	Comments
Source	Pristane/phytane	Very high in coal sourced oils (>3.0) (Hedberg, 1968).
Migration	Pristane/ <i>n</i> -C ₁₇	An increasing ratio through a source rock profile could indicate migration. Branched chained pristanes will be eluted less readily than straight chained <i>n</i> -C ₁₇ .
Maturity	Pristane/ <i>n</i> -C ₁₇ and Phytane/ <i>n</i> -C ₁₈	These ratios decrease with increasing maturity (Tissot et al., 1987).

Table 2.4. Isoprenoid ratios and interpretations.

2.5 Geography of the study area

The coals investigated are from the Longyear seam located on the Spitsbergen Island found within the Svalbard archipelago. Spitsbergen is the largest island on the Svalbard archipelago in the Arctic Ocean and is located in-between Norway and the North Pole (Harland, 1998). Svalbard consists of all the islands between latitude 74° North and latitude 81° North and between longitude 10° East and longitude 35° East (Fig 2.5). The Svalbard archipelago is located in the northern part of the kingdom of Norway covering an area of approximately 62,049 square kilometres (sq. Km) and is roughly centred on 78° North latitude and 20° East longitudes (Dallmann et al., 1988). In this region, the mean annual temperature ranges from -5°C at sea level to about -15°C within the mountains leaving the area covered with ice for more than 6 months of the year. The climate is arctic with extensive glaciations covering about 60% of the region (Svendsen et al., 2002). Svalbard is located within an area of extensive permafrost and permafrost related features. These features are more pronounced in the dry central area of Spitsbergen which is not fully covered by glaciers (Harland, 1998). Glacial cut troughs also known as Fjord's characterise this region. Heavy glaciations and the northern latitude generally choke up arable land hindering the growth of trees and shrubs on the island.



Fig. 2.5. The Svalbard archipelago

2.6 Geological setting of the investigated region

Svalbard has a very elegant and diverse geologic history which makes it a place where a complex variety of geologic activities can be studied. The Svalbard islands evolved through a series of uplifts/subsidence with episodes of re-deposition of re-worked sediments impeded by episodes of basalt and dyke volcanism (Harland, 1997). The archipelago symbolises an uplifted region of the Barents shelf and is bound by passive continental margins on the north and west (Fig 2.6). This uplift was more pronounced in the northern and western parts of the shelf allowing progressively older rocks to trend in this direction (Myhre and Eldholm, 1988). The plate margins in this region evolved during the Tertiary period and are closely related to the rifting and sea floor spreading of the Norwegian-Greenland Sea and the Eurasia basin. The tectonic history of western Spitsbergen in particular is greatly influenced by events affiliated to the splitting of the Greenland Sea (Myhre and Eldholm, 1988; Worsley, 1986).

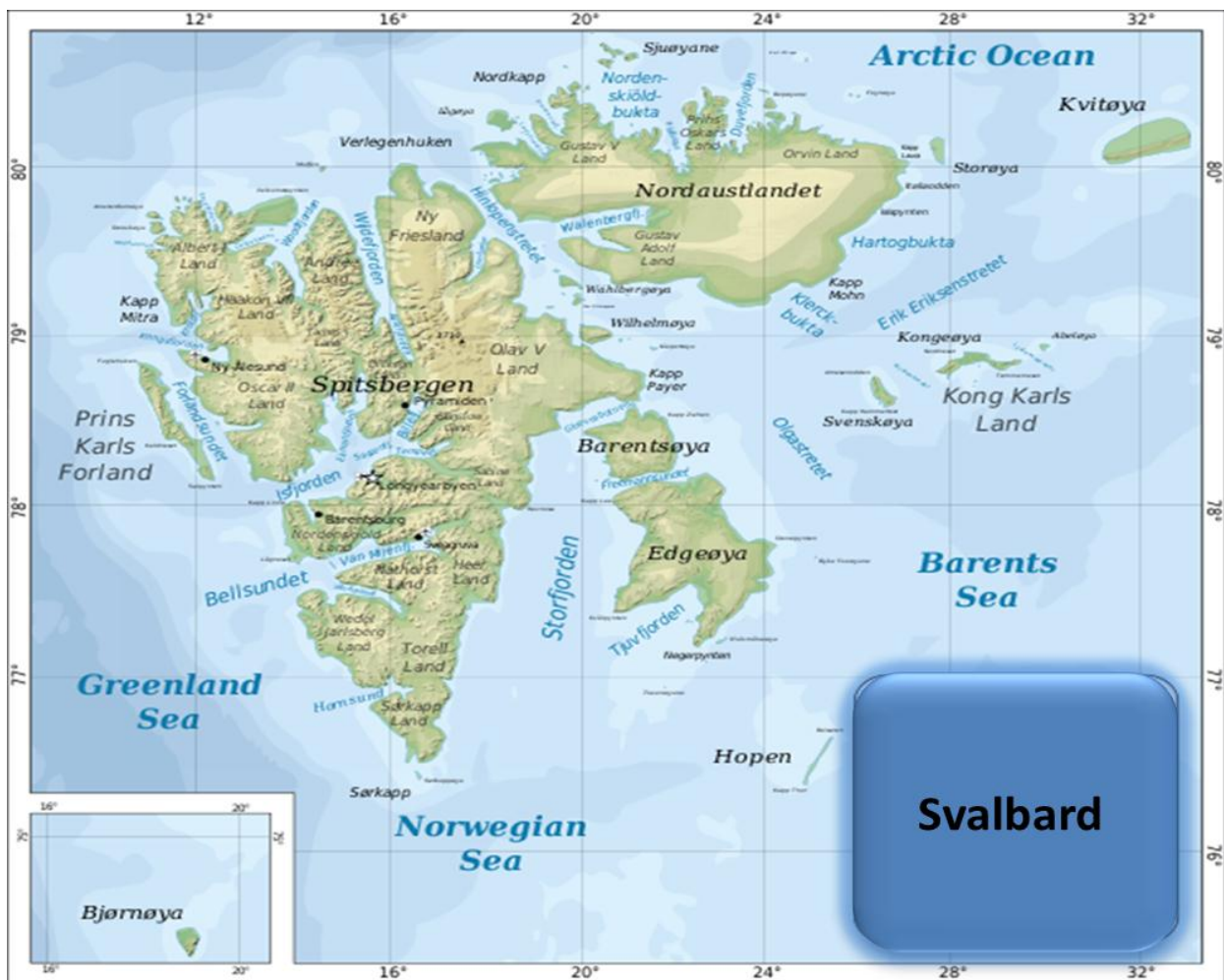


Fig. 2.6. Topographic Map of Svalbard

The sedimentary sequence of Svalbard appears to stretch from the upper Palaeozoic to the lower Tertiary periods. Abundant tertiary deposits exist within the central region of Spitsbergen in an extensive depression trending in the North, North, West (NNW) direction (Cmiel and Fabianska, 2004; Myhre and Eldholm, 1988). These central tertiary deposits exceed a 2300m thickness and consist mainly of sandstones, conglomerates, siltstones, claystones, coals and coaly shales. The Svalbard platform consists of a broad syncline with a fold belt trending west and a mildly ascending limb towards the east. Located within the syncline is the central basin which represents the middle part of Spitsbergen (Orheim et al., 2007).

Coal observations of Spitsbergen Central Basin.
 Important mining areas named.
 Vertical section along line A-A.

Height of columns indicate seam thickness as observed by
 core drilling (●) or surface trenching (○)

Seam headings:
 A= Askeladden, L= Longyear, T= Todal, S=Svea

After Major, H. & Nagy, J. 1972.
 Detailed coal information A.Orheim/Store Norske

- Tertiary
- Cretaceous
- Jurassic
- Triassic
- Carboniferous and Permian
- Lower Carboniferous
- Cambrium - Ordovicium
- Dolerite intrusions

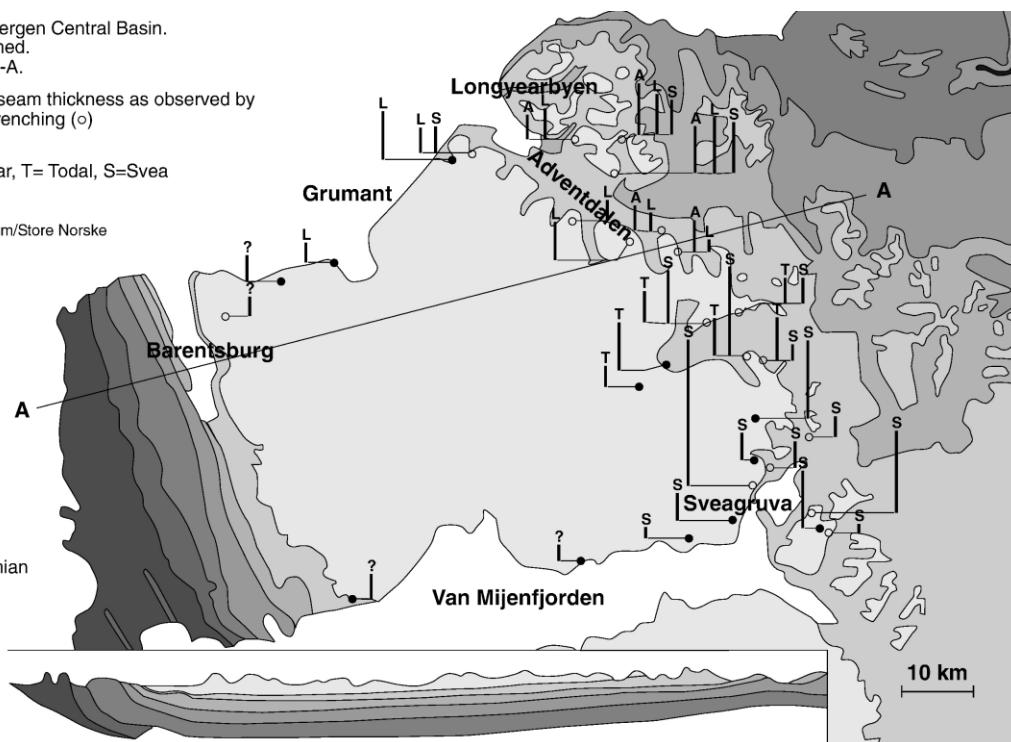


Fig. 2.7. The geologic map of Spitsbergen central basin (Orheim et al., 2007).

Within this central basin (the middle part of Spitsbergen), the principal Tertiary outcrop is the Van Mijenfjorden group which spans about 2km in thickness dominating most of the central basin of Spitsbergen (Fig 2.7). The Van Mijenfjorden group is typically subdivided into six lithologic formations (Fig 2.8). Coal seams and organic sediment traces are found in the Firkanten, Grumantbyes and Aspelintoppen formations within this group (Cmiel and Fabianska, 2004). However, the Firkanten formation is the principal source of coal in the Spitsbergen region.

Buchananisen Group Kaffioyra region		
Age	Formation	Member
O1	Balanuspynten	Sarstangen Sarsbukta
E	Marchaislaguna Krokodillen Reinhardpynten Sesshogda Selvagen Aberdeenflya	
Van Mijenfjorden Group Longyerbyen region		
Age	Formation	Member
E	Aspelintoppen Battfjellet Frysjaodden	
Pc	Grumantbyen Basilika Firkanten	Endalen Kolthoffberget Todalen
Billefjorden Group Sorkapp Land region		
Age	Formation	
C ₂	Sergeijevfjellet	
C ₁	Hornsundneset Adriabukta	

Fig. 2.8. The stratigraphic units of the central basin (Harland, 1998).

Spanning about 100-170Km in thickness, this generally transgressive sequence covers about three to eight coastal-tidal sequences with a conglomerate normally defining its base. The upper part of the Firkanten formation is represented by the Endalen member which contains mainly sandstones to the north with shale, dolomite and siltstone interfingers (Dallmann, 1993). The Todalen member represents the lower coal-bearing part of this formation and contains marine and lacustrine to brackish sandstones, shales and siltstones with relevant coal intercalations. The Todalen member consists of five principal coal seams starting from the top: Askeladden, Svarteper, Longyear, Todalen and Svea (Cmiel and Fabianska, 2004).

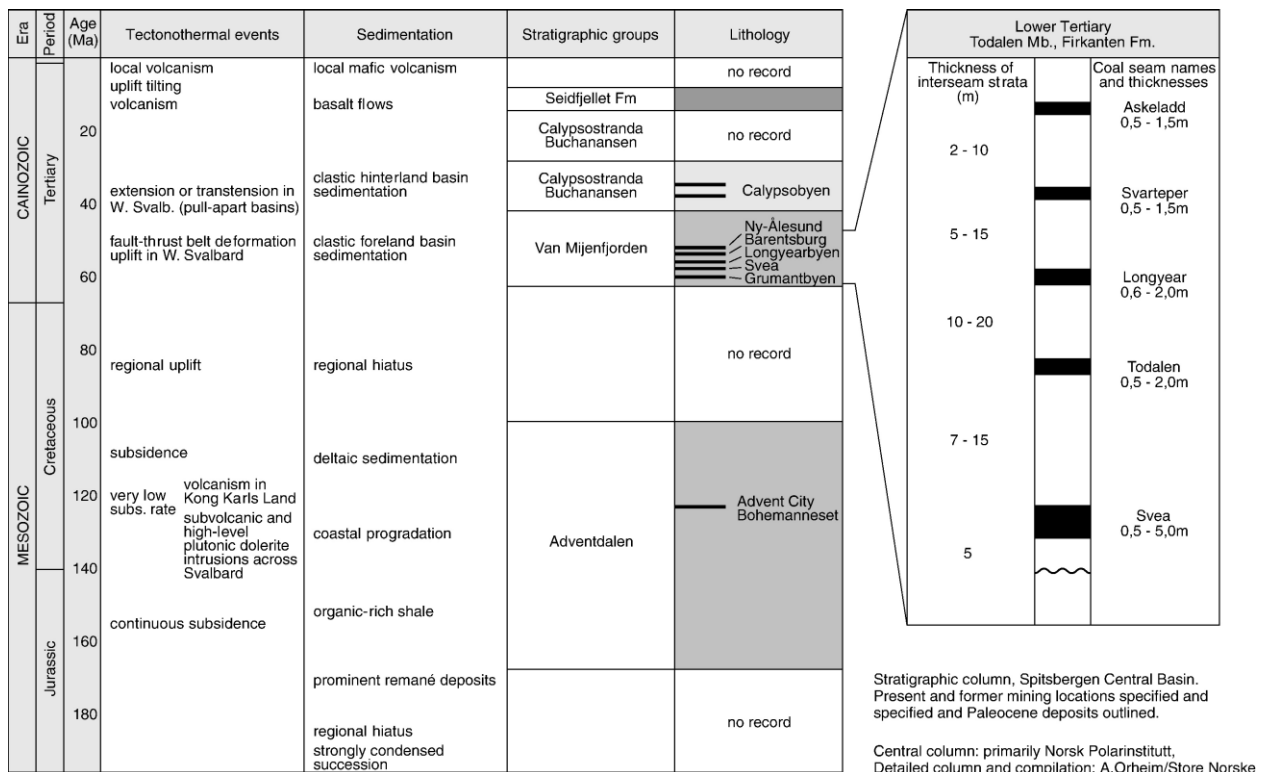


Fig. 2.9. The stratigraphic generalised column of the central basin (Orheim et al., 2007).

The coal samples investigated in this are from the Longyear seam in the Todalen member which is located within the middle part of the central basin.

2.7 The Longyear seam

To achieve an appropriate classification of the Todalen member, (Nagy, 2005) divided the member into lithologic intervals (Fig. 2.12). The Longyear falls into the interval B in this lithostratigraphic division. This interval generally displays a coarsening upward trend which is typical of a barrier back setting probably assembled along a deltaic coastline. These deposits are believed to have been created as a result of rapid deposition in a fresh water depression in a deltaic plain followed by subsequent sea-water flooding during the Paleogene transgression (Nagy, 2005). This process eventually transforms the lake into a brackish coastal lagoon. The presence of foraminifera in this section is indicative of the earliest Paleogene marginal marine incursion of this site. The fauna assemblage is absolutely bound and named *Trochammina* sp.1 after the most common species. However, the faunal diversities within this interval are acutely low and this is attributed to the hyposaline estuarine conditions (Nagy et al., 2011).

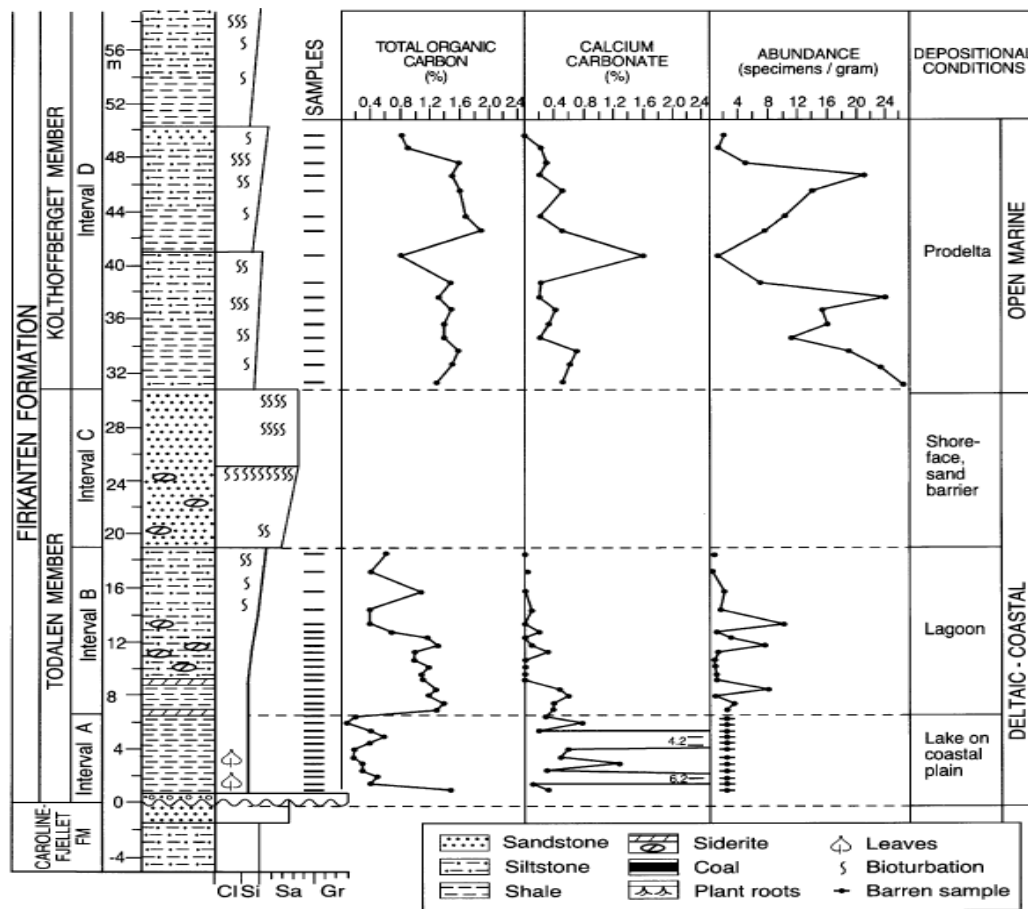


Fig. 2.10. The lithologic section of the Basilikaelva section of the Firkanten formation showing the Todalen member (Nagy, 2005).

The Longyear seam is located right at the middle of the Todalen member. This seam has an average thickness of 1-2 m and is laterally continuous. The total organic carbon (TOC) content is practically low averaging approximately 71% which is the lowest of all the seams at the Basilikaelva section (Dietmar Müller and Spielhagen, 1990). When compared with the Svarteper and the Askeladden coals, the Longyear coals display very little thickness variations and splitting. The lateral continuity and persistent thickness of the Longyear coal seam is as a result of sediment accumulation on a broad, gently subsiding plain typified by extended zones of marsh growth (Hvoslef et al., 1986). This is unlike the Svarteper and Askeladden coals that originated as a result of frequently flooded, mildly undulating delta plains. Although the Longyear is closer in quality to the Svea, the petrographic studies conducted by several workers places the Longyear ahead in quality because of its lower inertinite content. This makes the coals of the Longyear seam of high economic importance (Cmiel and Fabianska, 2004; Dallmann, 1993; Harland, 1998; Orheim et al., 2007).

CHAPTER THREE

EXPERIMENTAL TECHNIQUES AND METHODS

3.1 Experimental techniques

3.1.1 Gas Chromatography (GC)

Gas chromatography separates gaseous and liquid mixtures into individual components allowing each component to be analysed individually. When a sample is injected into the equipment, the sample is vapourised at high temperature and swept through a column by a mobile phase gas (carrier gas), usually an inert gas like helium or hydrogen. Helium and hydrogen are preferred because they facilitate faster separations due to the slow decrease of their chromatographic efficiency with increasing flow rate. The carrier gas forces the injected sample to the stationary phases which are usually polymers or a microscopic layer of liquid. The stationary phases are coated with different materials which will allow samples coming in contact with them to elute at different time known as the retention time of the compound. The interaction between the compounds in a mixture and the stationary phase occur at different rates. These interactions create electrical signals which are detected and sent to a computer for processing. The signals appear on the software in form of chromatograms.

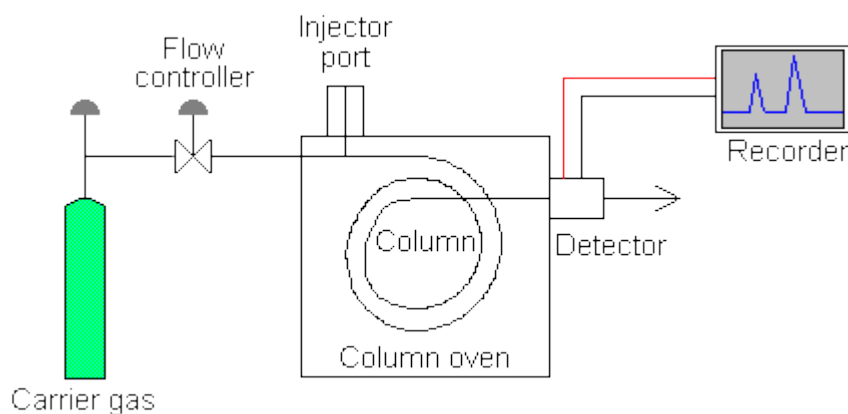


Fig. 3.1. Schematic diagram of a gas chromatograph

3.1.2 Gas chromatography-mass spectrometry (GC-MS)

GC-MS combines the functionality of a gas/liquid chromatogram and a mass spectrometer with the aid of an interface (a device which transports effluents from the gas chromatograph to the mass spectrometer) effectively linking both equipment (Fig 3.2). The gas chromatograph separates a mixture into its components and breaks the individual components into fragments, feeding them into the mass spectrometer which provides information that aids in the identification of the separated components. The chemical and structural information contained in these fragments can be detected either in full scan mode (SCAN) or by selected ion monitoring (SIM). The full scan mode analyses the currents generated by all the fragments of a compound which is proportional to the concentration of that compound in the ionising chamber of the mass spectrometer at that instant. The SIM mode monitors the ion current for a selected mass fragment (m/z) generating a signal value that is characteristic of a particular compound or a group of compounds. The SIM mode is generally more selective and often specific compared to the SCAN. This makes the SIM very useful in trace analysis. The GC-MS technique has been established as one of the most powerful tools for obtaining data on biological markers and isotopes in a petroleum system (Peters et al., 2007).

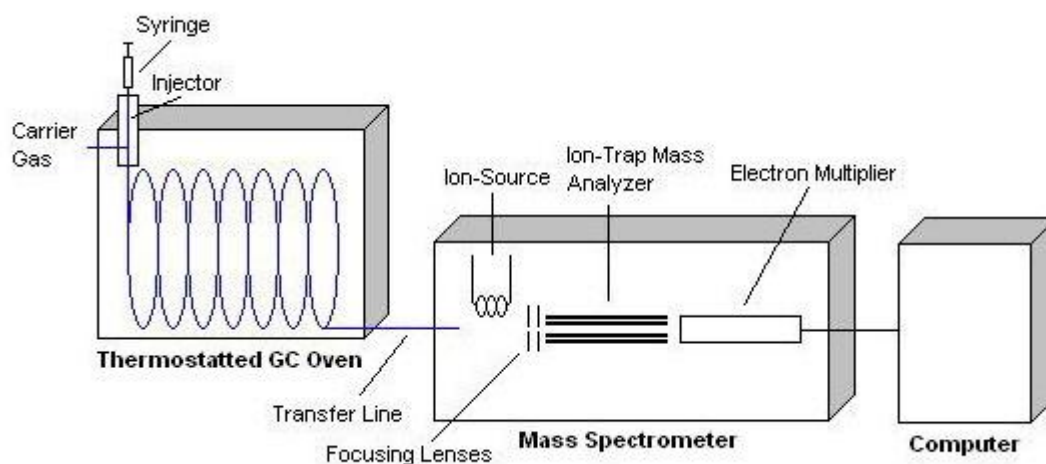


Fig. 3.2. Schematic diagram of the gas chromatograph-mass spectrometer.

3.1.3 Hydrous pyrolysis technique

Hydrous pyrolysis involves the high temperature decomposition of organic samples in an inert environment in the presence of water. This technique is applied by most geochemists to investigate hydrocarbon generation and source rock maturation of petroleum source rocks and coal. Hydrous pyrolysis is used to liberate the liquid and gaseous hydrocarbon constituents from a proven source rock or coal for further analysis.

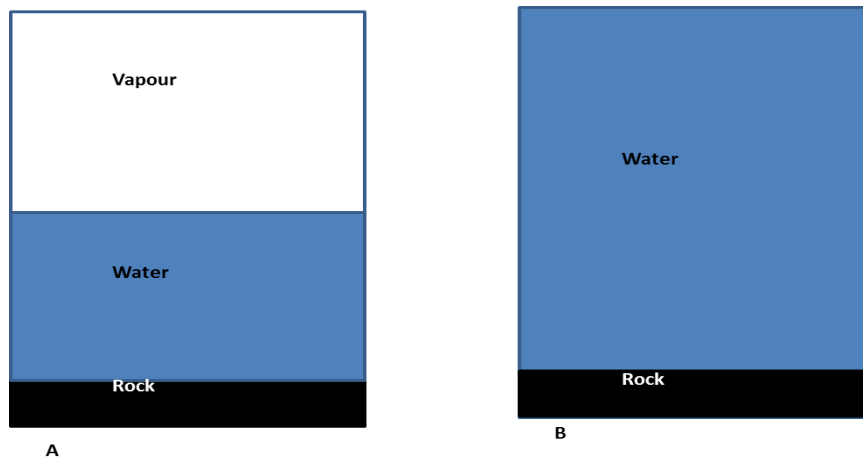


Fig. 3.3. Experimental configurations for the pyrolysis experiments, from (Carr et al., 2009).

The major components of hydrous pyrolysis equipment are the pressure vessel (reactor) and furnace or fluidized sand bath which is used to supply heat to the system. The reactor is designed with stainless steel or hastelloy to withstand very high temperature and pressure. Rock sample and water are introduced into the reactor using one of the configurations in figure 3.3. In one of the configurations, the reactor is totally covered with water and rock sample, leaving no space in the reactor (Fig. 3.3 b). For the second configuration, rock sample and water take up about 85% of the reactor volume leaving some space at the top (Fig 3.3 a). The space remaining is filled with an inert gas prior to the start of experimentation (Carr et al., 2009). For this configuration, vapour and liquid water are operating at experimental temperature.



Fig. 3.4. A typical hydrous pyrolysis experimental setup showing the sandbath, gauge and reactor and temperature controller.

3.2 Experimental methods

3.2.1 Samples studied

Approximately 1.5 m (150 cm) cores of undisturbed coal samples were retrieved from the Longyear seam. Six samples were taken from intervals approximately 23 cm apart for analysis to allow for adequate representation (table 3.1).

Sample Tag	Seam Depth (cm)
10201	5.5
10207	29
10220	66
10226	83
10231	117.5
10241	135.5

Table 3.1. Sample numbering and representation with seam depth.

* Samples above 135.5 cm were observed to have been slightly disturbed and contaminated with overlying organic matter.

The base, middle and top of the seam are represented by two samples each. The coal samples were crushed and sieved to sizes between 0.03 and 0.05 cm for the hydrous pyrolysis experiments. This is to ensure that the coals are in contact with water during the hydrous pyrolysis experiments (Uguna, 2007). However, samples for Soxhlet extraction were crushed to fine powdered form (< 0.001 cm) to aid better extraction. These samples are also used to compare the extraction efficiency of coarse and fine coal samples and the extraction results are recalculated to an average percentage. Approximately 5g of each prepared sample was placed in a new tightly capped vial and stored in a vinyl plastic bag to keep them air and contamination free.

Details of the geochemical characteristics of the Longyear coals prior to hydrous pyrolysis experiments are shown in table 3.2.

Depth (cm)	*HI (mg/g TOC)	*VR (%R_o)	*Vitrinite (%)	*Inertinite (%)	*Liptinite (%)
5.5	314	0.67	71.2	21.2	3.6
29	344	0.70	72.4	19.4	4.4
66	362	0.72	65.6	25.6	4.0
83	352	0.63	84.4	8.0	4.4
117.5	389	0.58	80.4	10.8	4.8
135.5	387	0.56	86.0	6.0	4.8

Table 3.2. The initial geochemical characteristics of Longyear coal

* Approximate value at depth.

3.2.2 Vitrinite reflectance and maceral composition determination

The vitrinite reflectance and maceral composition were obtained using reflected light microscopy with point counts of 100 and 500 for vitrinite reflectance and maceral composition respectively. Reflectance measurements are obtained using the Leitz Ortholux microscope fitted with an MPV control and photometer head. Polished and mounted samples were analysed under white light using 32X oil-immersion objectives and 10X oculars for the maceral composition while the reflectance is obtained using a green filter.

3.2.3 Elemental analysis of the samples

The hydrogen and total organic carbon (TOC) content of the coal sample was determined by combusting the samples in an oxygen-rich atmosphere using the thermo electron flashEA 1112 elemental analyser. The equipment is controlled by the EAGER300 software for windows. The equipment consists of a quartz reactor tube with beds of copper oxide as the oxidizing agent and a copper wire as the reductant. The furnace temperature is held at 900°C before the sample is introduced. When the sample is introduced and the equipment starts, an aliquot of pure oxygen is automatically injected into the reactor to aid flash combustion of the sample organic matter. A steady stream of helium gas (which acts as the carrier gas) is passed through the reactor at a rate of 140 L min⁻¹. The products of this initial reaction (CO₂, H₂O, SO_x and NO_x) are swept from the oxidation stage of the reactor by a stream of helium gas. These gases are reduced to CO₂, H₂O, SO₂ and N₂ in the reducing stage of the reactor and then passed into the GC column for separation. The separated components are quantified by comparing them to similar combustion products of a known standard material. The standard material used for this study was BBOT (2.5 Bis [5-tert-butyl-benzoxazol-2-yl] Thiophene).

3.2.4 Hydrous Pyrolysis

Hydrous pyrolysis experiment was conducted on 1g TOC of pre-extracted coal sample (1g TOC weight equivalent of sample was calculated from the TOC content of immature coals) at 350°C for 24 hours. Prior to heating, the sample was introduced into the Parr 4740 series hastalloy cylindrical pressure vessel with a 22 ml capacity (Fig. 3.5). 15 ml of distilled water is added to the reactor after which the reactor was assembled and connected to the pressure gauge rated to 690 bar (Fig 3.6). The reactor is flushed with nitrogen after which nitrogen is pumped into the reactor at 2 bar pressure. This is to produce a relatively inert atmosphere during the experiment. The volume of nitrogen eventually retained in the system is measured after trapping the nitrogen for 1 minute.

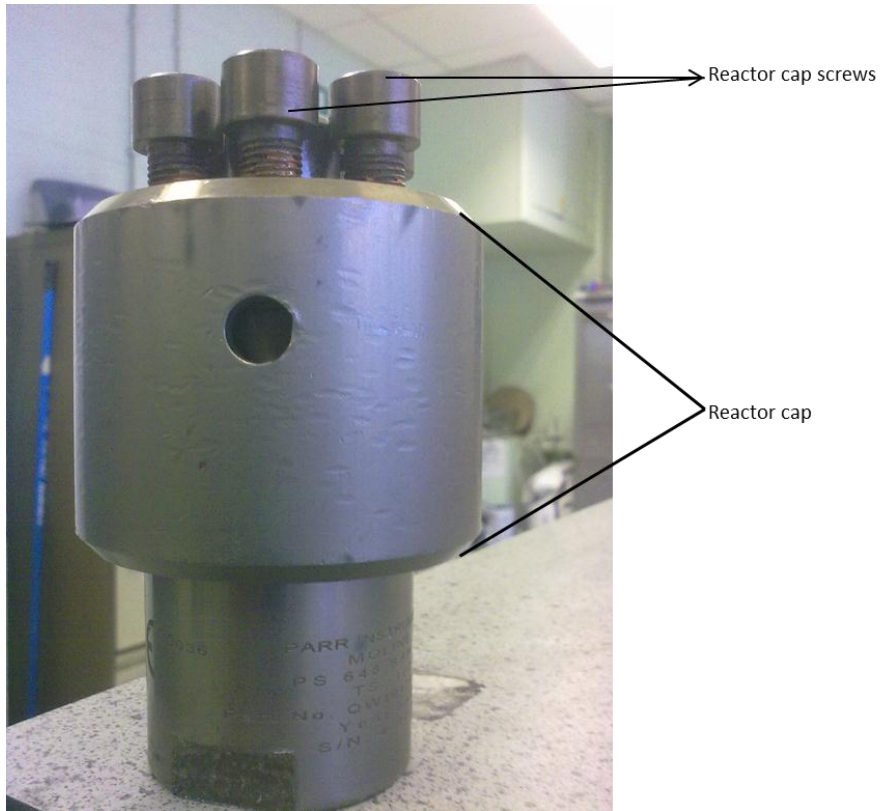


Fig. 3.5. The Parr 4740 series hastalloy cylindrical reactor vessel

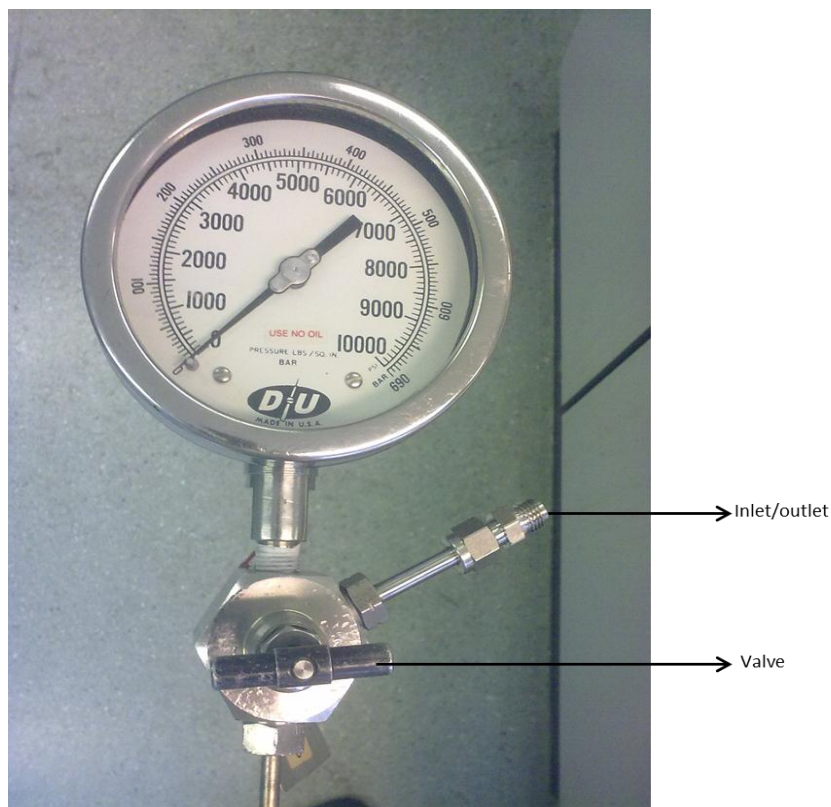


Fig. 3.6. Pressure gauge showing the inlet/outlet and valve.

The assembled reactor was then lowered into a pre-heated fluidised sand bath controlled by an external temperature controller. During the experiment, the reaction temperature is also monitored every 10 seconds by an additional K-type thermocouple connected to a computer. The average temperature of the experiment is recorded from the computer software just before the experiment is turned off. When the standard experimental time has elapsed, the sand bath is turned off and the reactor is allowed to cool to ambient temperature before product recovery.

3.2.5 Recovery and analysis of generated gas

The gas generated during the pyrolysis experiment was collected using a gas tight syringe and immediately transferred to a gas bag for analysis. Analysis of the gas is done on a Carlo Erba HRGC 5300 gas chromatograph fitted with FID and TCD detectors operating at 200°C and 180°C respectively. Hydrocarbon gases were determined by FID using a Chrompak CPPorapakplotQ capillary column (with a 27.5 m x 0.32 mm, 10µm film thickness) by injecting 10 µl of gas sample. Helium was the carrier gas used and an oven temperature programme of 70°C (hold 2 min) to 90°C (3 min) at 40°C min⁻¹, then to 140°C (3 min) at 40°C min⁻¹ and finally to 180°C (49 min) at 40°C min⁻¹. Individual gas yields were determined quantitatively in relation to an external gas standard (pure methane gas was used for this study). On completion of the experiment, the chromatograms produced are analysed for gas areas which are used to calculate individual gas volumes.

3.2.6 Recovery generated bitumen

The reactor vessel dismantled following gas collection and the water in the vessel is carefully decanted into a glass beaker. The Samples retained in the pressure gauge are forced out into a beaker by repeatedly injecting dichloromethane (DCM) into the gauge. The reactor vessel and coal residue collected in a beaker are transferred to a vacuum oven to dry at 45°C for 3 to 4 hours. The dry coal sample is then transferred to a pre-extracted cellulose thimble for soxhlet extraction and the vessel is rinsed with DCM to recover any product attached to the vessel wall. The reacted coal sample was extracted using a 250ml dichloromethane (DCM)-methanol mixture (93:7 vol/vol) for 72 hours. The dichloromethane-methanol mixture is separated from the generated bitumen using a rotary evaporator and the extracted bitumen transferred into a pre-weighed vial and allowed to evaporate. The coal residue is allowed to dry properly in a fume cupboard, weighed, and transferred to a tightly capped vial for TOC content analysis.

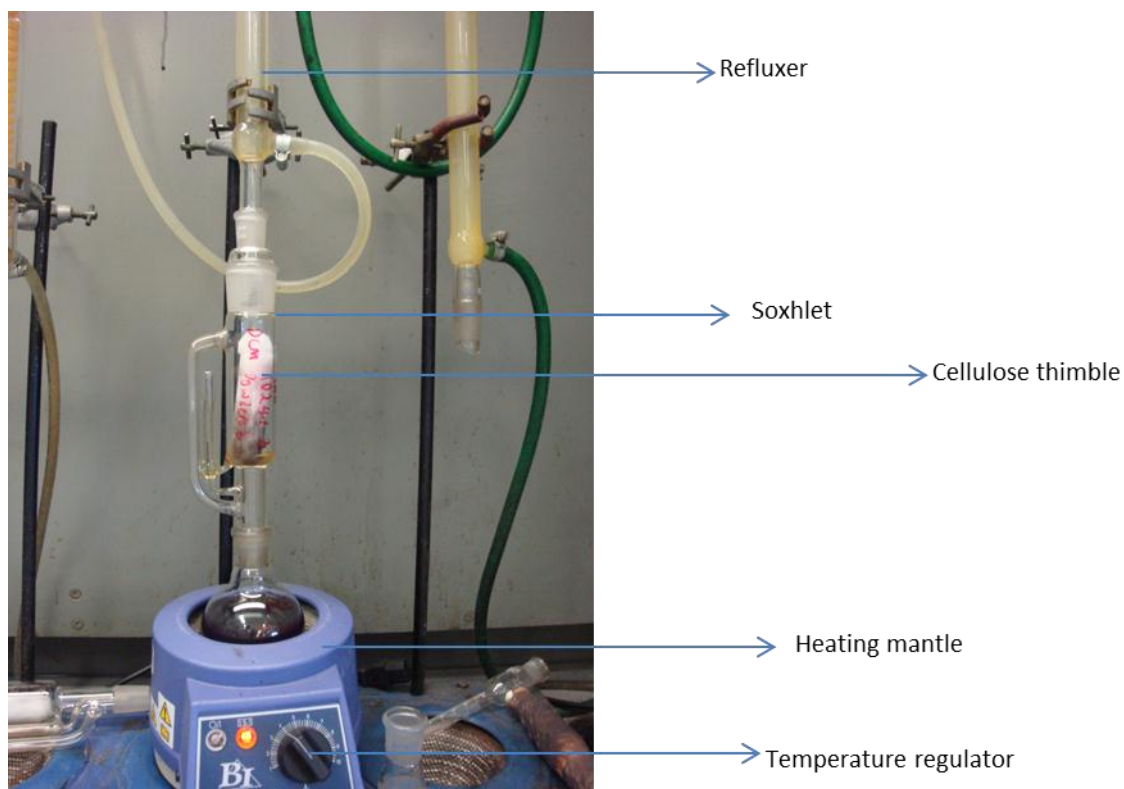


Fig. 3.7. Soxhlet extraction setup

3.2.7 Separation of bitumen into fractions

Bitumen yields before and after hydrous pyrolysis is separated into their aliphatic, aromatic and polar fractions using silica - alumina (ratio 1:4) adsorption column chromatography. The bitumen to be fractionated is absorbed onto clean silica (about 0.8g), which is then introduced into the packed column. The aliphatic fraction was eluted using 15ml *n*-hexane while the successive addition of 15ml *n*-hexane/DCM mixture (9:6 vol/vol) and 15ml DCM/methanol mixture (7.5:7.5 vol/vol) was used to elute the aromatic and polar constituents respectively. The eluted fractions are collected in a pre-weighed vial and the solvent allowed to evaporate leaving the fractions in the vial. The weight of each fraction is obtained and the fractions transferred to properly labeled GC- vials and stored in the refrigerator for further GC-MS analysis.

3.2.8 Gas chromatography mass spectrometry (GC-MS) analysis of aliphatic fractions

The gas chromatography-mass spectrometry analysis of the aliphatic hydrocarbon fractions was performed using a Varian CP-3800 gas chromatograph interfaced to a 1200

Quadrupole mass spectrometer (Electron ionisation mode, 70eV, source temperature 280°C). A VF-1MS fused silica column (50 m x 0.25 mm i.d., 0.25 µm thickness), with helium as the carrier gas used to achieve separation. An oven programme of 50°C (hold 2 min) to 450°C (hold 33 min) at 5°/min was used. The aliphatic fractions were diluted with 0.3 mL of dichloromethane and 1666 ng of cholane was injected into the samples to serve as an internal standard. Analyses were performed in both full scan (m/z 50 – 450), selective ion response (SIR) modes (ions – m/z: 69, 71, 113, 149, 151, 177, 183, 191, 205, 217, 218, and 259 monitored).

CHAPTER FOUR

RESULTS AND DISCUSSION

Results from experiments conducted will be used to investigate evidences of petroleum generation and migration within the Longyear seam. Hydrous pyrolysis and initial coal extract yields will be useful in determining the generative capacity for the coal seam. This will be backed up with other petroleum generation and maturity parameters like vitrinite reflectance, hydrogen index, elemental and maceral composition. Aliphatic aromatic and polar fractions from the pyrolysis and initial coal extract yields will also serve as clues to the composition of the bitumen and will also be used to examine the maturity and source of the bitumen present in the coal as well as petroleum migration within the coal seam.

4.1 Elemental composition of Longyear coal

Figure 4.1 shows the hydrogen contents of the initial Longyear coal samples.

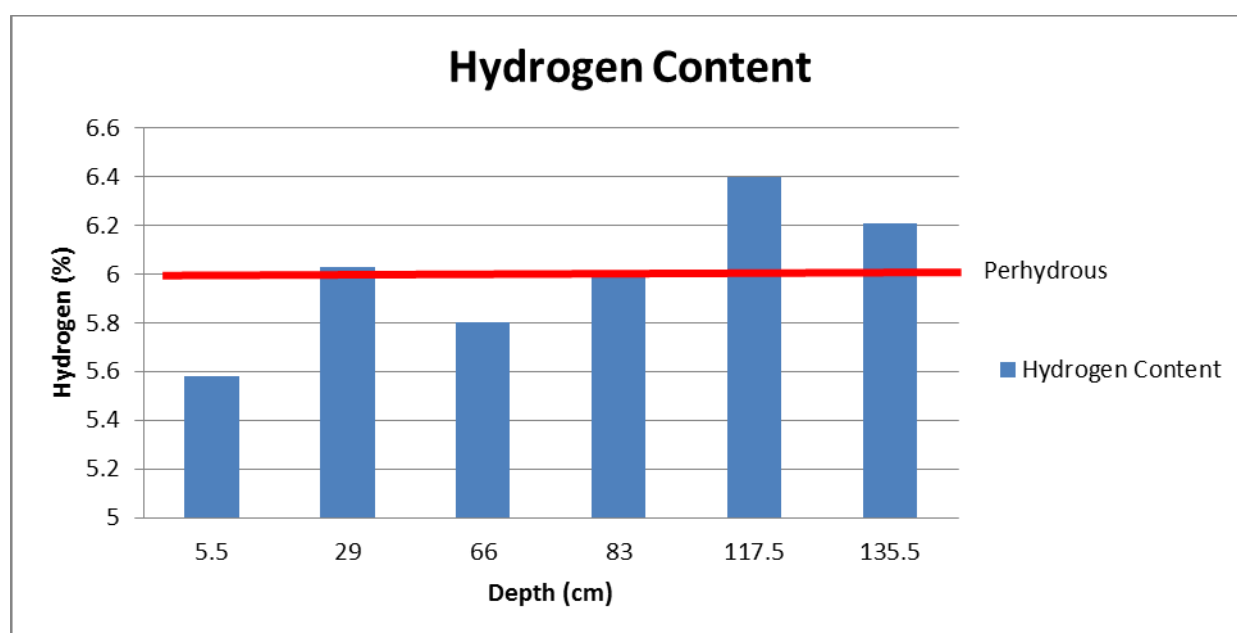


Fig. 4.1. Hydrogen content of initial Longyear samples at different depths showing the perhydrous line.

The average hydrogen content across the seam is 6% confirming the perhydrous nature of the Longyear coal. However, the upper portion of the seam is characterised by a higher hydrogen content of 6.4% compared to basal portion of the seam which recorded

a hydrogen content of 5.6%. The relatively high hydrogen content of the Longyear coals is due to the abundance of perhydrous vitrinites which has been reported by (Cmiel and Fabianska, 2004). According to Teichmuller (1987), the presence of the perhydrous vitrinites causes the coal organic matter to resemble type II organic matter. This is due to the incorporation of lipids within the biopolymer derived from plant materials (lignin, cellulose or tannings) which affects the chemical structure, properties and behavior of perhydrous vitrinites, enabling them to expel petroleum-like products. This ultimately affects the ability of such coals to generate and expel liquid hydrocarbons.

Figure 4.2 B shows the general hydrogen content trend within the seam. The seam displays a gradual enrichment of hydrogen from the bottom to the top of the seam with a sharp decrease at the middle of the seam (around 80cm). Marshall et al. (2011) attributed this decrease to a change in early peatland conditions from raised bog to fen at this portion of the seam. This reduction at the middle of seam could also be due to the deposition of a lamina of fine-grained mudstones or other organic debris. The increase in hydrogen content up-seam could be an indication of the trend of hydrocarbon generation through the seam. The vitrinite reflectance decreases up-seam in an opposing manner to the hydrogen content (Fig. 4.2 A). This reduction is due to the suppression of VR values by the hydrogen content of these samples. The suppression of vitrinite reflectance values by the hydrogen rich components of coals has previously been reported by (Diessel and Gammidge, 1998). The vitrinite reflection reduction in the Longyear coal was previously observed by (Orheim et al., 2007).

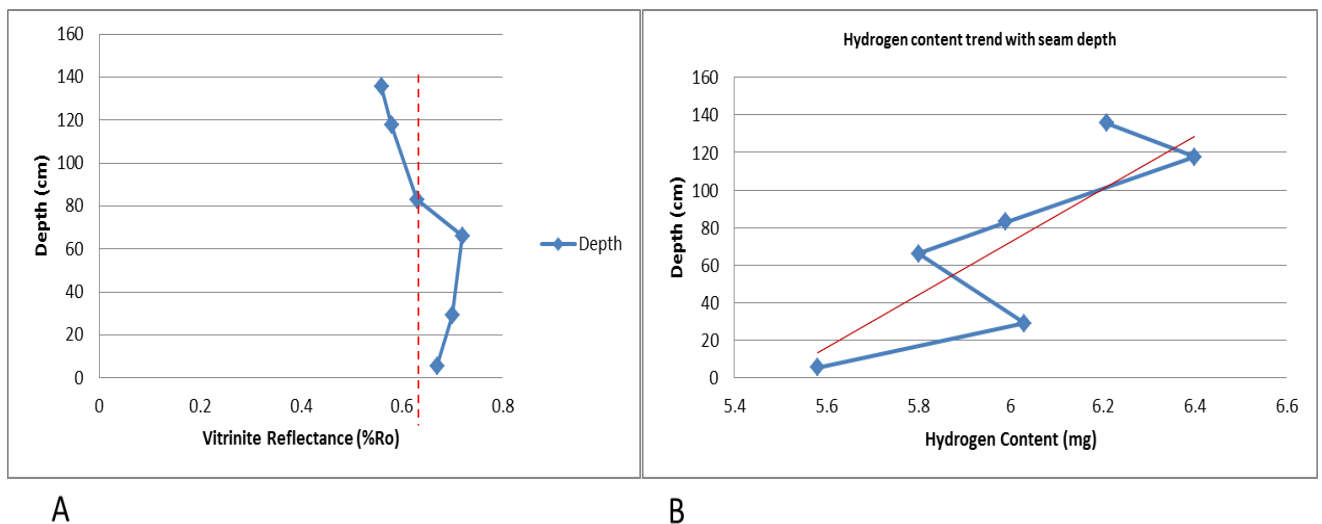


Fig. 4.2 A. The vitrinite reflectance profile of the Longyear seam. Red line showing the mean VR of 0.64% (B) The hydrogen trend of the Longyear seam.

Hydrogen content is not a definitive tool for determining petroleum generating capacity of coals because hydrogen enrichment may be as a result of impregnation of secondary bitumen from the seam surroundings or the inclusion of oil stained particles from other sediments. This is not the case in the Longyear coals because of the slight difference (average of 0.36%) in hydrogen content between the pre-extracted and post extracted samples (table 4.1). An average difference of 0.36% across the seam is negligible bearing in mind that some hydrogen would be lost while stripping off the mobile phase bitumen from the coal during the extraction of bitumen

Depth (cm)	Hydrogen Fresh (%)	Hydrogen extracted (%)	Hydrogen Pyrolysed (%)
5.5	5.58	5.24	4.44
29	6.03	5.70	4.82
66	5.80	5.52	4.59
83	5.99	5.75	4.64
117.5	6.41	5.93	4.76
135.5	6.21	5.69	4.72

Table 4.1. Hydrogen content of Longyear coal at various stages of experimentation.

The hydrogen content of the seam is also fairly consistent values with maturity (after pyrolysis) as seen from table 4.1. This is because the high temperature pyrolysis leads to the uniform degradation of hydrogen rich components within the coals (Iglesias et al., 2002).

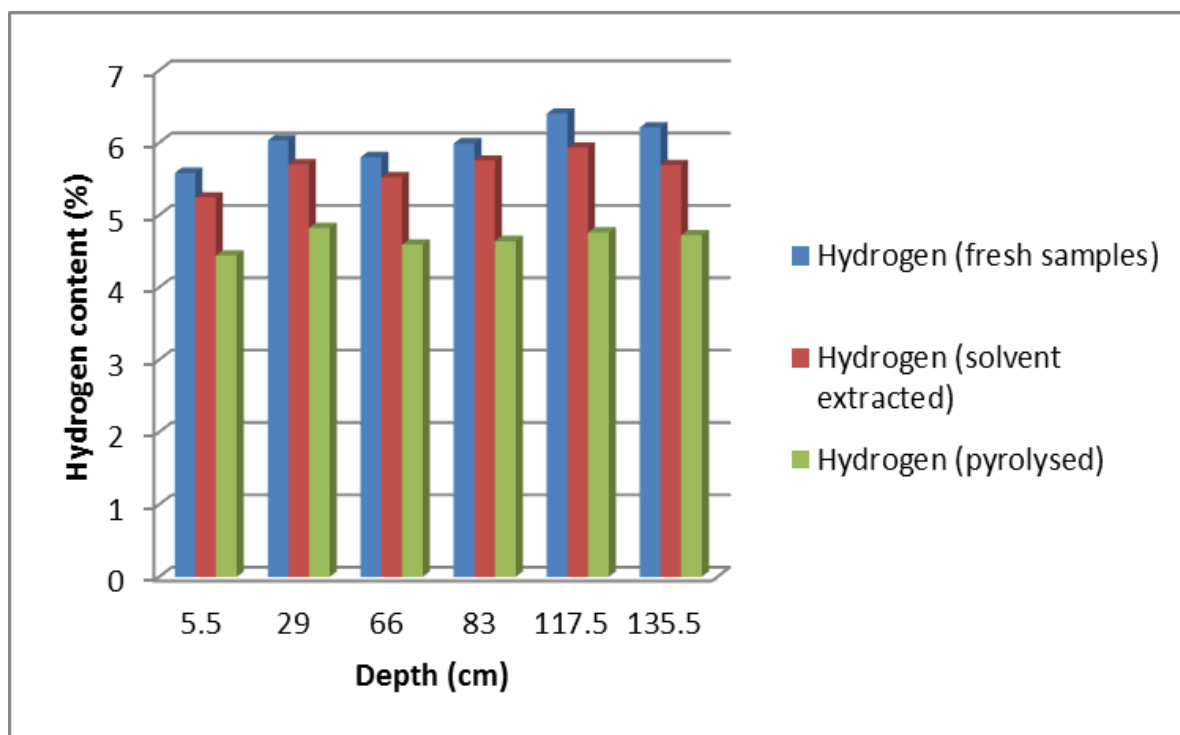


Fig. 4.3. Hydrogen content of the Longyear coal samples showing a decrease in hydrogen content with hydrocarbon generation.

The total organic carbon (TOC) content of the fresh Longyear coal samples fall between the range of 80.07% - 82.66% which is fairly consistent with the 81% - 83.05% range reported by Cmiel and Fabianska (2004) for the Longyear coals. An average of 3.5% decrease in TOC values was observed after solvent extraction. This is due to a carbon loss associated with the loss of hydrocarbons from the coal. After pyrolysis, the TOC values increase when compared with the solvent extracted samples. This is expected because during the process of coalification (which occurs during pyrolysis), there is a net increase in carbon content with rank. Similar TOC values are observed between the fresh samples and the mature samples with the only inconsistency at 117.5 cm probably due to residual bitumen trapped in the sample. The proximity in TOC values is an indication of the similarity in rank between the fresh and the mature samples.

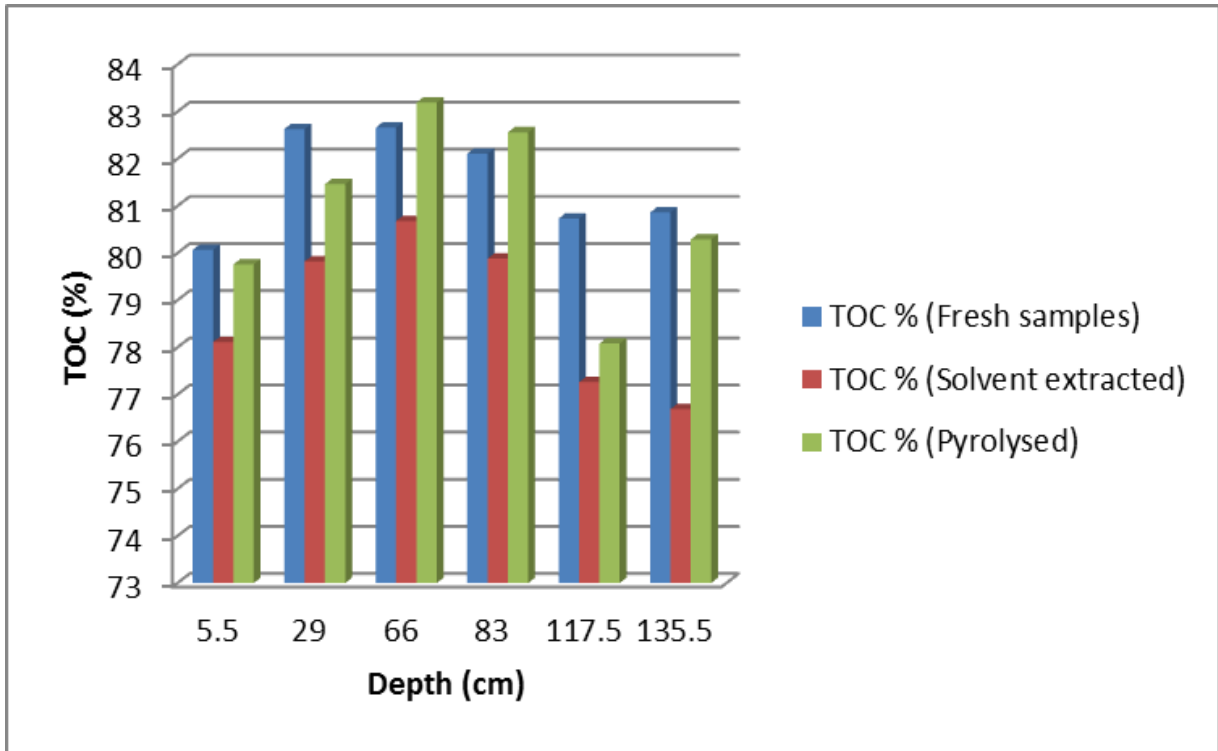


Fig. 4.4. Changes in the TOC content change with depth of Longyear coals at various stages of simulated maturity

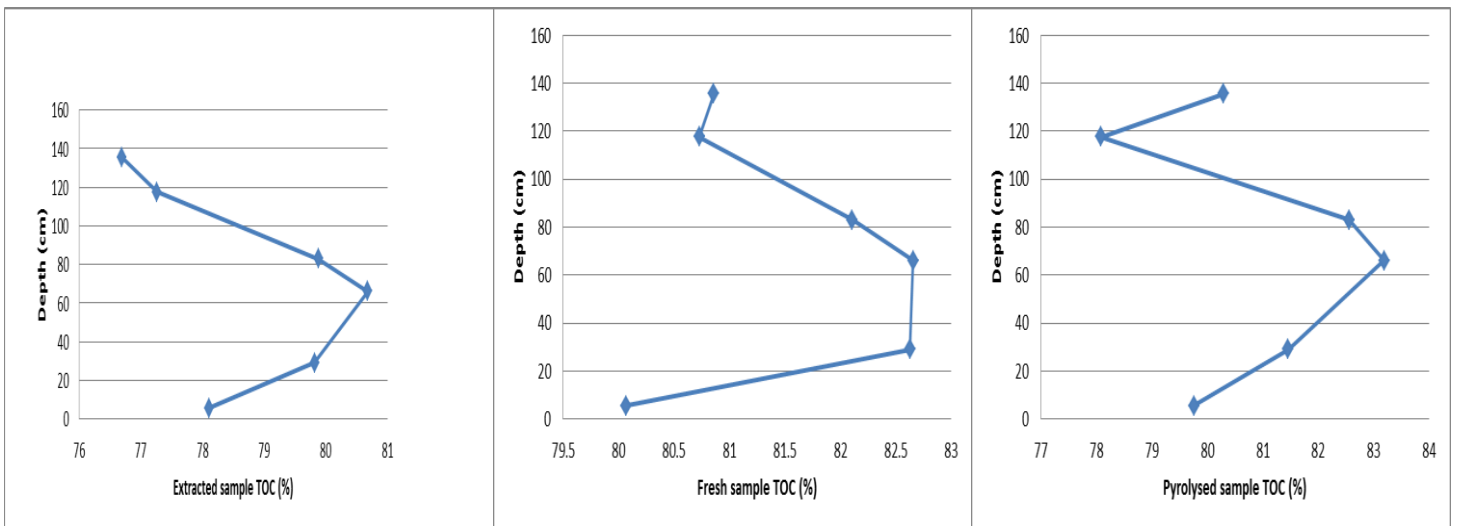


Fig. 4.5. TOC content change with depth of the Longyear coals at various stages of simulated maturity.

The Longyear coals show a general increase in TOC from the bottom of the seam to a peak at the middle of the seam and then start to decrease towards the upper portion of the seam (Fig. 4.5). Several scientists have previously correlated such decreases in TOC with an increase in hydrocarbon generation (Boreham and Powell, 1991; Cooles et al., 1986). The most probable reason for the decrease in TOC of Longyear coals is the loss

of carbon in form of free-oil carbon in the samples that have yielded more hydrocarbons. The TOC content of the Longyear coals falls within the range of some other proven oil prone coals like those found in the Cooper and Taranaki basin (Curry et al., 1994).

4.2 Gas yields

The individual and total ($C_1 - C_4$) hydrocarbon yields generated from hydrous pyrolysis are shown in Fig. 4.6. The range of gas generation for the Longyear coals after pyrolysis at 350°C fall between 5.74 – 9.93 mg/g TOC (Fig. 4.6). The maximum value for gas generated in this study is much lower than marine source rocks like the Kimmeridge clay (24.06 mg/g TOC at 350°C) which is renowned for its accumulation of commercial quantities of natural gas (Carr et al., 2009). However, it is believed that coals will generate greater amounts of gas at higher thermal maturity. Although there is little information available on the quantitative features of gas generation with relation to maturity, Powell et al. (1991) were able to relate the abundance of gas fractions (C_1 - C_4) from the Walloon coal measures with an increase in maturity. Highest gas yield was observed towards the top of the seam and also corresponded with the very higher hydrogen content of the coals and lower TOC. The general trend of gaseous hydrocarbon yields shows an increase from the bottom to the top of the seam (Fig. 4.7). The prolific gas generation of the Longyear coal can be compared to the tertiary Australian coals of the Cooper basin reported by (Vincent et al., 1985). At a thermal maturity similar to that simulated in the Laboratory, the Longyear coals could have sourced some of the commercial gas accumulations in the Barents Sea (that lies between 74°30'N and Spitsbergen).

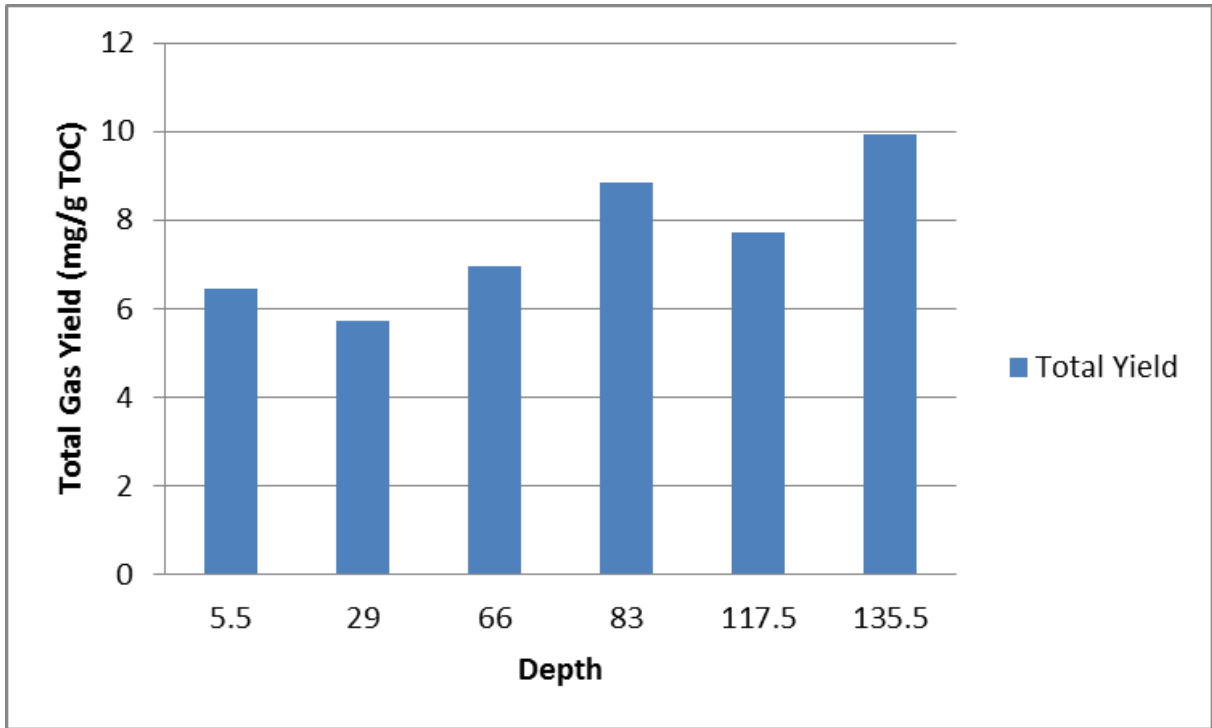


Fig. 4.6. Total gas yields of the Longyear seam at various depths.

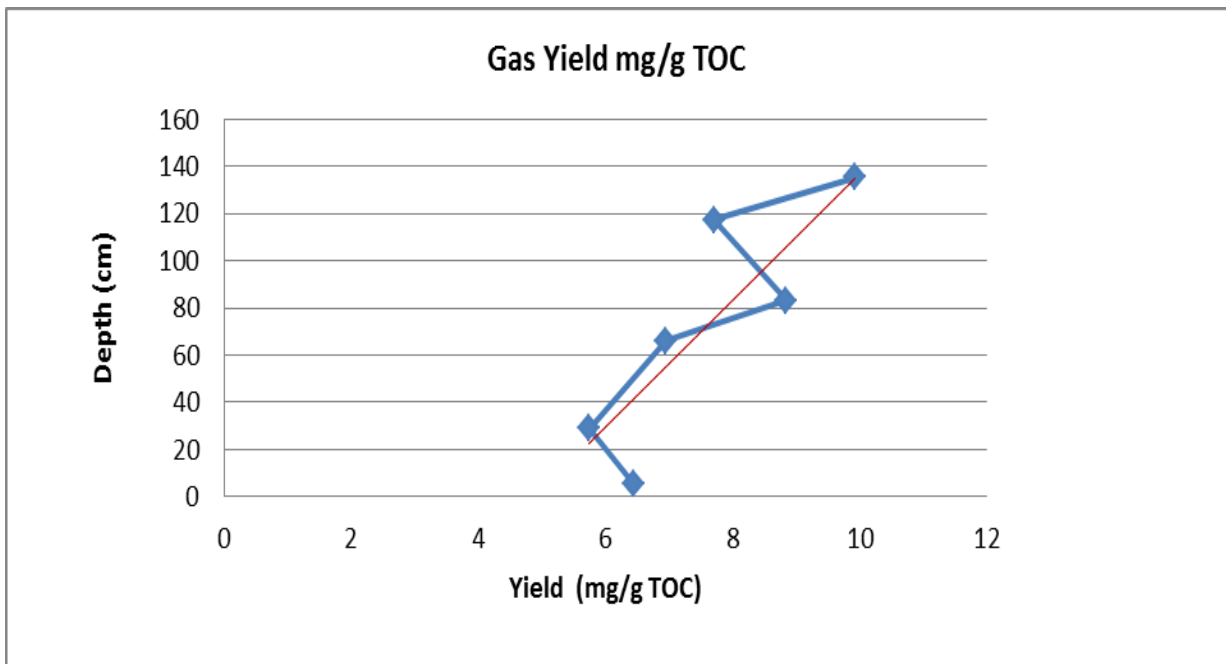


Fig. 4.7. Changes in generated gas yields with depth of the Longyear seam

On an individual gas component basis, the methane (CH₄) yield of the generated gas was highest with the alkanes generally dominating the alkenes (Fig. 4.8). Information on the gas to oil ratio and the gas composition is generally useful in assessing migration within a sequence (Hunt, 1979).

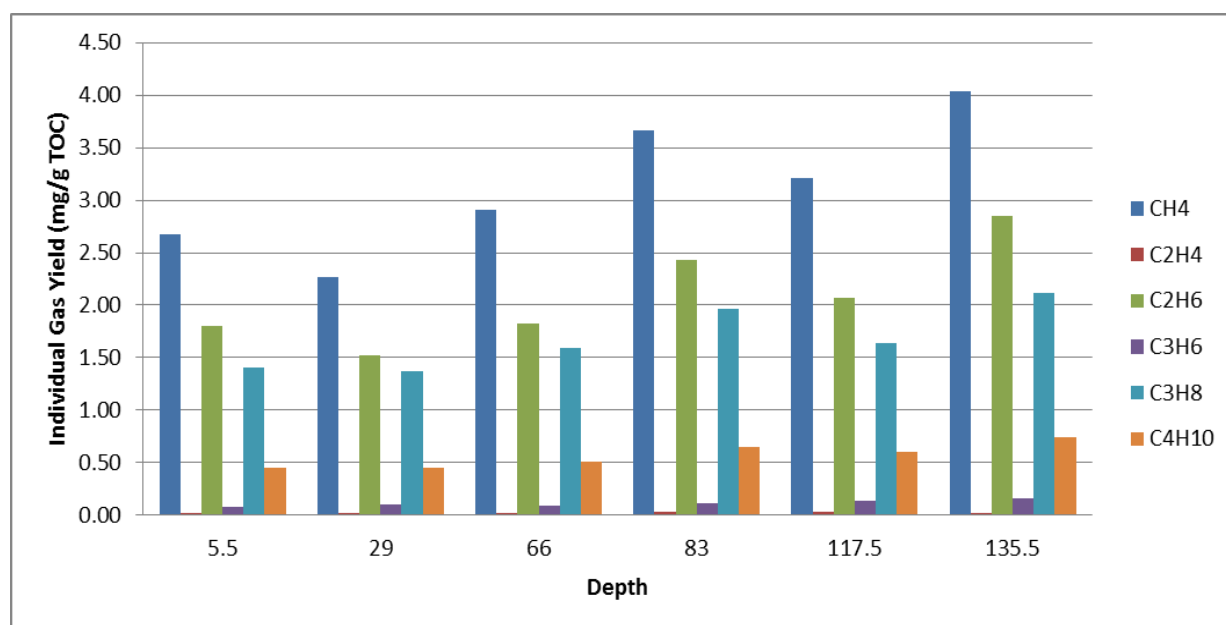


Fig. 4.8. C₁-C₄ gas fractions of the Longyear coals at different depths.

The dominance of low molecular weight gases is due to their small molecular weights and the ease with which they will be generated during the simulation of maturation. Zhao and Cheng (1998) have previously attributed the formation of low molecular weight volatiles to the cracking of larger hydrocarbons trapped within coals.

4.3 Bitumen yields

Initial coal bitumen yields ranged between 3.5% – 11% within the seam for the coarse (0.03-0.05 cm) Longyear coal samples. Solvent extraction was carried out on coarse and fine coal samples to compare to their extraction efficiency, but coarse samples are used for hydrous pyrolysis experiments. Powdered samples showed a 1.63% average increase in extract yields compared to the coarse samples through the seam (Fig.4.9). An increase in surface area is responsible for the increase in bitumen yield.

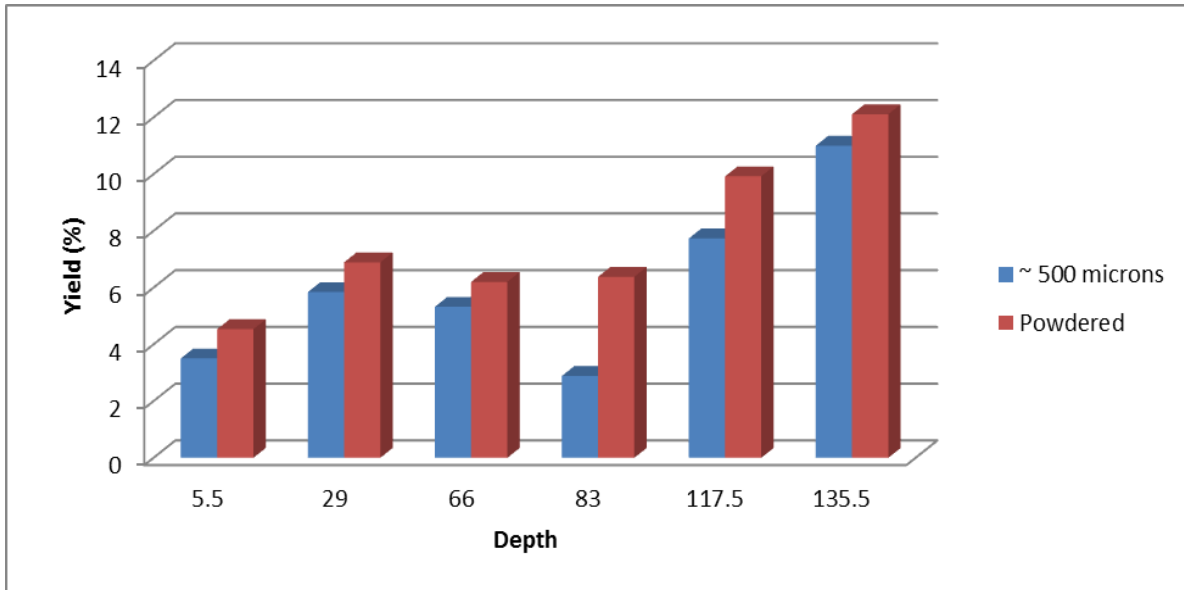


Fig. 4.9. Bitumen yields from extracted Longyear coal samples at different sample sizes

The bitumen yield generally increased from the bottom to the top of the seam with the lower portion of the seam (0-80 cm) showing variable increases with a maximum yield of approximately 6% and the basal contact yielding 4% (Fig. 4.10).

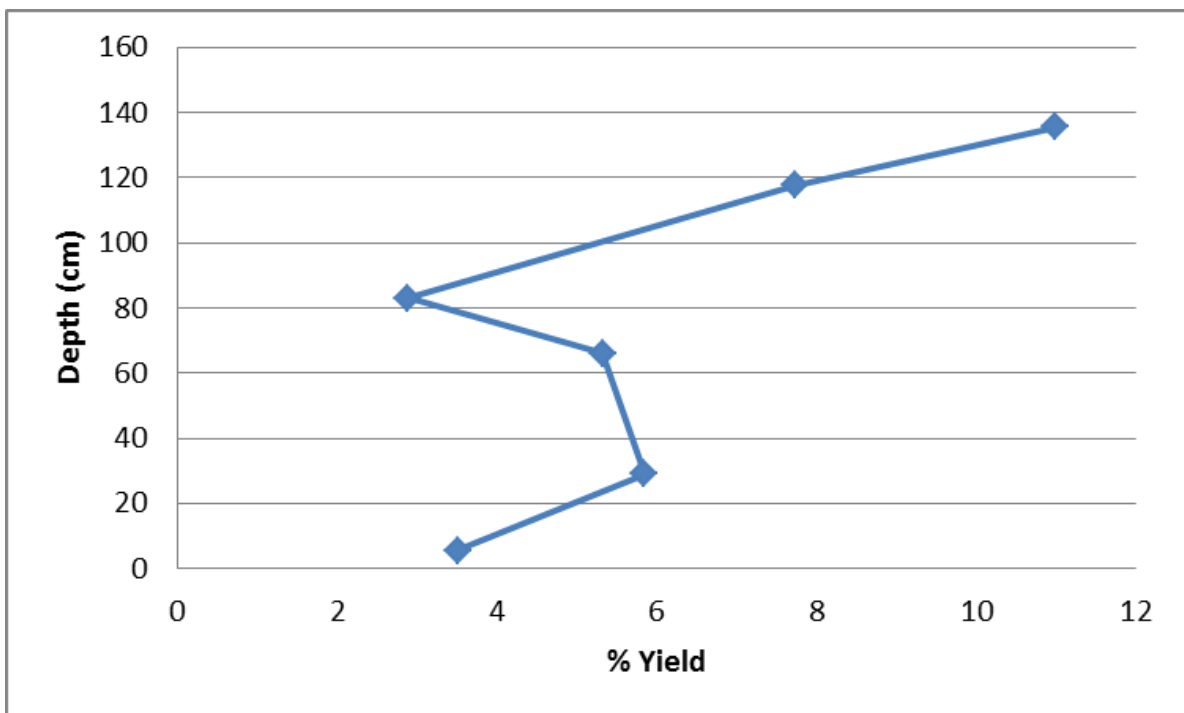


Fig. 4.10. Changes in bitumen yield with seam depth.

The reduction around the central portion of the seam coincides with that observed in the hydrogen content trend plot. The upper portion of the seam (80 – 140 cm) is characterised by a steady increase in bitumen yield attaining a maximum yield of 11% at about 135.5 cm. Beyond this point, the extractable yields decrease sharply (Appendix A1). This sharp decrease is due to lithologic changes and mixtures with other foreign materials as the seam thins out. Changes in concentration of bitumen from the top to the bottom of the seam can be a sign of liquid hydrocarbon migration within the seam. However, further evidence is required before migration can be inferred. Migration of liquid hydrocarbons from coal occurs under very stringent conditions and in the presence of abundance of bitumen (Huang, 1999; Huc and Hunt, 1980; Wilkins and George, 2002).

The bitumen yields from hydrous pyrolysis of the pre-extracted Longyear samples are shown in figure 4.11. A maximum yield of 22.5% (292mg/g TOC) was attained at the upper portion of the seam with the base recording the lowest bitumen yield of 15.26%. General trends resemble that of initial coal extract with yields increasing up the seam. Hydrous pyrolysis yield is an indication of the remaining generative potential of the coal and is function of the initial quality of the kerogen. Initial kerogen quality is assessed from the hydrogen index of the samples. Close examination of the total bitumen yields (initial coal yield plus pyrolysis yield) show that there is an increase from the bottom to the top of the seam. Total bitumen yields range from 18.76% - 31.6% (240-404 mg/g TOC).

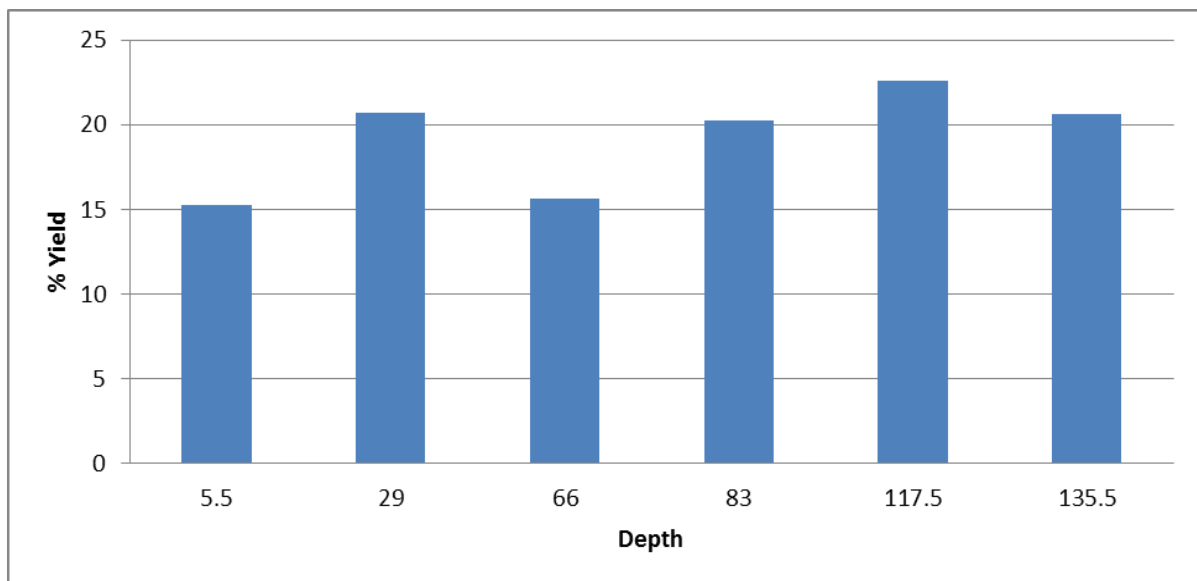


Fig. 4.11. Hydrous pyrolysis yields from Longyear coals samples at various depths.

The ability to generate bitumen during laboratory simulation experiments suggests that this coal will generate petroleum like products when subjected to similar temperature and pressure conditions in a geologic basin. The total (pyrolysis and initial coal extract) maximum yield for the Longyear coal came to 408 mg/g TOC at 350°C for 24 hours (table 4.2).

Depth (cm)	Yield (mg/g TOC)					
	5.5	29	66	83	117.5	135.5
Soxhlet	44.80	73.20	65.90	36.0	100.1	139.70
Pyrolysis	195.4	259.0	193.60	253.0	292.10	268.70
Total	44.80	332.10	259.50	289.0	392.20	408.40

Table 4.2. Total bitumen yield of each sample

The bitumen yield from the Longyear coal is significantly lower than common marine source rocks like the type II Kimmeridge clay which generated approximately 765 mg/g TOC of bitumen plus oil at 350°C for 24 hours (Carr et al., 2009). This is because of the ability of these source rocks to generate and expel liquid petroleum at lower temperatures than coals, which is as a result of the source rocks being more reactive and of higher starting HI than the Longyear coal. However, coals being less reactive could generate higher volumes of bitumen during higher temperature simulations (depending on their starting HI). This has been investigated and found to be the case (Horsfield et al., 1988; Tissot et al., 1987). Snowdon (1991) also noted that coals that exhibit high resinite (Liptinite) content which is labile in nature would generate high yields of liquid hydrocarbons at relatively lower temperatures.

Oil generation within the Longyear seam is far from uniform. The coal samples at the upper portion of the seam (117 – 140 cm) display a more constant and prolific generating capacity when compared with the basal portions. The increase in bitumen generation of each portion of the seam coincides with an increase in HI (Fig. 4.12). This is an indication of higher bitumen generation with improved kerogen quality. The increasing portions of the bitumen generation curve are also matched with decreases in TOC content. Simple material balance considerations would indicate that the loss of carbon (hydrogen and oxygen as well) would lead to the liberation of carbon and hydrogen rich molecules. Powell et al. (1991) attributed such increased carbon losses to a greater generating capacity.

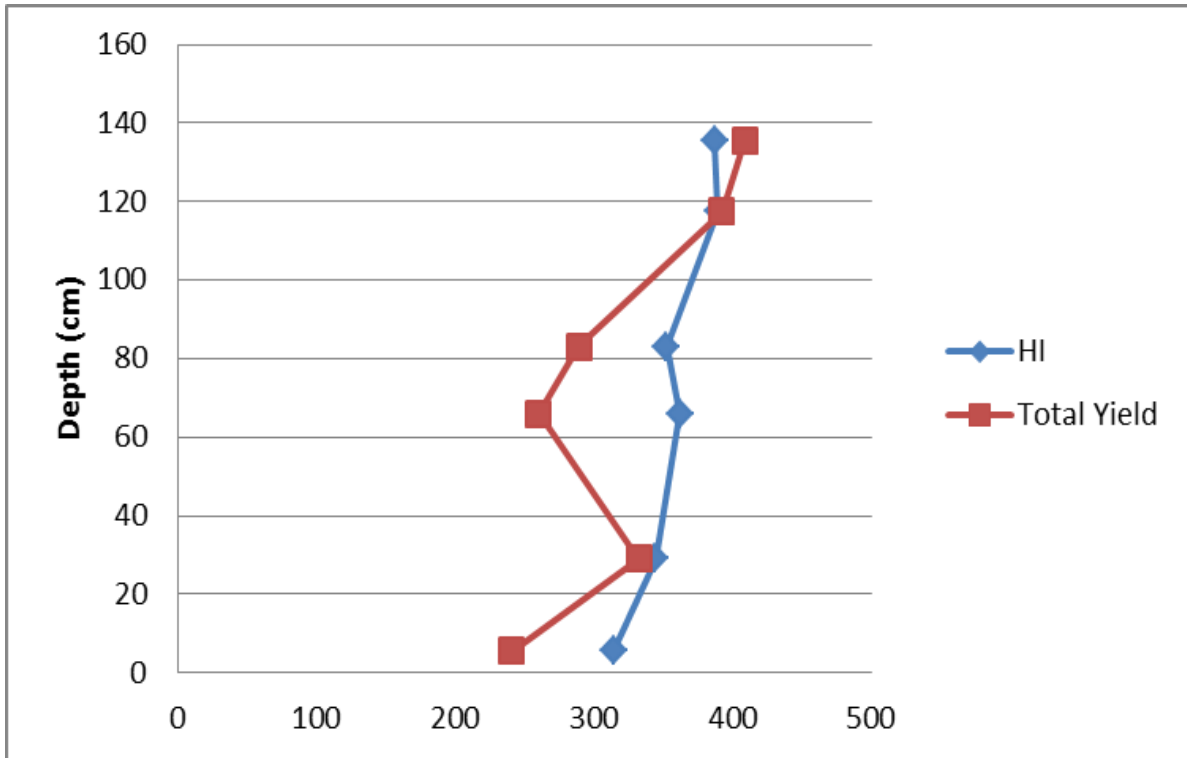


Fig. 4.12. Comparism between HI and bitumen yield of the Longyear coal samples. The figure shows a relative increase in bitumen yield with increasing HI.

Despite the impressive hydrocarbon yields of the Longyear coals, the threshold liquid hydrocarbon concentration at which migration of hydrocarbons within the seam would occur remain ambiguous and difficult to predict. Thus the question of the lower limit of pyrolysable hydrocarbon yield for which these coals would act as effective source rocks for waxy oil is difficult to answer since this depends mainly on the migration mechanism and generative capacity of the coal. However, it is possible to make some general observations based on suggestions by Powell et al. (1991), that close examination of the composition of oil generated could help predict migration within and out of a sequence. These observations could only be made after careful examination of the composition of the generated bitumen.

4.4 Bitumen composition

Table 4.3 shows the percentages of the aliphatic, aromatic and polar fractions present in the bitumen at various depths.

Depth (cm)	Extracted Bitumen composition (%)					
	5.5	29	66	83	117.5	135.5
Aliphatics	11.42	13.01	11.97	12.36	6.06	6.10
Aromatics	33.46	30.14	25.70	42.18	35.93	24.41
Polar	38.98	52.05	51.06	30.55	42.86	52.20

Table 4.3. Percentage composition of fractions in initial the coal bitumen at various depths.

A graphical representation of this table (Fig 4.13) shows a clear dominance of polar and aromatic compounds throughout the seam. This initial polar dominance is truncated at the middle portion of the seam with the aromatic compounds dominating. This truncated region coincides with the portion where changes in TOC and hydrogen content occurred and it supports evidence of paleoenvironmental change.

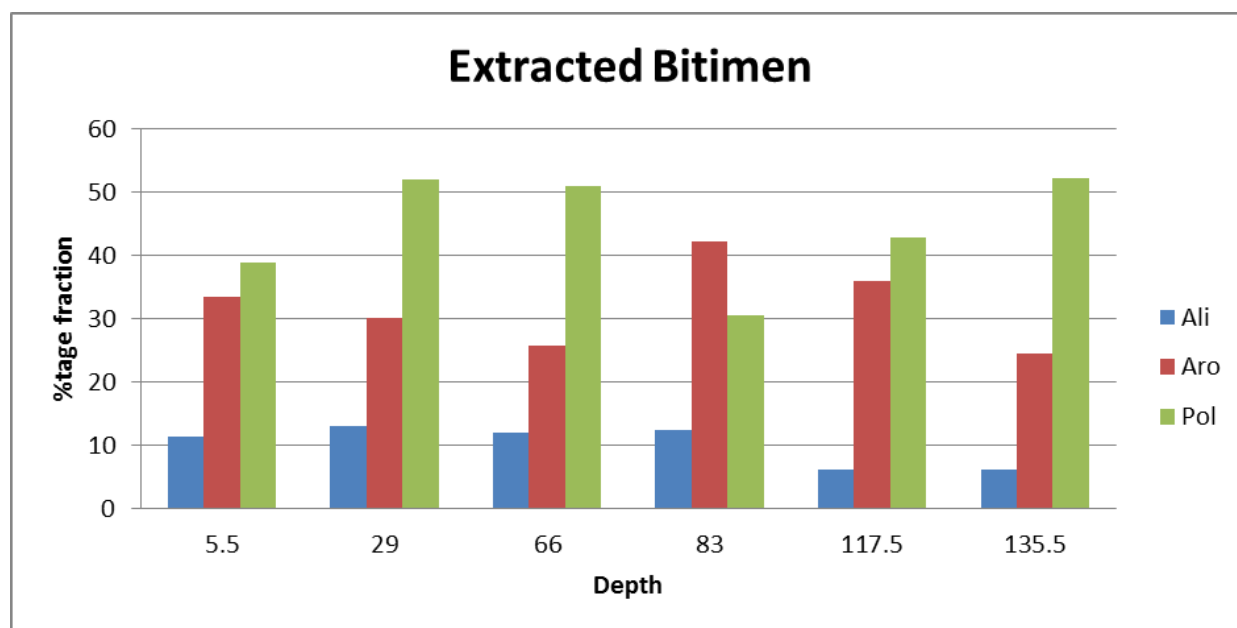


Fig. 4.13. Percentage composition of each fraction in extracted bitumen at various depths.

The aliphatic fraction of the bitumen is of extreme importance because of its role in determining the overall quality of the bitumen. This fraction has also been used to assess oil migration within a sedimentary sequence by virtue of its ability to migrate more freely than other fractions (Leythaeuser et al., 1988). The Longyear seam has its highest aliphatic content of 13.01 % occurring at the lower portion of the seam and the least content of 6.06 % at the upper portion. A plot of the aliphatic composition versus depth is shown in figure 4.14. The plot shows a reducing aliphatic trend from the bottom to the top of the seam. The seam base is characterized by approximately twice the amount of aliphatics as the upper portion of the seam. The loss of lower molecular weight hydrocarbon fractions from the bottom towards the top of the seam could be a sign of hydrocarbon migration within the seam. Karlsen et al. (1988) observed this type of light hydrocarbon redistribution with depth and attributed it to the effect of petroleum migration within a sequence. Leythaeuser and Schaefer (1984) also noted that that hydrocarbon migration is associated with compositional fractionation effects. For control purposes, bitumen from a sample above (142.5 cm) the highest studied sample (135.5 cm) was fractionated. This sample yielded 5.60 % of aliphatics which was lower than the 135.5 cm sample (Appendix A2).

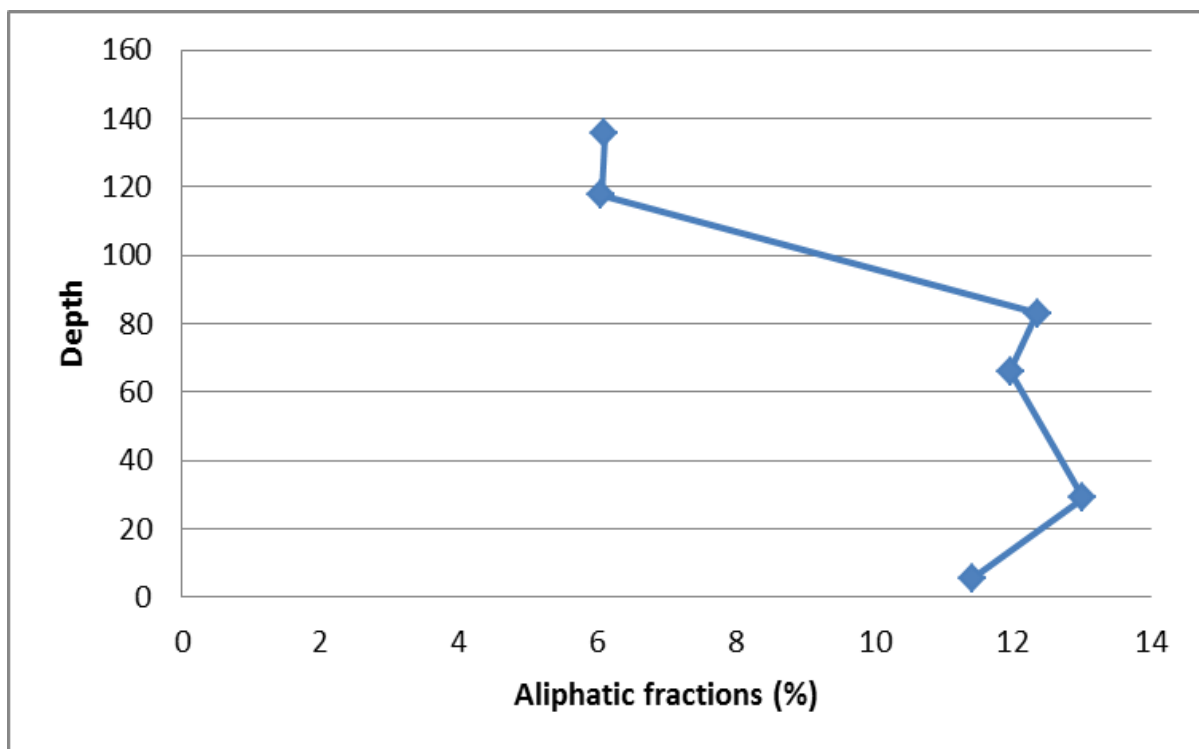


Fig. 4.14. Change in aliphatic yields from initial coal extracts with depth of the seam.

The hydrous pyrolysis bitumen fractions are fairly uniform throughout the seam. The polar and aromatic fractions still dominate. This is because the bitumen generated has not started to crack to oil. The polar fractions comprise of 46-67% while the aromatics comprise of 10-16 % and the aliphatics remain the smallest fraction comprising of 4-11 % (Fig 4.15).

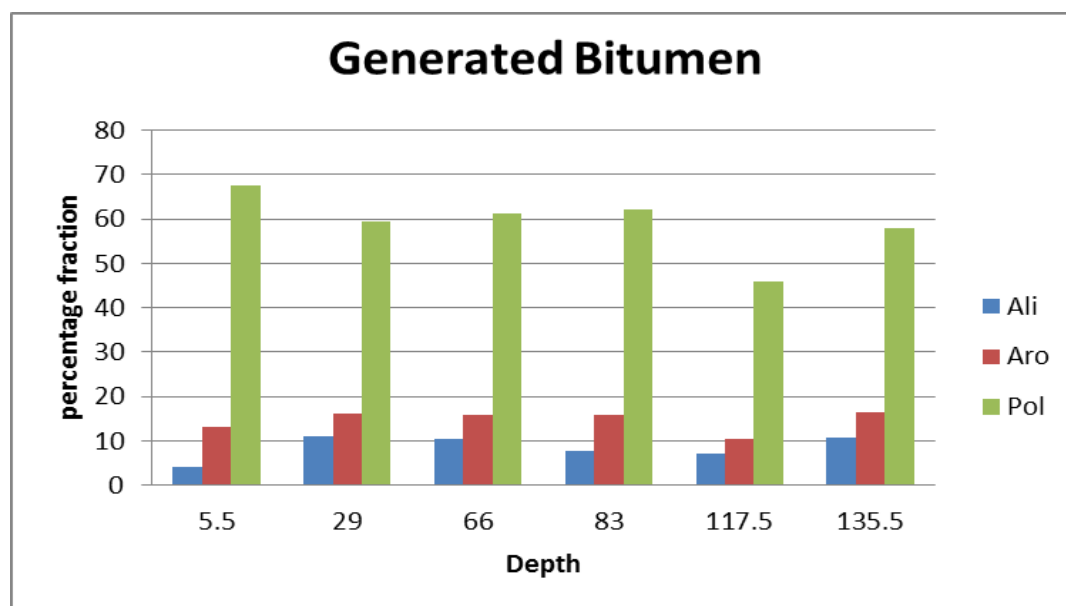


Fig. 4.15. Percentage composition of each fraction in generated bitumen at various depths.

4.5 Biological marker distribution in the aliphatic fraction of Longyear coals

Sterane peaks viewed on the m/z 217 chromatograms (Appendix A3-A8) are fairly uniform throughout the seam for both the initial coal extract and the hydrous pyrolysis generated bitumen. This correlates well with the C_{29} ($\alpha\beta\beta/\alpha\beta\beta+aaa$) and $C_{29}(S/S+R)$ sterane maturity ratios. The C_{29} ($\alpha\beta\beta/\alpha\beta\beta+aaa$) ratios range from 0.49-0.52 for the initial coal extracts and 0.40-0.45 for the pyrolysis yield while the $C_{29}(S/S+R)$ ratios range from 0.19-0.41 for the initial extract and 0.40-0.54 for the pyrolysis yields (table 4.4). The $C_{29}(S/S+R)$ ratio of both extracted and generated bitumen indicate a moderate to high thermal maturity. Seifert (1978) reported that the $C_{29}(S/S+R)$ and C_{29} ($\alpha\beta\beta/\alpha\beta\beta+aaa$) sterane maturity ratios increase from 0-0.5 (0.52-0.55 at equilibrium) with increasing thermal maturity. However, the C_{29} ($\alpha\beta\beta/\alpha\beta\beta+aaa$) ratio is most often ignored because of inconsistencies that could arise due to the contamination of the C_{29} $aaaS$ isomer by other sterane isomers (Gallegos and Moldowan, 1992).

Depth	Sterane ratios			
	Extracted (solvent extraction)		Generated (pyrolysis)	
	29(S/S+R)	29($\beta\beta/\beta\beta+\alpha\alpha$)	29(S/S+R)	29($\beta\beta/\beta\beta+\alpha\alpha$)
5.5	0.40	0.51	0.45	0.41
29	0.41	0.52	0.41	0.41
66	0.41	0.52	0.49	0.33
83	0.45	0.50	0.53	0.37
117.5	0.43	0.50	0.54	0.19
135.5	0.45	0.49	0.40	0.25

Table 4.4. Relevant sterane ratios at various depths of the Longyear seam.

The proportion of C_{27} , C_{28} and C_{29} steranes in bitumen is related to the palaeoenvironment of deposition and the type of organic matter in the source rock (Volkman et al., 1983). During the examination of the total composition of regular C_{27} , C_{28} and C_{29} steranes distributed within the aliphatic fraction of the bitumen, the C_{29} steranes shows a clear dominance. The total sterane ranges for C_{27} , C_{28} and C_{29} fall between 2-27%, 2-18% and 54-95% respectively. From the data in table 4.5, there is a close similarity of the sterane distribution between the extracted and generated bitumen. This similarity suggests uniformity in the original organic matter from of both extracted and generated bitumen. The absence of any consistent changes in the regular sterane distribution is indication that these oils are from a similar source.

Depth	Total Steranes (%)					
	Extracted (solvent extraction)			Generated (pyrolysis)		
	C_{27}	C_{28}	C_{29}	C_{27}	C_{28}	C_{29}
5.5	14.07	14.91	71.03	16.57	5.59	77.84
29	13.23	15.47	71.30	27.42	18.13	54.44
66	14.48	14.81	70.71	10.43	14.16	75.40
83	13.89	16.19	69.91	14.31	9.67	76.03
117.5	12.93	16.29	70.78	10.07	9.44	80.49
135.5	2.42	1.91	95.67	24.83	7.71	67.45

Table 4.5. Total sterane concentrations of the Longyear seam at various depths.

The distribution of C_{27} , C_{28} and C_{29} homologs can be plotted on a ternary diagram for differentiating ecosystems (Huang and Meinshein, 1979). The abundance of C_{29} steranes can be seen clearly on the tri plot in Fig. 4.16. The predominance of C_{29} steranes relative to C_{27} and C_{28} is attributed to higher plant input in the bitumen (Lockhart et al., 2008). This is characteristic of oils derived from terrigenous source rocks. Similar sterane distribution has been reported in coal derived oils from the Cooper-Eromanga basin in South Australia (Hunt, 1991). Sterane ternary diagrams have been used

extensively by Peters (2000) to show the relationship between oils and source rock bitumen. This plot is very reliable for this study because the samples plot around the same position showing that they are from the same source and depositional environment. According to Mackenzie et al. (1983a), this plot has had limited success with steranes in source rocks and crude oil from various source-rock depositional environments.

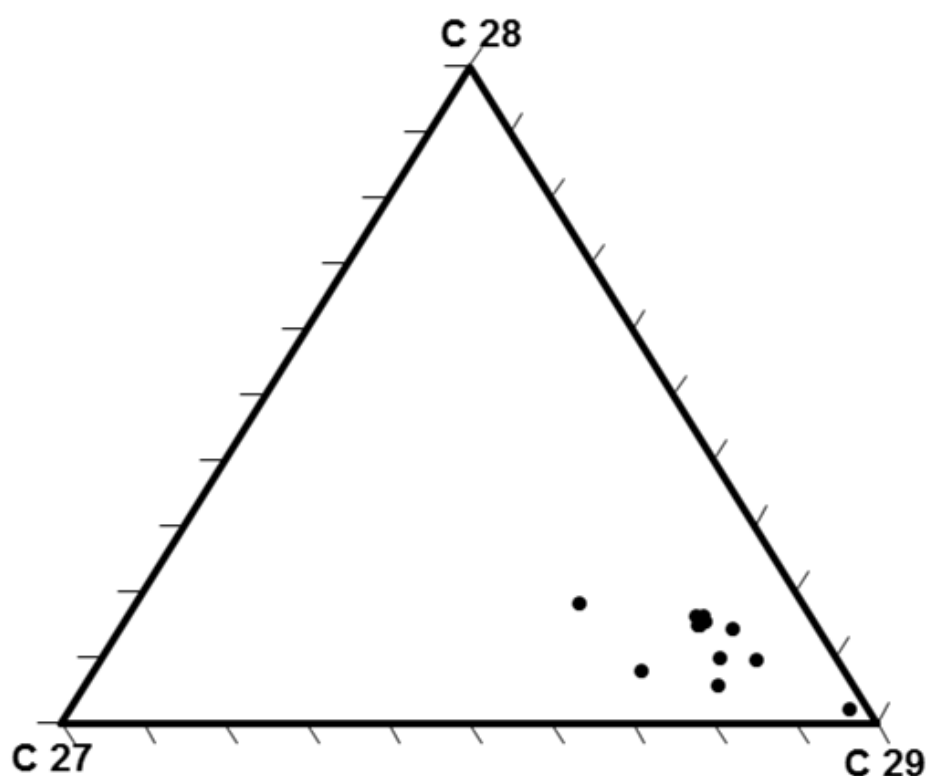


Fig. 4.16. Tri-plot of the C₂₇, C₂₈ and C₂₉ steranes. Samples plot much closer to the C₂₉ steranes.

The *m/z* 191 chromatogram (Appendix A9-A14) shows the full array of hopanes with the excellent preservation of the longer chain carbon homologues. Hopane peaks from the hydrous pyrolysis yields and initial coal extracts show a striking similarity, with the C₂₉ and C₃₀ hopanes dominating. C₃₀ peaks are particularly higher when compared to C₂₉ in all the bitumen. Higher C₂₇ 18a (H) - 22,29,30 - trisnorneohopane (T_s) peaks relative to C₂₇ 17a (H) - 22,29,30 - trisnorneohopane (T_m) is common in all the hopane peaks. Nytoft and Bojesen-Koefoed (2001) reported relatively higher T_s peaks compared to T_m peaks in more mature bitumen. This is because C₂₇ 17a (H) - 22,29,30 - trisnorneohopane is less stable than C₂₇ 18a (H) - 22,29,30 - trisnorneohopane during catagenesis. The T_s/T_s+T_m ratio is a maturity parameter which is fairly reliable when

evaluating bitumen from a common source (Philp and Gilbert, 1982). The T_s/T_s+T_m ratio ranges for both oils are uniform throughout the seam averaging 0.94 and 0.89 for the extracted and generated bitumen respectively (table 4.6). This ratio increases with thermal maturity and approaches equilibrium at 0.8 (Seifert et al., 1980). The uniformity of this maturity ratio in both extracted and generated bitumen is a further indication that they are of the same source.

The stereoisomer ratios (S and R) can be calculated for any of the C_{31} to C_{35} compounds. Typically, the C_{31} and C_{32} homohopane proportions are used to calculate the S/S+R ratios. The C_{31} hopane ratios for the initial coal bitumen extracts fall in the range of 0.60-0.61 and 0.58-0.60 for the generated bitumen. The C_{32} ratio is fairly similar, falling in the range of 0.57-0.59 and 0.56-0.58 for extracted and generated bitumen respectively (table 4.6). The S/S+R ratio increases from 0-0.60 (0.57-0.62 representing an equilibrium maturity range) during maturation (Seifert et al., 1980). Average values for C_{31} homologue is 0.60 for bitumen extracts and 0.59 for the generated bitumen. The C_{32} hopanes show averages of 0.58 and 0.57 for the extracted and generated bitumen respectively. These values are higher than the 0.55 and 0.58 averages reported for low maturity crude oils (Zumberge, 1987b). Ratios within the 0.57-0.62 range indicate that the essential phase of petroleum generation has been attained or probably surpassed (Moldowan et al., 1995). However some sediments have generated liquid hydrocarbons at S/S+R hopane ratios less than 0.5 by virtue of increased thermal stress. Such sediments have been observed in the Grippsland basin and have been extensively discussed by (Philp and Gilbert, 1982). The average S/S+R ratio for the extracted Longyear coals approach an equilibrium value of 0.59 at a mean vitrinite reflectance of 0.64% R_o . Immediately this equilibrium is reached, these ratios remain constant, providing no further maturity information. This is observed by the negligible difference in difference (0.01) in average equilibrium ratios between the extracted and generated bitumen samples. Hence, these ratios can be calibrated against other maturity parameters (such as HI and VR) and regarded as the mean entry maturity values for petroleum generation in the Longyear coals.

Dept h	Hopane ratios					
	Extracted (solvent extraction)			Generated (pyrolysis)		
	$C_{31}(S/S+R)$	$C_{32}(S/S+R)$	T_s/T_s+T_m	$C_{31}(S/S+R)$	$C_{32}(S/S+R)$	T_s/T_s+T_m
5.5	0.60	0.57	0.94	0.59	0.58	0.89
29	0.61	0.58	0.93	0.59	0.57	0.92
66	0.61	0.58	0.93	0.60	0.56	0.87
83	0.60	0.59	0.95	0.59	0.58	0.89
117.5	0.60	0.57	0.94	0.58	0.57	0.92
135.5	0.60	0.59	0.93	0.58	0.58	0.89

Table 4.6. Relevant hopane ratios at various depths of the Longyear seam.

The effectiveness in which hopanes are used to predict thermal maturity is often affected by the effects of biodegradation in oils. The destruction of hopanes has been observed in severely biodegraded oils. Alexander et al. (1981) also reported the relative susceptibility of $\alpha\beta$ hopanes to biodegradation when compared with the $\beta\alpha$ hopanes. Hence an enrichment of $\beta\alpha$ hopanes can serve as an indication of biodegradation. However, the excellent preservation of hopanes in the oils derived from the Longyear coals is an indication that these oils have not been biologically degraded at any portion of the seam. The uniform preservation of the $\alpha\beta$ hopanes in the extracted and generated bitumen reduces any possibility of biodegradation. Hence, hopane ratios serve as one of the most reliable tools in determining and correlating the maturity of oils from the Longyear coals.

Isoprenoid and *n*-alkane distribution were viewed on the *m/z* 71 chromatograms (Appendix A15-A20). Bitumen extracts are dominated by long chain *n*-alkane series starting around C_{15} and diminishing on the chromatogram at around C_{34} . This range of *n*-alkane is expected from high wax oils which are mainly derived from terrigenous sources (Hedberg, 1968). Although oils from terrigenous sources have high wax content, not all waxy oil samples are necessarily terrigenous, hence care should be taken not to draw early conclusions on this basis. Certain *n*-alkane ratios can be applied in the identification the primary source input in bitumen. The amount of land plant input relative to that of marine organisms in bitumen can be ascertained using the terrigenous aquatic ratio (TAR) (Peters et al., 2007). The TAR is derived from the equation, $TAR = (nC_{27}+nC_{29}+nC_{31})/(nC_{15}+nC_{17}+nC_{19})$. Higher TAR values indicate greater terrigenous input relative to aquatic sources (Bourbonniere and Meyers, 1996). TAR values for the extracted bitumen range between 0.7-2 while those for the generated bitumen range between 0.4-0.6. The generally low TAR values and the inconsistency of the values are attributed to the high sensitivity of TAR to maturity and biodegradation (Moldowan et al., 1995). The relative abundance of odd against even carbon numbered *n*-alkanes

provides a reasonable estimate of source input and thermal maturity. The alkanes show a slight dominance of the odd numbered *n*-alkanes over the even numbered *n*-alkanes. This odd over even predominance is consistent in both the solvent extraction and hydrous pyrolysis yields. The carbon preference index (CPI) is one of the measurements and can be calculated from the equation, $CPI = \frac{2(C_{23}+C_{25}+C_{27}+C_{29})}{C_{22}+C_{30}+2(C_{24}+C_{26}+C_{28})}$. CPI values approach 1.0 and an odd carbon number preference at high thermal maturity (Bray and Evans, 1961). CPI ratios of extracted and pyrolysed samples all within a similar range of 1.6-2.1 indicating relatively high thermal maturity (table 4.7).

Depth	<i>n</i> -alkane ratios			
	Extracted (solvent extraction)		Generated (pyrolysis)	
	CPI	TAR	CPI	TAR
5.5	1.82	0.67	1.53	0.51
29	2.05	1.00	1.58	0.52
66	1.99	1.06	1.57	0.56
83	2.18	2.04	1.63	0.50
117.5	1.94	1.80	1.62	0.57
135.5	1.92	1.69	1.61	0.43

Table 4.7. Relevant *n*-alkane ratios

Pristane peaks in the extracted bitumen stand high above any other peak in the *m/z* 71 chromatograms. This is quite unexpected because these high peaks are indicative of low thermal maturity (Tissot et al., 1987). High pristane peaks could remain in oils that have matured early in geologic time (Tissot et al., 1987). Young mature oils like those from the tertiary could exhibit such characteristics. Leythaeuser and Schwarzkopf (1985) observed that anomalous pristane values could arise as a result of other factors which include source input, biodegradation, migration and geologic age. The height of the pristane peaks reduce considerably in the hydrous pyrolysis yields and stand much shorter than the *n*-alkanes. Table 4.8 shows some relevant isoprenoid and isoprenoid/*n*-alkane ratios.

Pristane/phytane (Pr/Ph) ratios are commonly used for palaeoenvironmental interpretation. The determination of redox conditions as well as source input has been achieved by Didyk et al. (1978) using Pr/Ph ratios. According to Hedberg (1968) anoxic conditions favour the formation of phytane and oxic conditions promote the conversion of phytol to pristane while the Pr/Ph ratios of > 3 are indicative of terrigenous plant input under oxic conditions.

Depth	Isoprenoid ratios					
	Extracted (solvent extraction)			Generated (pyrolysis)		
	Pr/Ph	Pr/nC ₁₇	Ph/nC ₁₈	Pr/Ph	Pr/nC ₁₇	Ph/nC ₁₈
5.5	12.31	2.34	0.16	3.52	0.34	0.07
29	13.60	6.20	0.35	3.80	0.41	0.09
66	12.84	5.63	0.36	3.21	0.37	0.09
83	13.48	16.22	0.87	3.82	0.41	0.09
117.5	12.06	19.62	1.28	3.72	0.36	0.08
135.5	6.63	20.71	2.24	3.23	0.29	0.06

Table 4.8. Relevant isoprenoid and isoprenoid/*n*-alkane ratios

Maximum values of 13.48 for the extracted oils and 3.82 for the pyrolysis yields correspond to terrigenous organic matter input. The ability of Pr/Ph ratios to accurately describe the redox state and palaeoenvironments is affected by several factors. These factors include a variation in the source biomolecules that give rise to pristane or phytane and maturity of the oils. Pr/Ph ratios generally increase with thermal maturity (Connan, 1973; Radke et al., 1980). This is not the case in maturity simulations of the Longyear coals using hydrous pyrolysis as the yielded bitumen show much lower Pr/Ph values than the solvent extracted oils. Such a case was also identified by Burnham et al. (1982) after pyrolysis of the Green River oil shale. This decrease is due to the ease with which pristanes are released compared with phytane precursor from kerogen during catagenesis.

Isoprenoid/*n*-alkane ratios like the Pr/nC₁₇ and Ph/nC₁₈ ratios are maturity sensitive parameters and generally decrease with increase in thermal maturity. This is due to the formation of more *n*-alkanes from kerogen by cracking as thermal maturity increases. Hydrous pyrolysis bitumen yields show fairly stable Pr/nC₁₇ and Ph/nC₁₈ ranges throughout the seam height (table 4.8). This is because the uniform simulation of maturity cracks the isoprenoids under heightened thermal stress. However, the Pr/nC₁₇ and Ph/nC₁₈ values for the initial coal bitumen vary extensively. These variations are probably due to the effects of maturity difference, biodegradation, source variation or migration (Leythaeuser and Schwarzkopf, 1985). The previously examined biological markers have dealt with the possibilities of biodegradation, maturity differences and source variations leaving migration as the probable factor for this extensive anomaly.

The Pr/nC₁₇ ratios of the extracted oil show a steady increase from the bottom to the top of the seam (Fig. 4.17). The sampled profile of the seam shows a generally high Pr/nC₁₇ ratio but the enrichment of pristane is more prominent up-seam. The seam base is characterised by a Pr/nC₁₇ ratio of 2.3 while the top of the seam approaches a ratio of 20. This extreme variation is attributed to nC₁₇ being more readily expelled than pristane leading to the relative enrichment of pristane in the residual bitumen. This

relative enrichment of pristane towards the top of the seam has been recognized and used as an indicator for the recognition of hydrocarbon migration (Leythaeuser and Schwarzkopf, 1985). The Pr/nC_{17} ratios of source rocks experiencing migration increase sharply towards the rock contact with surrounding rocks (Mackenzie et al., 1983a). The increase in pristane concentration towards the upper portion of the Longyear seam suggests that migration could have occurred in the upward direction. The direction of migration coincides with an improved kerogen quality (from HI = 314 mg/g TOC at the seam base to the 389 mg/g TOC at the top of the seam) and an increase in hydrocarbon generation. In addition to the increase in Pr/nC_{17} ratios up-seam, there is a general decrease in the light-end hydrocarbons in this direction as shown by the aliphatic yields. The Ph/nC_{18} also increases in an exactly same manner like the Pr/nC_{17} ratio (Appendix A21). Similar isoprenoid/n-alkane distributions have been reported in the terrestrially derived coals of the Taranaki basin and in the organic rich shales of Paleocene Firkanten formation (Curry et al., 1994; Leythaeuser and Schwarzkopf, 1985). These sequences have experienced hydrocarbon migration and subsequent expulsion.

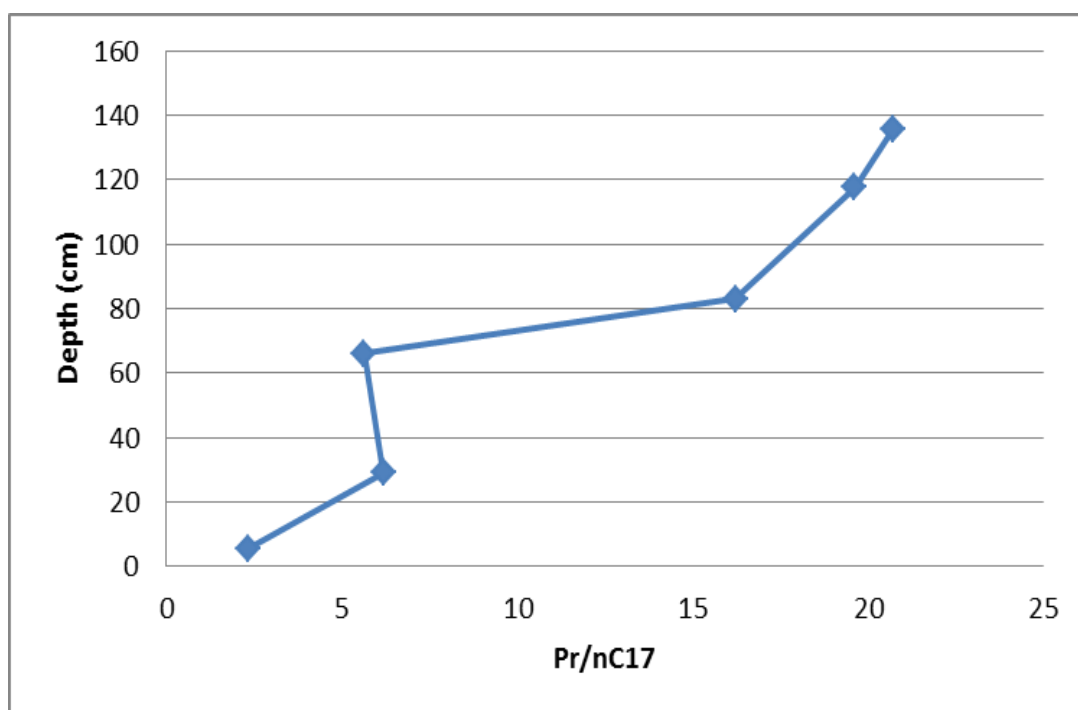


Fig. 4.17. Pr/nC_{17} trend with depth in the aliphatic fraction of initial coal bitumen extract.

CHAPTER FIVE

CONCLUSIONS AND FUTURE WORK

5.1 Conclusion

This study was aimed at determining the source of the bitumen present in the Longyear coal and investigating the possibility of oil migration within the coal seam. The potential of the Longyear coals to serve as a source rock for oil and a source of oil via retorting has also been examined. Conclusion drawn from the geochemical and biomarker analyses of these coals are summarised below:

- The average hydrous pyrolysis bitumen yields show that approximately 40-60% of liquid hydrocarbons are yet to be generated. This is a clear indication of the petroleum generative capacity of the Longyear coal. When subjected to similar geochemical conditions in-situ, these coals will generate significant liquid hydrocarbons. The volume of generated bitumen suggests that the Longyear coal has the potential to produce significant volumes of liquid hydrocarbons retorting (see appendix B for approximate calculations).
- The similarity of the hopane and pristane ratios used to ascertain the source and maturity of the initial coal extract and that generated from the coal after hydrous pyrolysis provides sufficient evidence to conclude that the bitumen found in-situ was generated by the coal.
- The loss of lower molecular weight hydrocarbon fractions and the steady increase of the Pr/nC₁₇ ratio towards the upper portion of the seam are signs of the possibility of upward migration of liquid hydrocarbon in the Longyear seam.
- Mean vitrinite reflectance and hydrogen index values can be correlated against the average biological maturity parameters. This could serve as a rule of thumb for determining the maturity range for which hydrocarbons will be generated by the Longyear coals. A good example will be to say that at a mean vitrinite reflectance of 0.64% R_o, hydrogen index of 358 mg/g TOC and a hopane ratio of 0.62 is the range for which liquid hydrocarbons will be generated from the Longyear coals.
- The change observed in all the applied geochemical data (TOC, gas and bitumen yield) at the middle portion of the Longyear seam is an indication of a change in depositional setting and peatland conditions during the formation of the Longyear seam.

5.2 Future work

A more detailed study of generative capacity of the Longyear coal should to be carried out using a technique that can be scaled up to industrial level.

A more detailed evaluation of the pathway and extent of migration in the Longyear seam is also necessary. The possibility of nearby hydrocarbon pools being sourced by the Longyear coal should be examined.

The truncation of several geochemical data observed at the middle portion of the Longyear seam should be looked into in greater detail. The horizontal extent and the impact of this truncation on the geological and engineering properties of this seam should be considered.

A study of the petrographic properties of the Longyear coal as they affect its pore size and structure with relation to the ease at which hydrocarbons will migrate is necessary.

REFERENCES

- Alexander, R., et al. (1981) Geochemical correlation of Windalia oil and extracts of Winning Group (Cretaceous) potential source rocks, Barrow Subbasin, Western Australia. *American Association of Petroleum Geologists Bulletin* 65-2, pp 235-250.
- Behar, F., et al. (1995) Experimental simulation of gas generation from coals and a marine kerogen. *Chemical Geology*, 126, pp 247-260.
- Boreham, C. J. & Powell, T. G. (1991) Variation in pyrolysate composition of sediments from the Jurassic Walloon Coal Measures, eastern Australia as a function of thermal maturation. *Organic Geochemistry*, 17, pp 723-733.
- Bourbonniere, R. A. & Meyers, P. A. (1996) Sedimentary geolipid records of historical changes in the watersheds and productivities of Lake Ontario and Erie. *Limnology and Oceanography*, 41, pp 352-359.
- Brassell, S. C., et al. (1986) Biological marker compounds as indicators of the depositions! history of the Maoming oil shale. *Organic Geochemistry*, 10, pp 927-941.
- Bray, E. E. & Evans, E. D. (1961) Distribution of n-paraffins as a clue to recognition of source beds. *Geochemica et Cosmochimica Acta*, 22, pp 2-15.
- Burnham, A. K., et al. (1982) Biological markers from Green River kerogen decomposition. *Geochemica et Cosmochimica*, 46, pp 1243-1251.
- Carr, A. D., et al. (2009) The effect of water pressure on hydrocarbon generation reactions: Some inferences from laboratory experiments. *Petroleum Geoscience*, 15, pp 17-26.
- Chandru, K., et al. (2008) Characterization of alkanes, hopanes, and polycyclic aromatic hydrocarbons (PAHs) in tar-balls collected from the East Coast of Peninsular Malaysia. *Marine Pollution Bulletin*, 56, pp 950-962.
- Cmiel, S. R. & Fabianska, M. J. (2004) Geochemical and petrographic properties of some Spitsbergen coals and dispersed organic matter. *International Journal of Coal Geology*, 57, pp 77-97.
- Connan, J. (1973) Diagenese naturelle et diagenese artificielle de la matiere organique a element vegataux predominants. In: Tissot, B. P. & Bienner, F. (Eds.), *Advances in organic geochemistry*. Paris: Editions Technip, pp 73-95.
- Cooles, G. P., et al. (1986) Calculation of petroleum masses generated and expelled from source rocks. *Organic Geochemistry*, 10, pp 235-245.
- Crelling, J. C. 1987. Separation, identification and characterisation of single coal maceral types. In: *Proceedings of the International Conference on Coal Science*, Amsterdam, The Netherlands. Elsevier Science Publishers, pp 119-122.

- Crelling, J. C. (2008) Coal Carbonization. In: Isabel, S.-R. & John, C. C. (Eds.), *Applied Coal Petrology*. Burlington: Elsevier, pp 173-192.
- Crelling, J. C., et al. (1988) Reactivity of coal macerals and lithotypes. *Fuel*, 67, pp 781-785.
- Curry, D. J., et al. (1994) Geochemistry of aliphatic-rich coals in the Cooper basin, Australia and Taranaki basin, New Zealand: implications for the occurrence of potentially oil-generative coals. In: Scott, A. C. & Fleet, A. J. (Eds.), *Coal and coal-bearing strata as oil-prone source rocks?* London: The Geological Society Special Publication, pp 149-181.
- Curtis, J. B., et al. (2004) Oil/source rock correlations in the Polish Flysch Carpathians and Mesozoic basement and organic facies of the Oligocene Menilite Shales: insights from hydrous pyrolysis experiments. *Organic Geochemistry*, 35, pp 1573-1596.
- Czochanska, Z., et al. (1988) Geochemical application of sterane and triterpane biomarkers to a description of oils from the Taranaki Basin in New Zealand. *Organic Geochemistry*, 12, pp 123-135.
- Dallmann, W. K. (1993) Notes on the stratigraphy, extent and tectonic implications of the Minkinfjellet Basin, Middle Carboniferous of central Spitsbergen. *Polar Research*, 12, pp 153-160.
- Dallmann, W. K., et al. (1988) Tertiary tectonics of Svalbard. Extended abstracts from symposium held in Oslo 26 and 27 April 1988. *Norsk Polarinstitutt Rapportserie*, 46, pp.
- Didyk, B. M., et al. (1978) Organic geochemical indicators of palaeoenvironmental conditions of sedimentation. *Nature*, 272, pp 216-222.
- Diessel, C. F. K. (1983) Carbonization reactions of inertinite macerals in Australian coals. *Fuel*, 62, pp 883-892.
- Diessel, C. F. K. (1992) *Coal-bearing depositional systems*, Berlin: Springer-Verlag, pp 4-41.
- Diessel, C. F. K. & Gammidge, L. (1998) Isometamorphic variations in the reflectance and fluorescence of vitrinite--a key to depositional environment. *International Journal of Coal Geology*, 36, pp 167-222.
- Dietmar Müller, R. & Spielhagen, R. F. (1990) Evolution of the Central Tertiary Basin of Spitsbergen: towards a synthesis of sediment and plate tectonic history. *Palaeogeography, Palaeoclimatology, Palaeoecology*, 80, pp 153-172.
- Durand, B., And M. Paratte (1983) *Oil potential of coals: a geochemical approach*, in *Petroleum geochemistry and exploration of Europe*, Boston: Blackwell Scientific Publications, pp 255-265.
- England, W. A. (1993) Migration systems analysis. *Marine and Petroleum Geology*, 10, pp 633-633.

- Fleet, A. J. & Scott, A. S. (Eds.) (1994) Coal and coal-bearing strata as oil-prone source rocks: an overview, Geological society special publication, pp
- Gallegos, E. J. & Moldowan, J. M. (1992) The effect of hold time on GC resolution and the effect of collision gas on mass spectra in geochemical biomarker research. In: Moldowan, J. M., Albrecht, P. & Philp, R. P. (Eds.), Biological markers in sediments and petroleum. Englewood Cliffs, NJ: Prentice-Hall, pp 156-181.
- Given, P. H. (1984) Essay on the organic geochemistry of coal. *Coal Science*, 3, pp 63-252.
- Harland, W. B. (1997) Proto-basement in Svalbard. *Polar Research*, 16, pp 123-147.
- Harland, W. B. (1998) The geology of Svalbard, Bath: Geological Society, pp 3-37.
- Hedberg, H. D. (1968) Significance of high-wax oils with respect to genesis of petroleum. *American Association of Petroleum Geologists -- Bulletin*, 52, pp 736-750.
- Horsfield, B., et al. (1988) Determining the petroleum-generating potential of coal using organic geochemistry and organic petrology. *Organic Geochemistry*, 13, pp 121-129.
- Huang, D. (1999) Advances in hydrocarbon generation theory: II. Oils from coal and their primary migration model. *Journal of Petroleum Science and Engineering*, 22, pp 131-139.
- Huang, W. Y. & Meinshein, W. G. (1979) Sterols as ecological indicators. *Geochimica et cosmochimica acta*, 43, pp 739-745.
- Huc, A. Y. & Hunt, J. M. (1980) Generation and migration of hydrocarbons in offshore South Texas Gulf Coast sediments. *Geochimica et Cosmochimica Acta*, 44, pp 1081-1089.
- Hunt, J. M. (1979) *Petroleum geochemistry and geology*, San Fransisco: W. H. Freeman, pp 186-284.
- Hunt, J. M. (1991) Generation of gas and oil from coal and other terrestrial organic matter. *Organic Geochemistry*, 17, pp 673-680.
- Hunt, J. M., et al. (1967) Chapter 7 The Origin of Petroleum in Carbonate Rocks¹. *Developments in Sedimentology*. Elsevier, pp 225-251.
- Hvoslef, S., et al. (1986) A combined sedimentological and organic geochemical study of the Jurassic/Cretaceous Janusfjellet formation (Svalbard), Norway. *Organic Geochemistry*, 10, pp 101-111.
- Iglesias, M. J., et al. (2002) Control of the chemical structure in perhydrous coals by FTIR and Py-GC/MS. *Journal of Analytical and Applied Pyrolysis*, 62, pp 1-34.
- Isaksen, G. H., et al. (1998) Controls on the oil and gas potential of humic coals. *Organic Geochemistry*, 29, pp 23-44.
- Issler, D. R. & Snowdon, L. R. (1990) Hydrocarbon generation kinetics and thermal modelling, Beaufort- Mackenzie Basin. *Bulletin of Canadian Petroleum Geology*, 38, pp 1-16.

- Ji-Yang, S., et al. (1982) A biological marker investigation of petroleums and shales from the Shengli oilfield, The People's Republic of China. *Chemical Geology*, 35, pp 1-31.
- Jiamo, F., et al. (1990) Application of biological markers in the assessment of paleoenvironments of Chinese non-marine sediments. *Organic Geochemistry*, 16, pp 769-779.
- Karlsen, D. A., et al. (1988) Light hydrocarbon redistribution in a shallow core from the Ravnefjeld formation on the Wegener Halvø, East Greenland. *Organic Geochemistry*, 13, pp 393-398.
- Kearey, P. (1996) *The New Penguin Dictionary of Geology*. Dictionary of Geology. 2nd ed. London, Penguin books.
- Killops, S., et al. (2002) Maturity-related variation in the bulk-transformation kinetics of a suite of compositionally related New Zealand coals. *Marine and Petroleum Geology*, 19, pp 1151-1168.
- Killops, S. D., et al. (1998) Predicting generation and expulsion of paraffinic oil from vitrinite-rich coals. *Organic Geochemistry*, 29, pp 1-21.
- Klerk, A. (2009) *Beyond Fischer-Tropsch: Coal-to-liquids Production and Refining*: Elsevier Science & Technology, pp 16-145.
- Larter, S. (2011). Petroleum composition, petroleum systems, source rocks and petroleum generation, petroleum generation, migration of petroleum [Online]. Available from: <http://science.jrank.org/pages/47993/petroleum.html> (last accessed 07-06-2011).
- Larter, S. R. (1995) *Coal and coal bearing strata as oil-prone source rocks* : Edited by A. SCOTT and A. FLEET. Geological Society Special Publication No. 77. 1994. *Organic Geochemistry*, 23, pp 467-467.
- Lewan, M. D. (1997) Experiments on the role of water in petroleum formation. *Geochimica et Cosmochimica Acta*, 61, pp 3691-3723.
- Leythaeuser, D. & Schaefer, R. G. (1984) Effects of hydrocarbon expulsion from shale source rocks of high maturity in upper carboniferous strata of the Ruhr area, Federal Republic of Germany. *Organic Geochemistry*, 6, pp 671-681.
- Leythaeuser, D., et al. (1988) Geochemical effects of primary migration of petroleum in Kimmeridge source rocks from Brae field area, North Sea. I: Gross composition of C15+-soluble organic matter and molecular composition of C15+-saturated hydrocarbons. *Geochimica et Cosmochimica Acta*, 52, pp 701-713.
- Leythaeuser, D. & Schwarzkopf, T. (1985) Pristane/n-haptadecane ratio as an indicator for recognition of hydrocarbon migration effects. *Organic Geochemistry*, 10, pp 191-197.

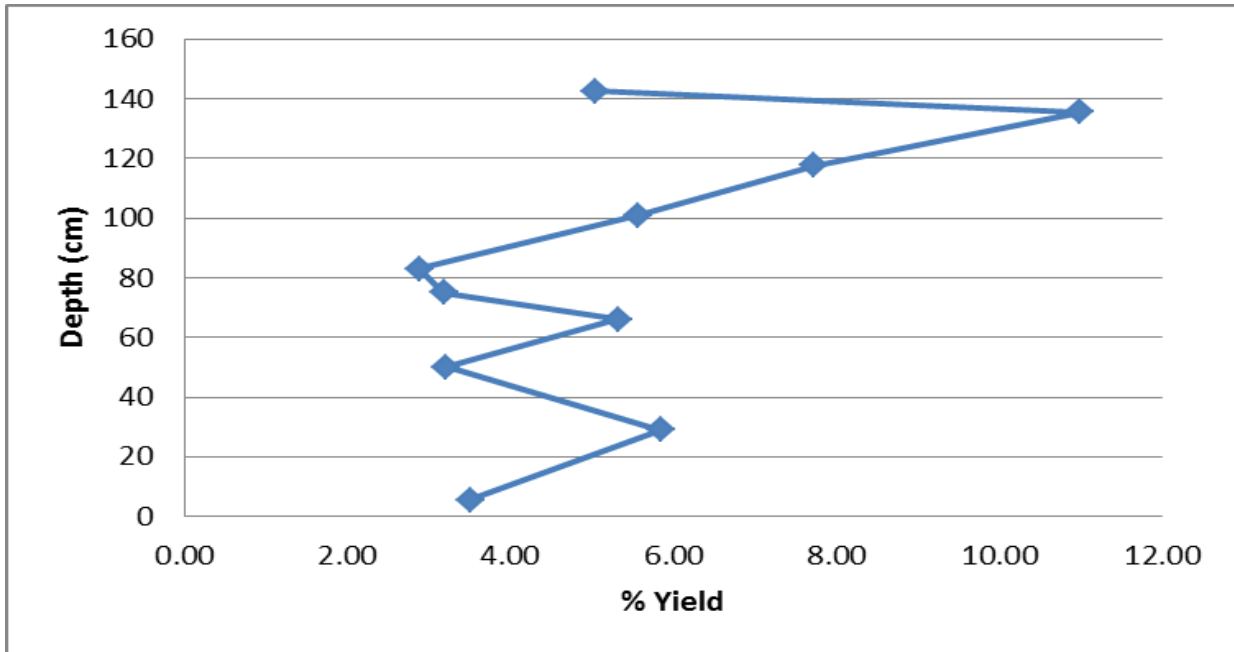
- Littke, R., et al. (1990) Petroleum generation and migration in coal seams of the Carboniferous Ruhr Basin, northwest Germany. *Organic Geochemistry*, 16, pp 247-258.
- Lockhart, R. S., et al. (2008) Release of bound aliphatic biomarkers via hydrolysis from Type II kerogen at high maturity. *Organic Geochemistry*, 39, pp 1119-1124.
- Mackenzie, A. S., et al. (1983a) Determination of hydrocarbon distribution in oils and sediment extracts by gas chromatography-high resolution mass spectrometry. *Organic Geochemistry*, 5, pp 57-63.
- Marshall, C., et al. 2011. Biomarker and Petrographic Evidence for the Origin and Maturity of Abundant Palaeocene Oil-Prone Type III Kerogen Deposits, Spitsbergen. In: 3P Arctic, The Polar Petroleum Potential Conference & Exhibition, 30 August-2 September, 2011. Halifax. (Abstract).
- Melendez, R. B. 2001. The characterisation and combustion of South American coals. PhD Thesis, University of Nottingham.
- Moldowan, J. M., et al. (1991) Rearranged hopanes in sediments and petroleum. *Geochimica et Cosmochimica Acta*, 55, pp 3333-3353.
- Moldowan, J. M., et al. (1995) Relationship between petroleum composition and depositional environment of petroleum source rocks. *American Association of Petroleum Geologists -- Bulletin*, 69, pp 1255-1268.
- Moore, L. R. (1969) Geomicrobiology and geomicrobiological attack on sedimented organic matter In: Eglinton, G. & Murphy, M. T. J. (Eds.), *Organic geochemistry: methods and results*. Berlin-Heidelberg-New York: Springer-Verlag, pp 265-303.
- Moore, P. S., et al. (1992) Integrated source, maturation and migration analysis, Gippsland Basin, Australia. *Australian Petroleum Exploration Association Journal*, 32, pp 313-324.
- Morris, P. J. (1998). Formation of coal [Online]. Available from: <http://www.athro.com/geo/trp/gub/coal.html> (last accessed 24/04/2011).
- Murchison, D. G. (1991) Petrographic aspects of coal structure: reactivity of macerals in laboratory and natural environments. *Fuel*, 70, pp 296-315.
- Myhre, A. M. & Eldholm, O. (1988) The western Svalbard margin (74°-80°N). *Marine and Petroleum Geology*, 5, pp 134-156.
- Nagy, J. (2005) Delta-influenced foraminiferal facies and sequence stratigraphy of Paleocene deposits in Spitsbergen. *Palaeogeography, Palaeoclimatology, Palaeoecology*, 222, pp 161-179.
- Nagy, J., et al. (2011) Marine shelf to paralic biofacies of Upper Triassic to Lower Jurassic deposits in Spitsbergen. *Palaeogeography, Palaeoclimatology, Palaeoecology*, 300, pp 138-151.

- Nytoft, H. P. & Bojesen-Koefoed, J. A. (2001) 17[alpha],21[alpha](H)-hopanes: natural and synthetic. *Organic Geochemistry*, 32, pp 841-856.
- Orem, W. H. & Finkelman, R. B. (2003) Coal Formation and Geochemistry. In: Heinrich, D. H. & Karl, K. T. (Eds.), *Treatise on Geochemistry*. Oxford: Pergamon, pp 191-222.
- Orheim, A., et al. (2007) Petrography and geochemical affinities of Spitsbergen Paleocene coals, Norway. *International Journal of Coal Geology*, 70, pp 116-136.
- Pepper, A. S. & Corvi, P. J. (1995) Simple kinetic models of petroleum formation. Part I: oil and gas generation from kerogen. *Marine and Petroleum Geology*, 12, pp 291-319.
- Peters, K. E. (2000) Petroleum tricyclic terpanes: predicted physiochemical behavior from molecular mechanics calculations. *Organic Geochemistry*, 31, pp 497-507.
- Peters, K. E., et al. (2007) *The Biomarker Guide: Volume 1, Biomarkers and Isotopes in the Environment and Human History*: Cambridge University Press, pp
- Petersen, H. I. (2002) A re-consideration of the "oil window" for humic coal and kerogen type III source rocks. *Journal of Petroleum Geology*, 25, pp 407-431.
- Petersen, H. I. (2006) The petroleum generation potential and effective oil window of humic coals related to coal composition and age. *International Journal of Coal Geology*, 67, pp 221-248.
- Petersen, H. I. & Nytoft, H. P. (2006) Oil generation capacity of coals as a function of coal age and aliphatic structure. *Organic Geochemistry*, 37, pp 558-583.
- Petersen, H. I., et al. (2009) Application of integrated vitrinite reflectance and FAMB analyses for thermal maturity assessment of the northeastern Malay Basin, offshore Vietnam: Implications for petroleum prospectivity evaluation. *Marine and Petroleum Geology*, 26, pp 319-332.
- Philp, R. P. & Gilbert, T. D. (1982) Unusual distribution of biological markers in Australian crude oil. *Nature*, 299, pp 245-247.
- Powell, T. G. (1986) Petroleum geochemistry and depositional setting of lacustrine source rocks. *Marine and Petroleum Geology*, 3, pp 200-219.
- Powell, T. G., et al. (1991) Petroleum source rock assessment in non-marine sequences: pyrolysis and petrographic analysis of Australian coals and carbonaceous shales. *Organic Geochemistry*, 17, pp 375-394.
- Radke, M., et al. (1984) Relationship between rank and composition of aromatic hydrocarbons for coals of different origins. *Organic Geochemistry*, 6, pp 423-430.
- Radke, M., et al. (1980) Composition of soluble organic matter in coals: relation to rank and liptinite fluorescence. *Geochimica et Cosmochimica Acta*, 44, pp 1787-1800.
- Schlumberger (2011). Source rocks [Online]. Available from: <http://oilfieldglossary.com/search.cfm> (last accessed 02/08/2011).

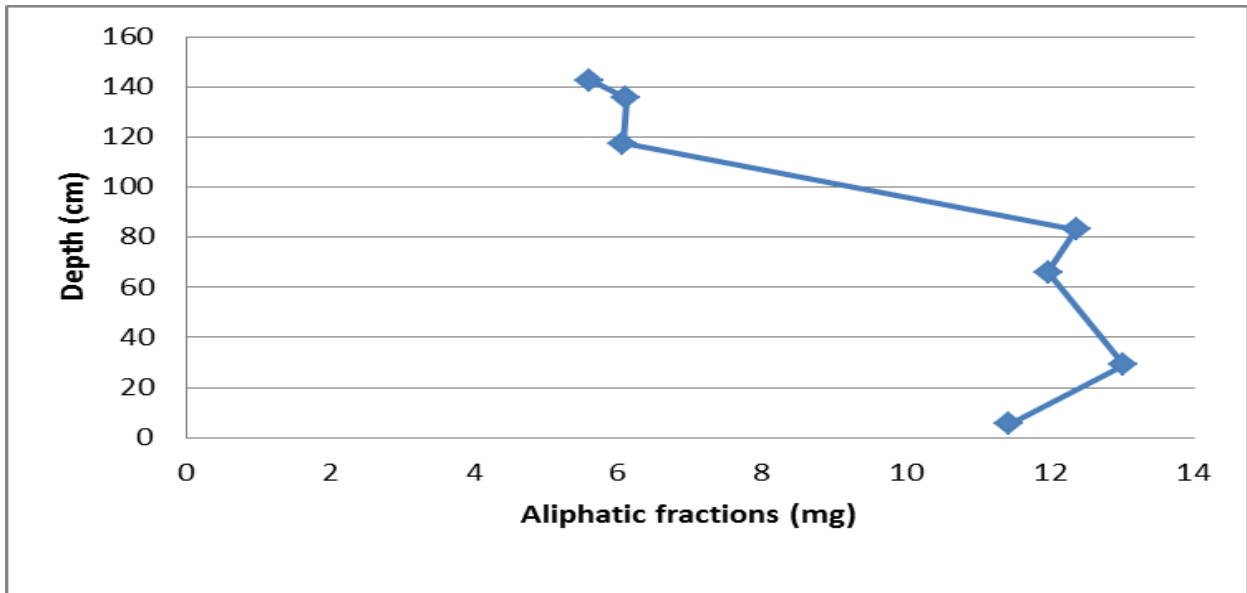
- Scott, A. C. (2002) Coal petrology and the origin of coal macerals: a way ahead? *International Journal of Coal Geology*, 50, pp 119-134.
- Seifert, W. K. (1978) Steranes and terpanes in kerogen pyrolysis for correlation of oils and source rocks. *Geochimica et Cosmochimica Acta*, 42, pp 473-484.
- Seifert, W. K., et al. 1980. Application of biological marker chemistry to petroleum exploration. In: Tenth world petroleum congress, Philadelphia. Heyden & sons, Inc, pp 425-440.
- Snowdon, L. R. (1991) Oil from Type III organic matter: resinite revisited. *Organic Geochemistry*, 17, pp 743-747.
- Stach, E. (1982) The macerals of coal. In: Stach, E., Mackowsky, M.-T., Teichmüller, M., Taylor, G. H., Chandra, D. & Teichmüller, R. (Eds.), *Stach's textbook of coal petrology*. 3rd ed. Berlin-Stuttgart: Gebruder Borntraeger, 3, pp 87-144.
- Svendsen, H., et al. (2002) The physical environment of Kongsfjorden-Krossfjorden, and Arctic fjord system in Svalbard. *Polar Research*, 21, pp 133-166.
- Sykes, R. & Snowdon, L. R. (2002) Guidelines for assessing the petroleum potential of coaly source rocks using Rock-Eval pyrolysis. *Organic Geochemistry*, 33, pp 1441-1455.
- Tatsch, J. H. (1980) Coal deposits: origin, evolution, and present characteristics, 1980. Trace Substances in Environmental Health: Proceedings of University of Missouri's Annual Conference on Trace Substances in Environmental Health, pp 6-14.
- Teichmüller, M. (1987) Recent advances in coalification studies and their application to geology. *Coal and Coal-bearing Strata: Recent Advances*, pp 127-169.
- Teichmüller, M. (1989) The genesis of coal from the viewpoint of coal petrology. *International Journal of Coal Geology*, 12, pp 1-87.
- Teichmüller, M. & Teichmüller, R. (1967) Diagenesis of Coal (Coalification). In: Gunnar Larsen & Chilingar, G. V. (Eds.), *Diagenesis in sediments*. Elsevier, pp 391-415.
- Teichmüller, M. & Teichmüller, R. (1979) Chapter 5 Diagenesis of Coal (Coalification). pp 207-246.
- Teichmüller, M. & Teichmüller, R. (1982) The geological basis of coal formation. In: Stach, E., Mackowsky, M. T., Teichmüller, M., Taylor, G. H., Chandra, D. & Teichmüller, R. (Eds.), *Stach's textbook of coal petrology*. Berlin: Gebruder Borntraeger, pp 5-82.
- Thomas, L. (1992) *Handbook of practical coal geology*, Chichester: John Wiley & Sons, pp 55-60.
- Tissot, B. (1969) Preliminary data on mechanics and kinetics of oil formation in sediments. computer simulation of geochemical reactions. 24, pp 470-501.
- Tissot, B. P. (1988) *Migration of Hydrocarbons in Sedimentary Basins: Geological and Geochemical Aspects*

- La migration des hydrocarbures dans les bassins sedimentaires: aspects geologiques et geochemiques. *Revue de l'Institut Francais du Petrole*, 43, pp 143-153.
- Tissot, B. P., et al. (1987) Thermal history of sedimentary basins, maturation indices, and kinetics of oil and gas generation. *American Association of Petroleum Geologists Bulletin*, 71, pp 1445-1466.
- Tissot, B. P. & Welte, D. H. (1984) *Petroleum formation and occurrence*, Berlin: Springer, pp 229-253.
- Uguna, C. 2007. Effect of water pressure on hydrocarbon generation, maturation and cracking. PhD Thesis, University of Nottingham.
- Van Krevelen, D. W. (1982) Development of coal research-a review. *Fuel*, 61, pp 786-790.
- Van Krevelen, D. W. (1984) Organic geochemistry--old and new. *Organic Geochemistry*, 6, pp 1-10.
- Vandenbroucke, M. & Largeau, C. (2007) Kerogen origin, evolution and structure. *Organic Geochemistry*, 38, pp 719-833.
- Verheyen, T. V., et al. (1984) An evaluation of Rock-Eval pyrolysis for the study of Australian coals including their kerogen and humic acid fractions. *Geochimica et Cosmochimica Acta*, 48, pp 63-70.
- Vincent, P. W., et al. (1985) Hydrocarbon generation, migration and entrapment in the Jackson-Nacowlah area, atp 259p, South-Western Queensland. *APEA journal*, 25, pp 62-84.
- Volkman, J. K., et al. (1983) A geochemical reconstruction of oil generation in the Barrow Sub-basin of Western Australia. *Geochimica et Cosmochimica Acta*, 47, pp 2091-2105.
- Ward, C. R. (1984) *Coal geology and coal technology*, Boston: Blackwell Scientific Publications, pp 1-40.
- Wilkins, R. W. T., et al. (2002) Comparison of two petrographic methods for determining the degree of anomalous vitrinite reflectance. *International Journal of Coal Geology*, 52, pp 45-62.
- Wilkins, R. W. T. & George, S. C. (2002) Coal as a source rock for oil: a review. *International Journal of Coal Geology*, 50, pp 317-361.
- Worsley, D. (1986) *Evolution of an Arctic archipelago; The Geological History of Svalbard*, Statoil, 121pp. pp.
- Zhao, C. & Cheng, K. (1998) Expulsion and primary migration of the oil derived from coal. *Science China Earth Sciences*, 41, pp 345-353.
- Zumberge, J. E. (1987b) Terpenoid biomarker distribution in low maturity crude oils. *Organic Geochemistry*, 11, pp 479-496.

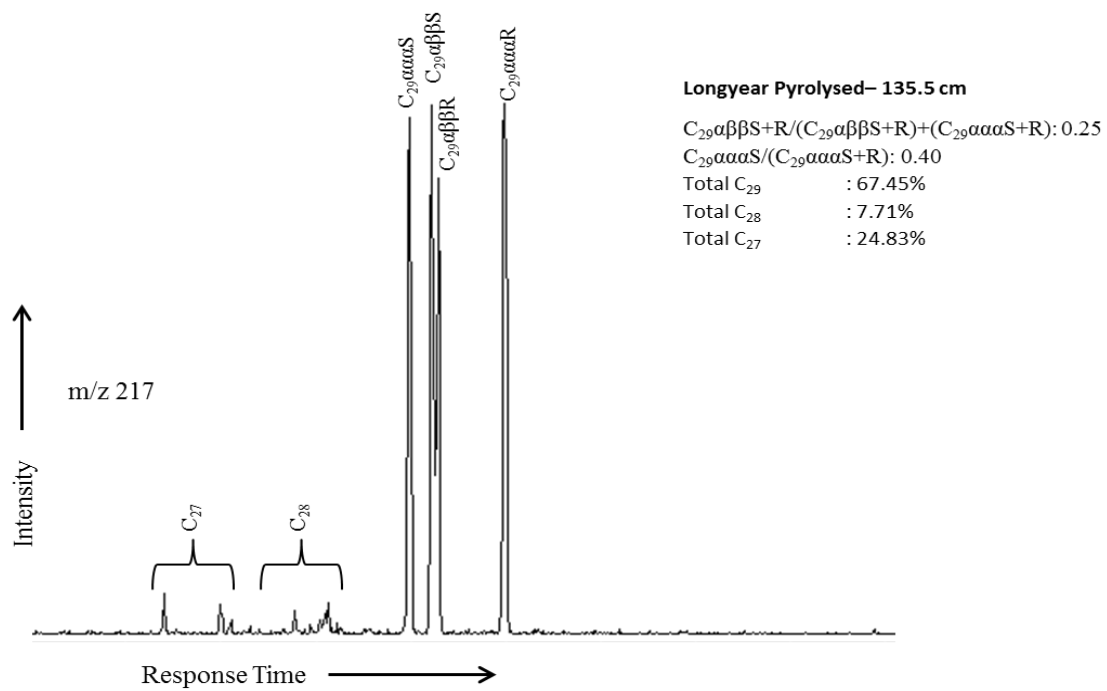
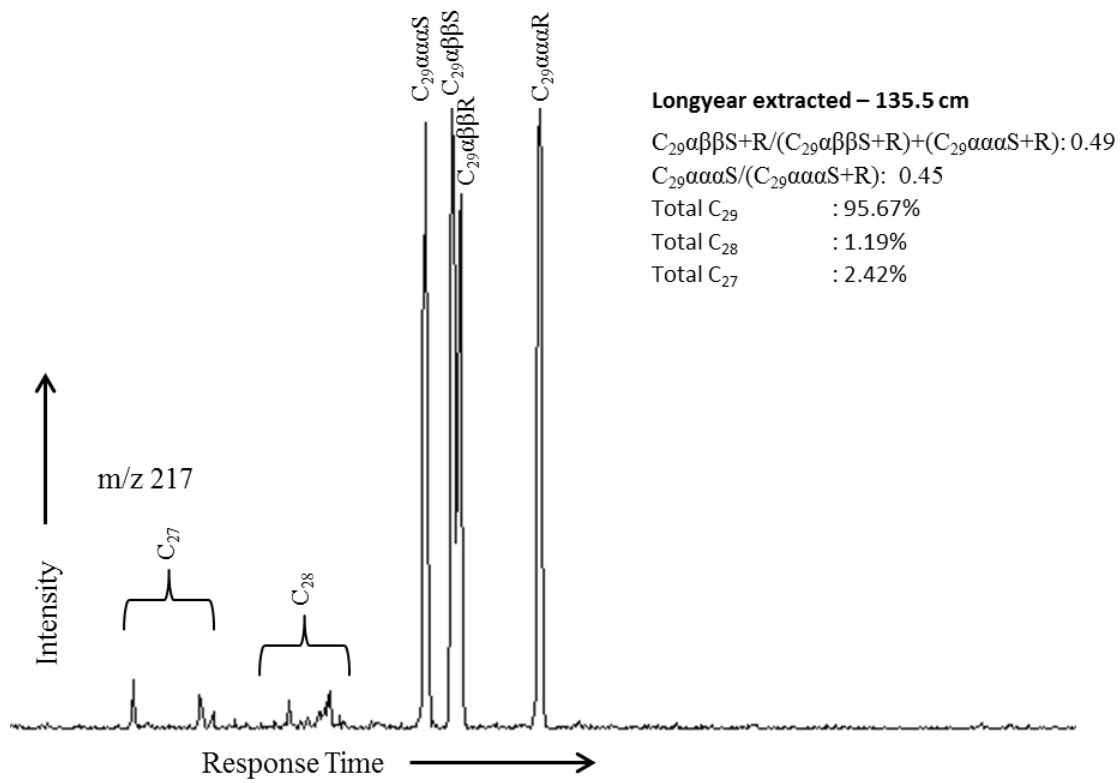
APPENDIX A-Figures



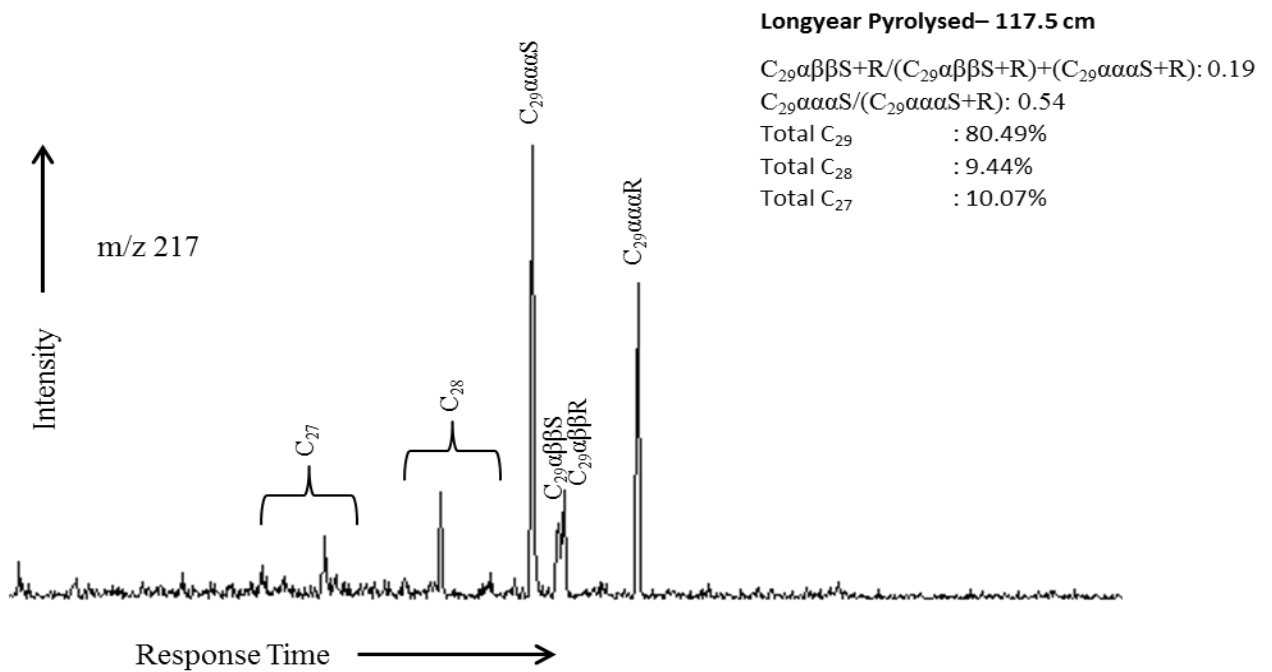
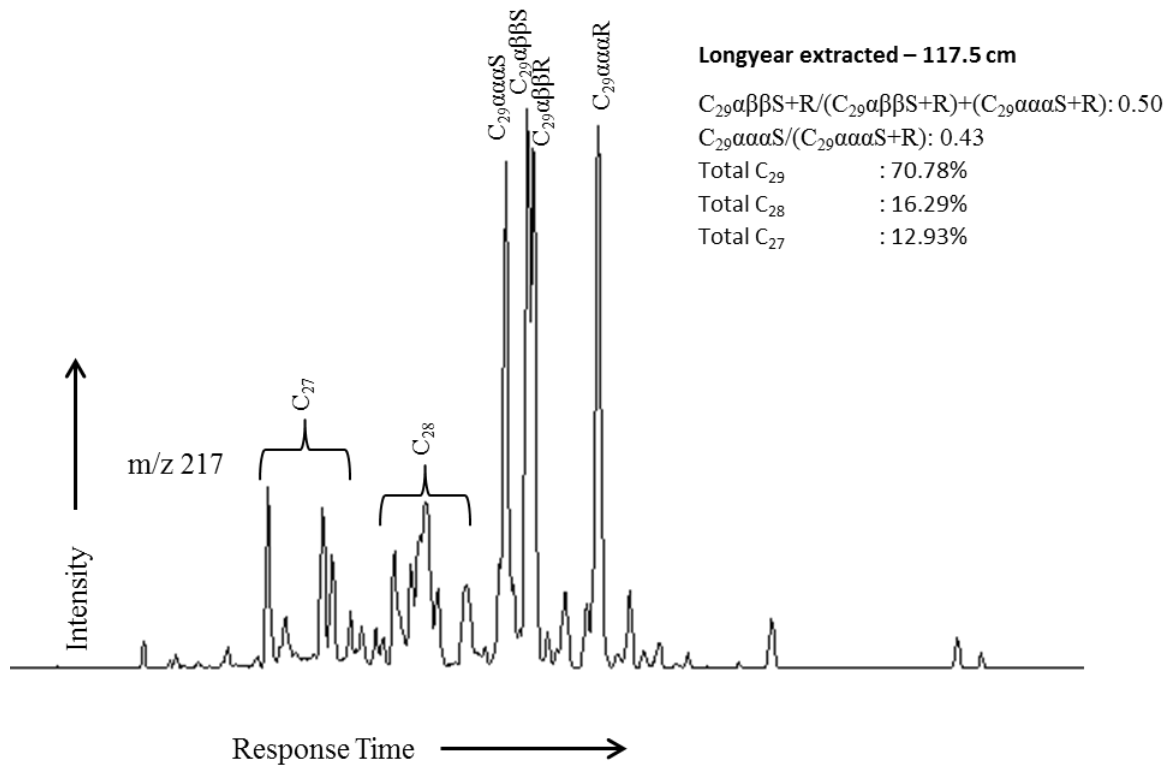
A1: Full profile of extractable bitumen from the Longyear seam. This profile shows experiments carried out on more samples



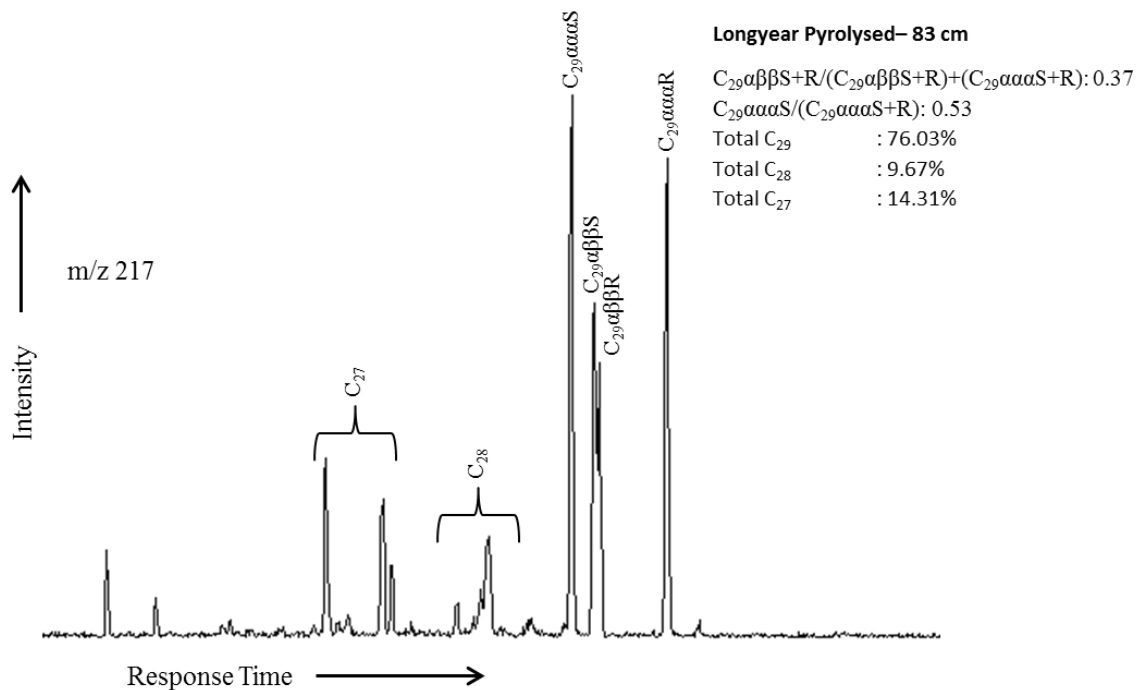
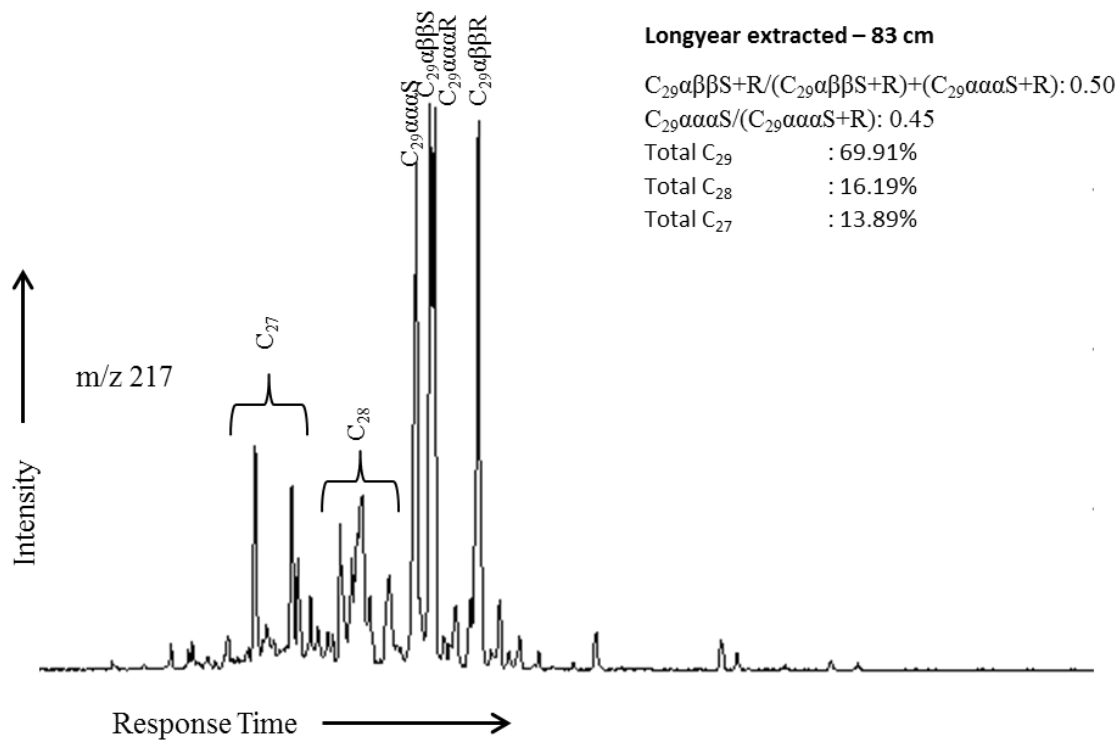
A2: Change in percentage of aliphatic fractions with depth of the Longyear seam. This profile shows added sample at the upper portion of the seam.



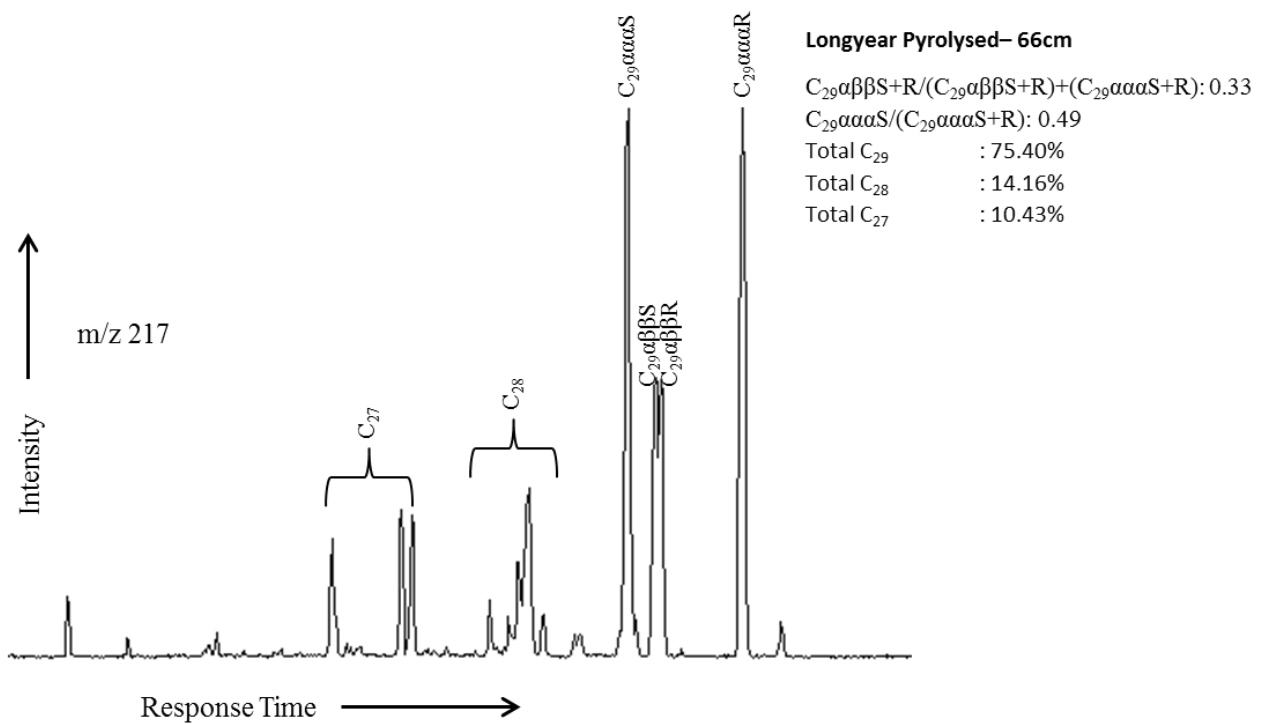
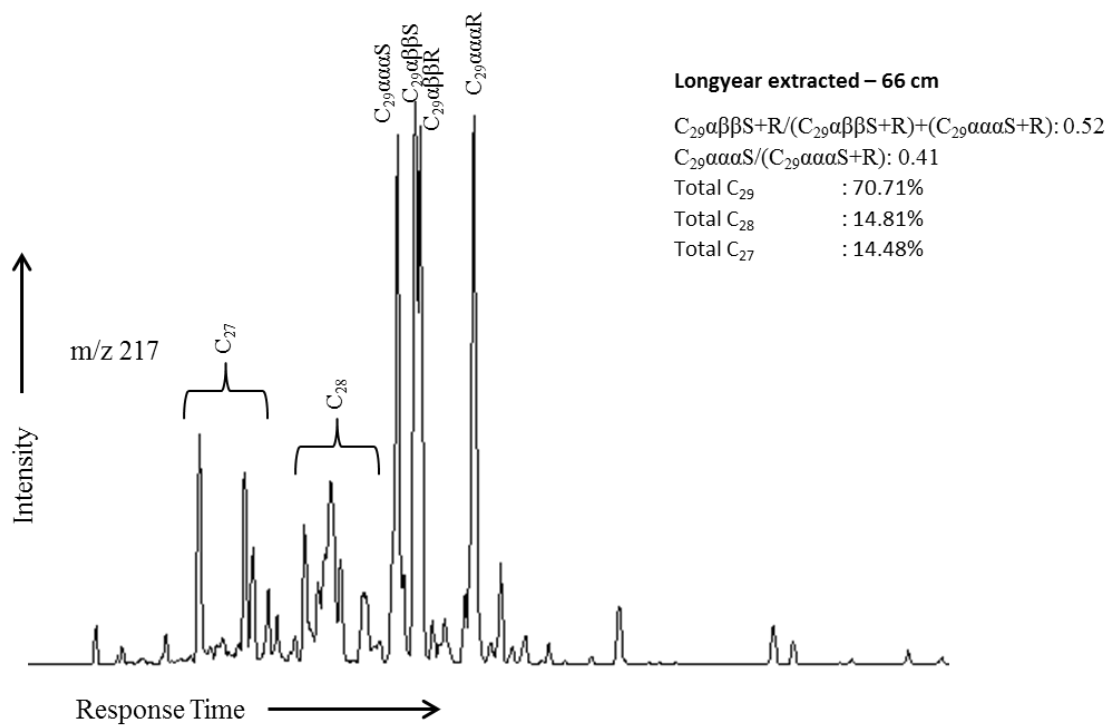
A3: Sterane chromatograms from the aliphatic content of the long year seam at 135.5 cm.



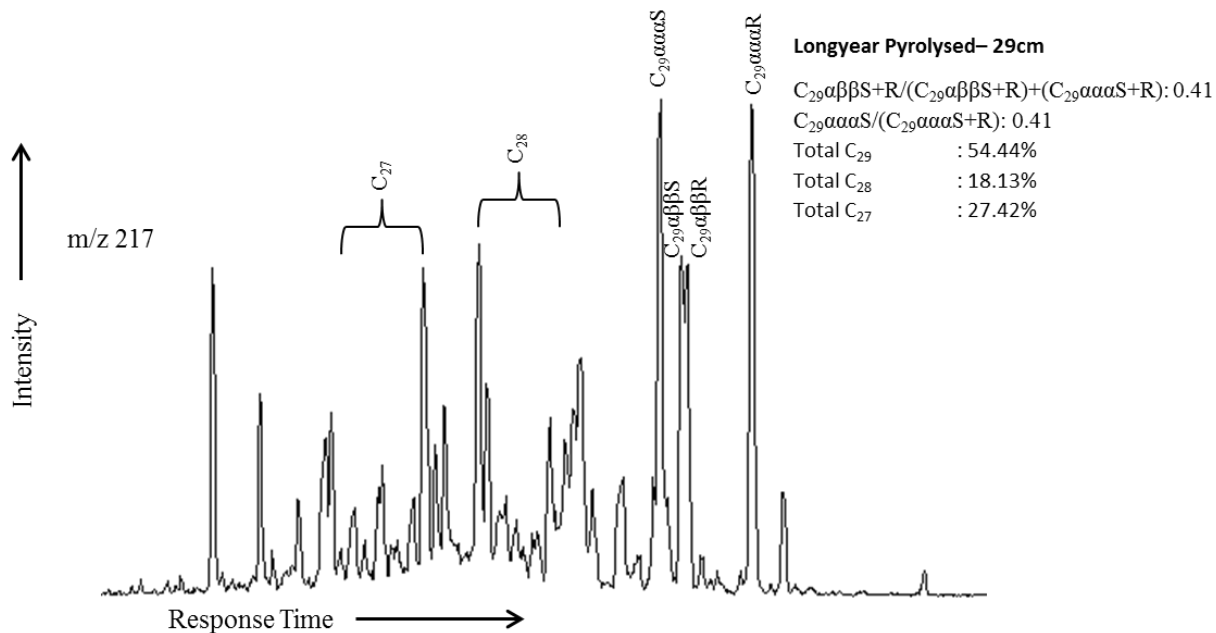
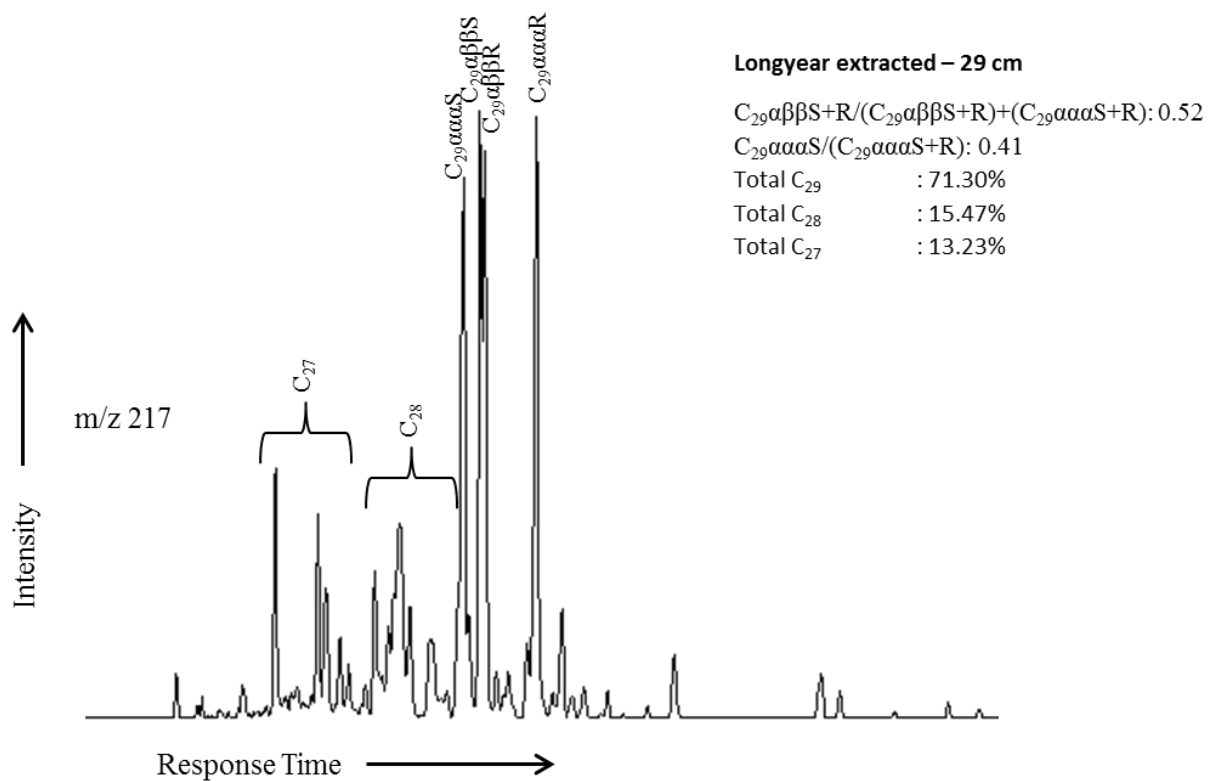
A4: Sterane chromatograms from the aliphatic content of the long year seam at 117.5 cm.



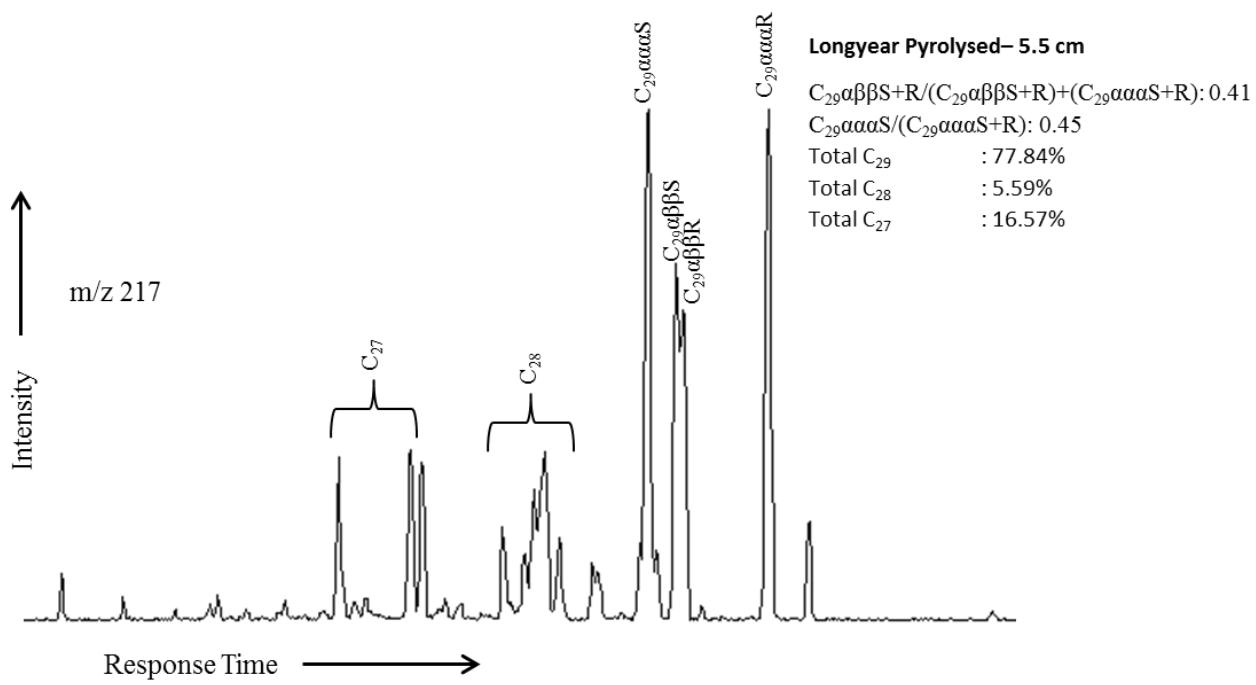
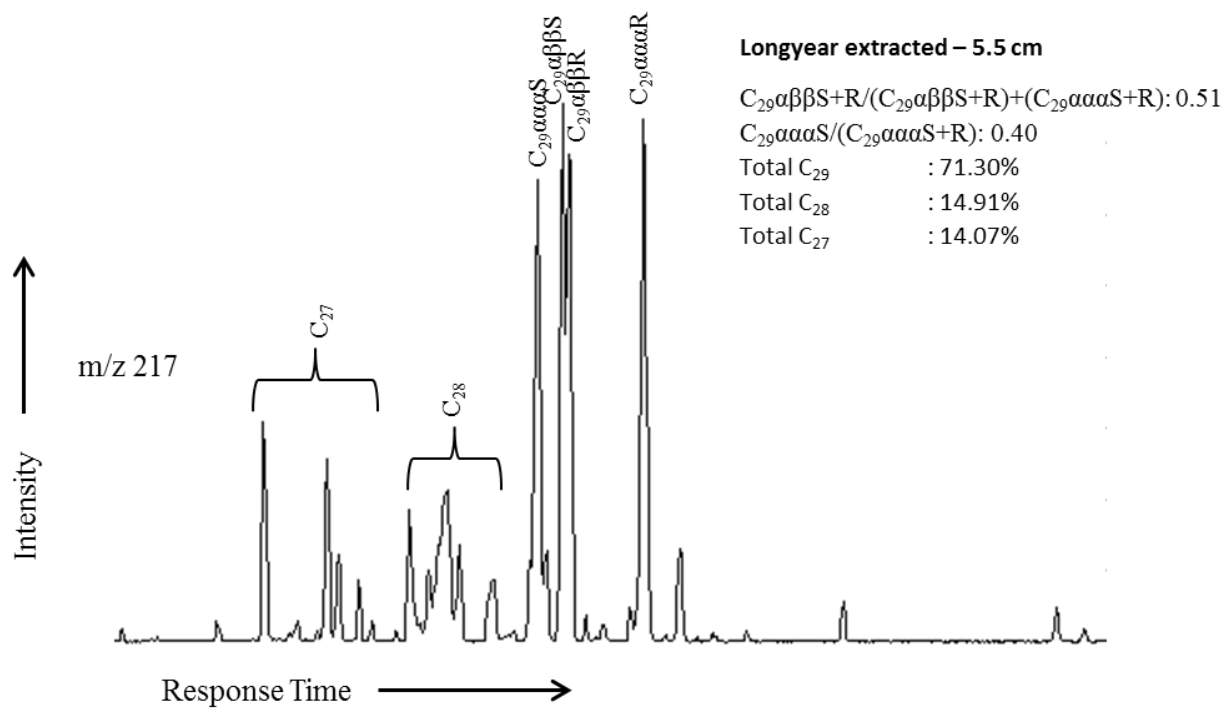
A5: Sterane chromatograms from the aliphatic content of the long year seam at 83 cm.



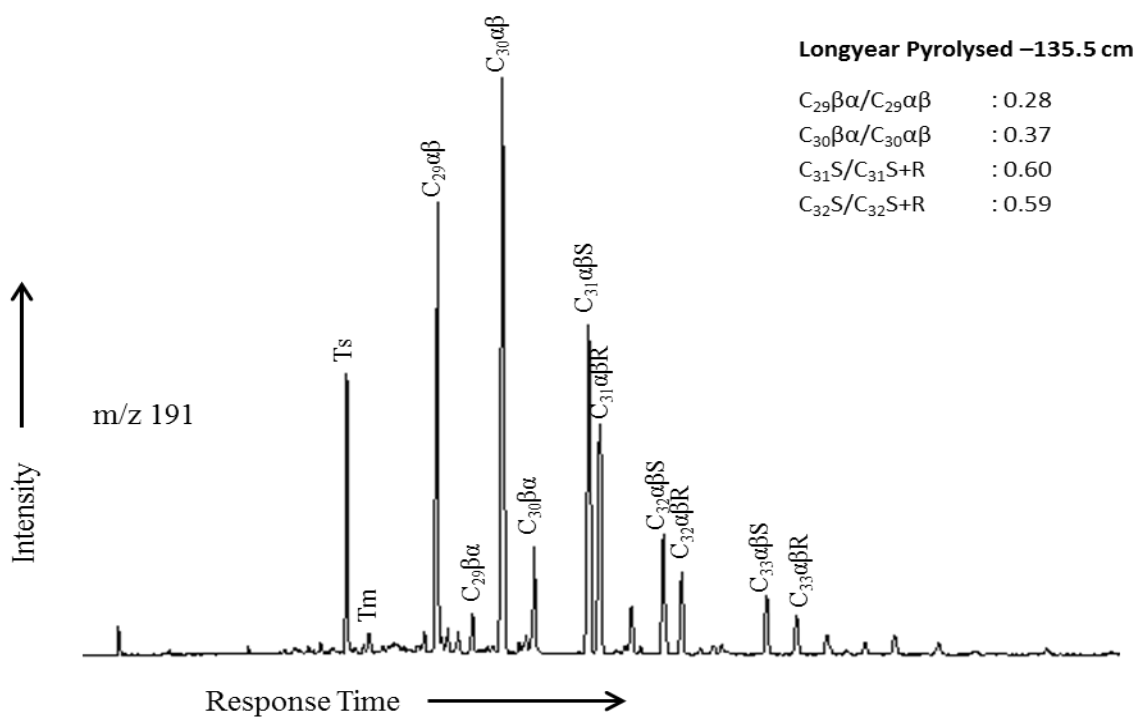
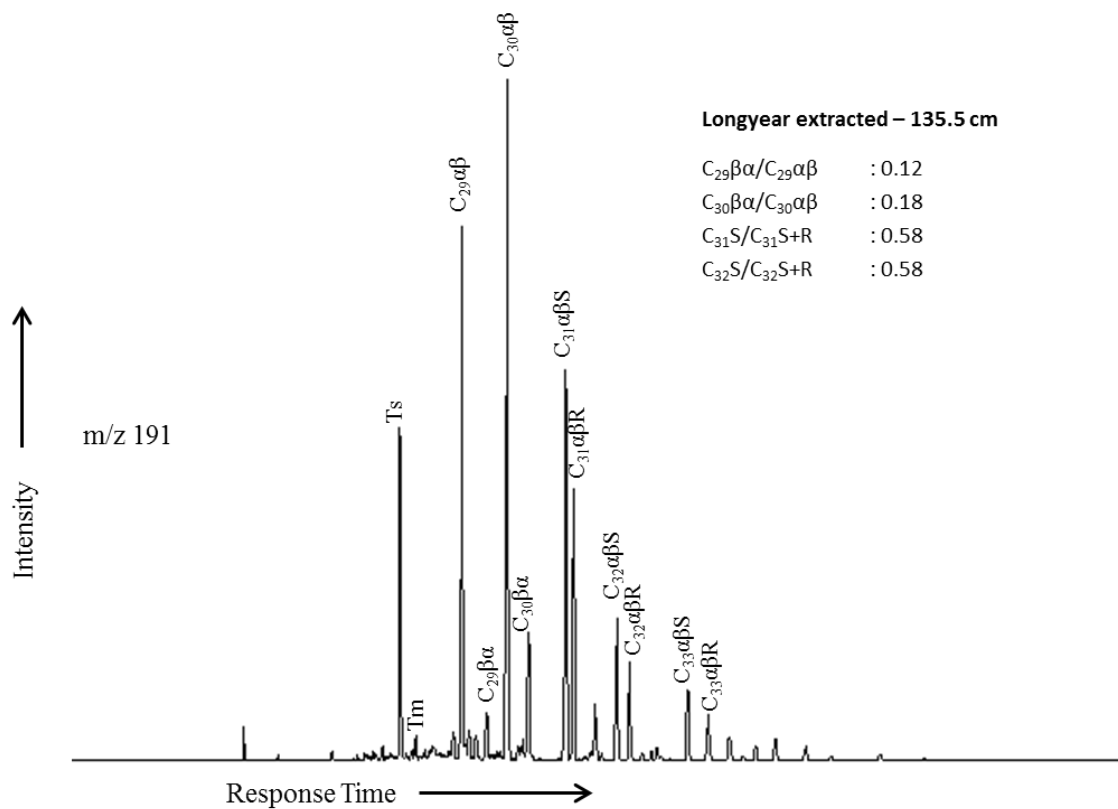
A6: Sterane chromatograms from the aliphatic content of the long year seam at 66 cm.



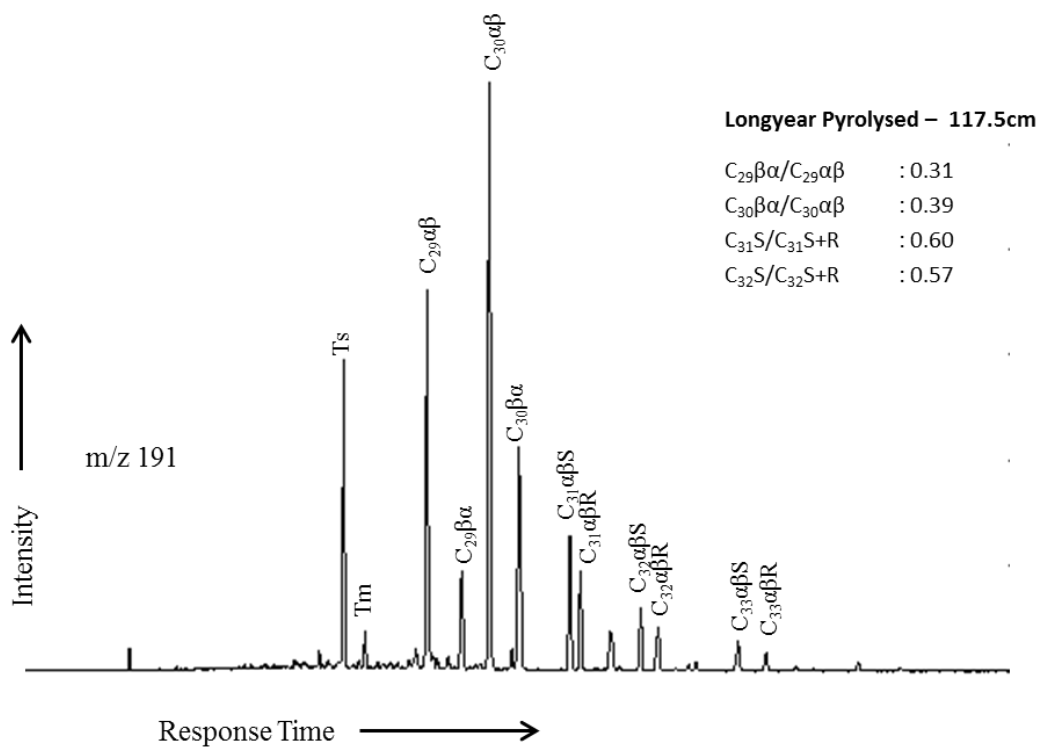
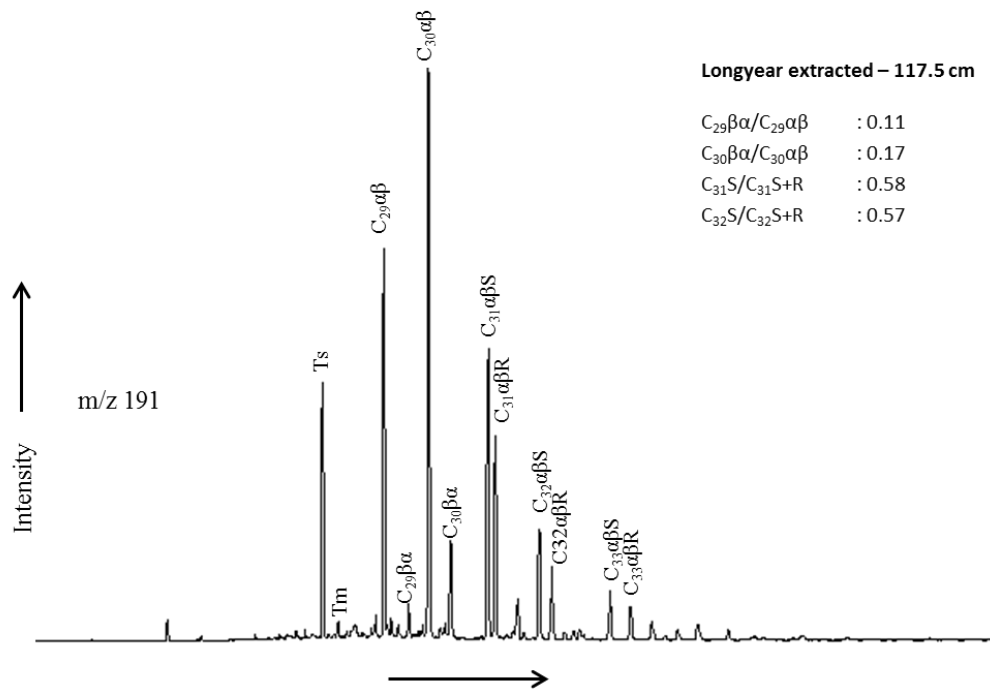
A7: Sterane chromatograms from the aliphatic content of the long year seam at 29 cm.



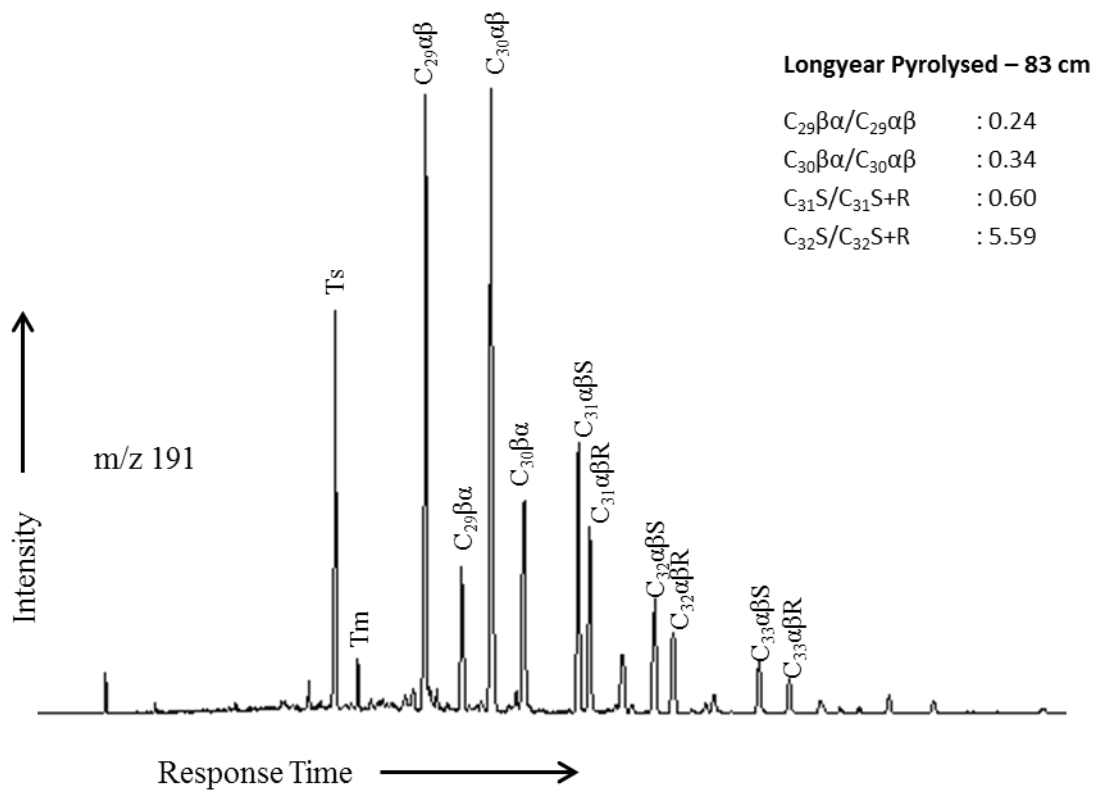
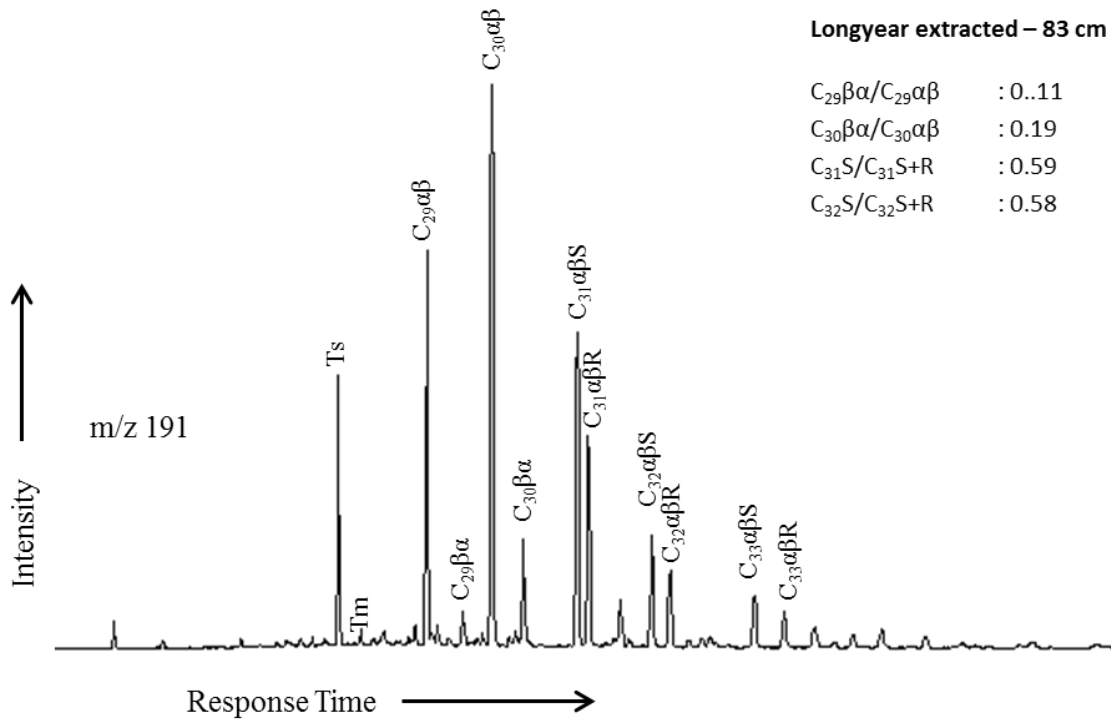
A9: Sterane chromatograms from the aliphatic content of the long year seam at 5.5 cm.



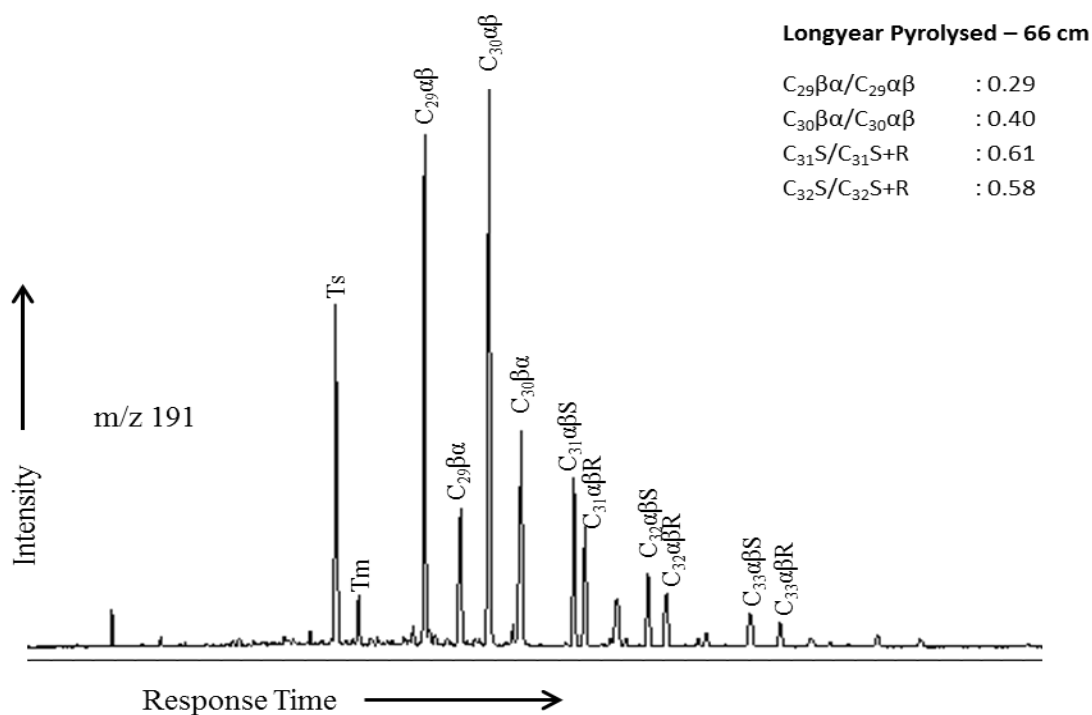
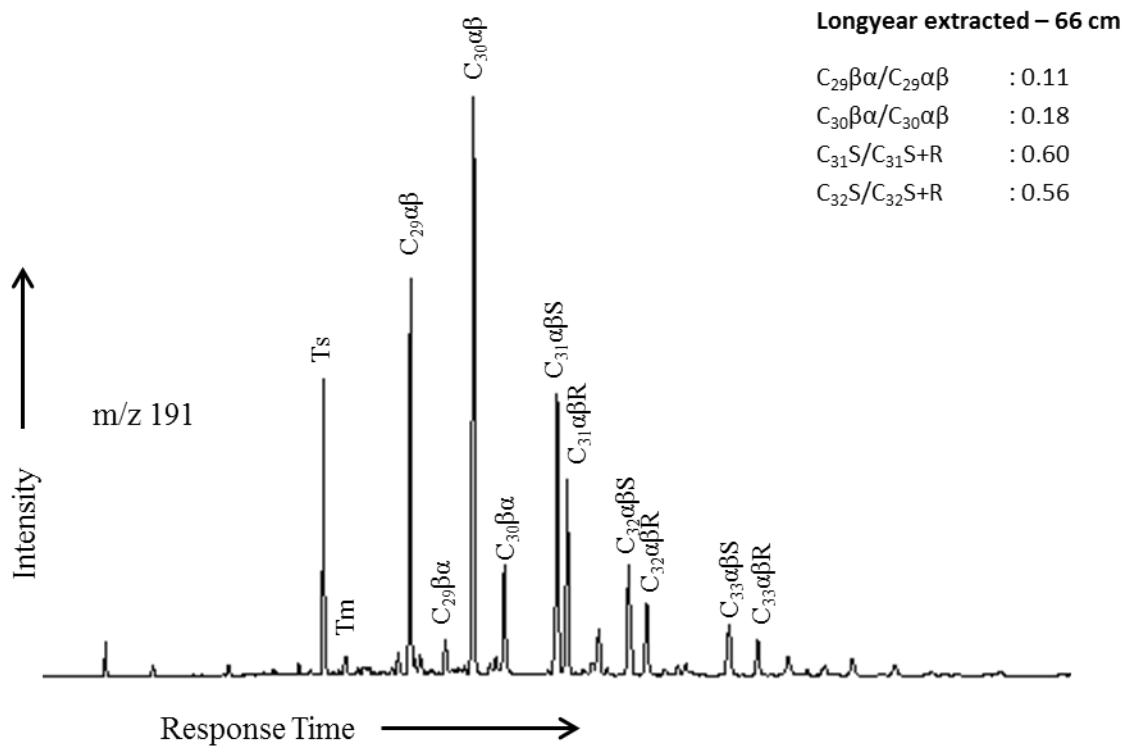
A9: Hopane chromatograms from the aliphatic composition of the Longyear seam at 135.5 cm



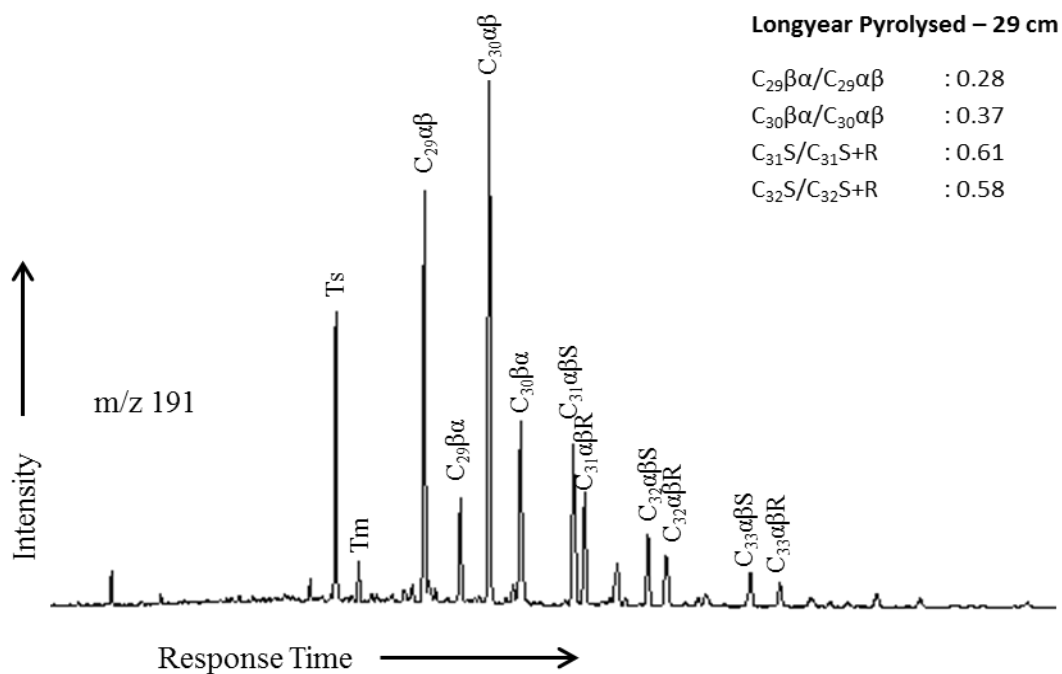
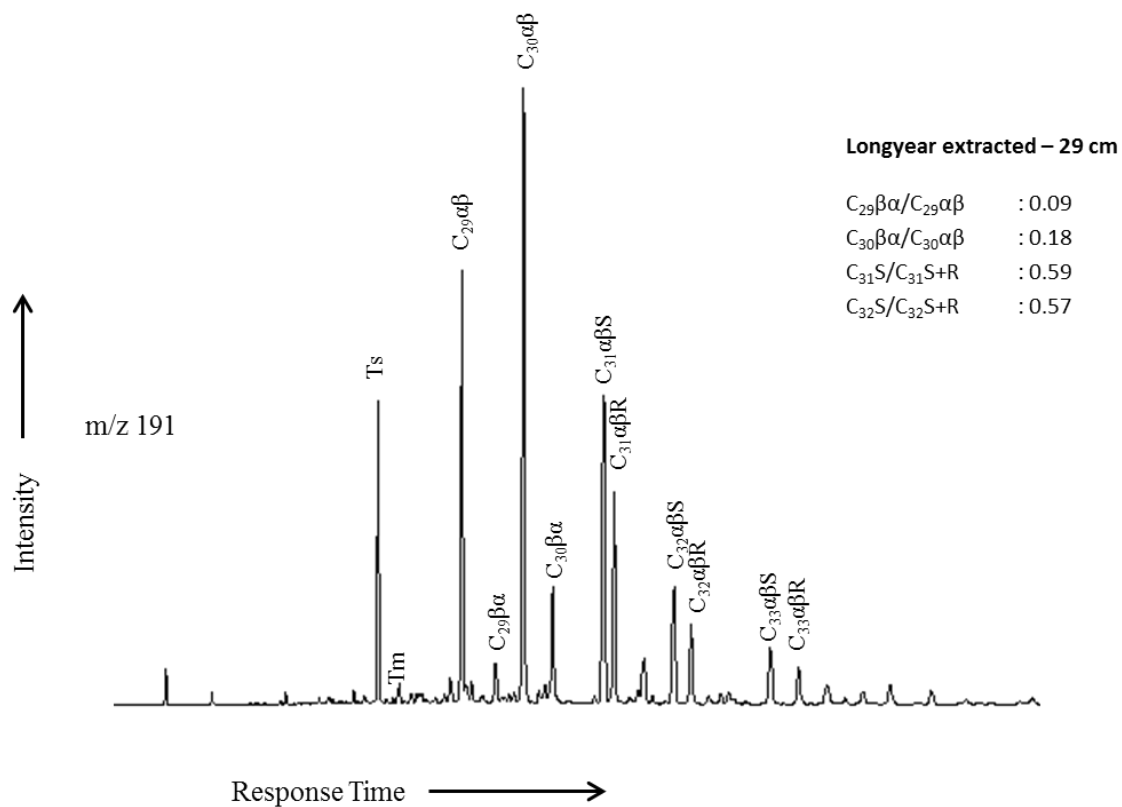
A10: Hopane chromatograms from the aliphatic composition of the Longyear seam at 117.5 cm.



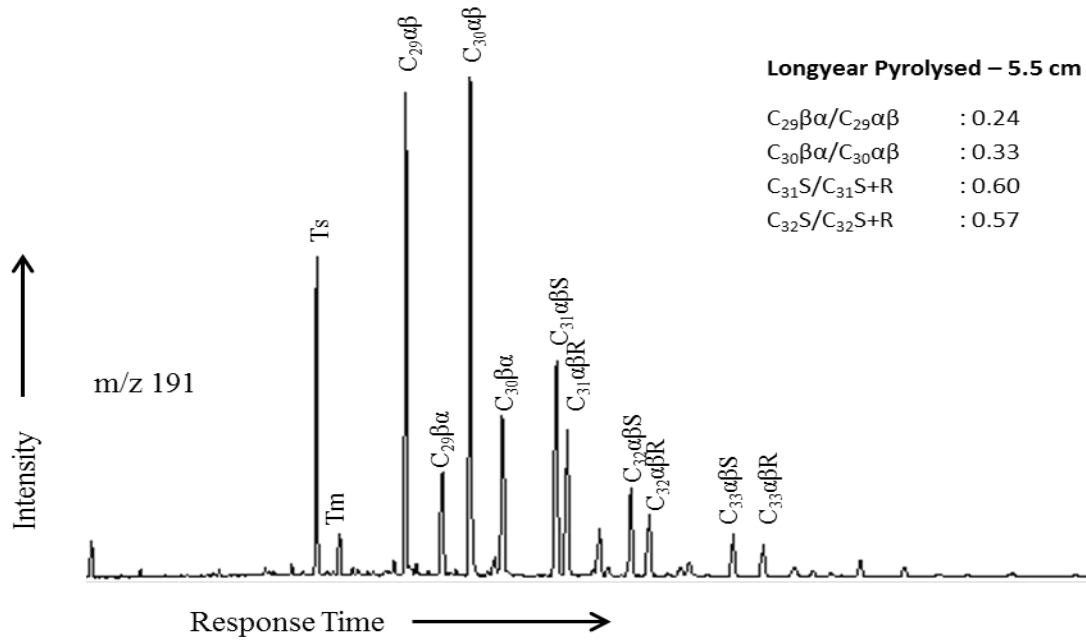
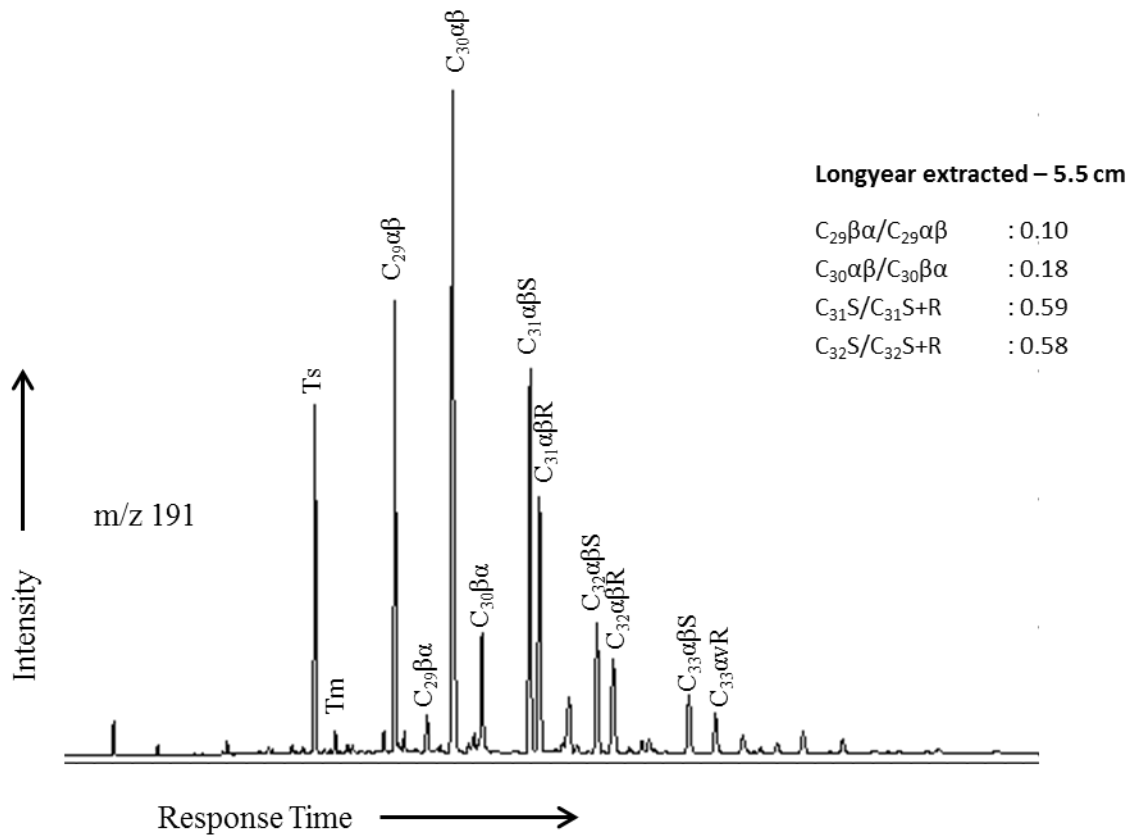
A11: Hopane chromatograms from the aliphatic composition of the Longyear seam at 83 cm.



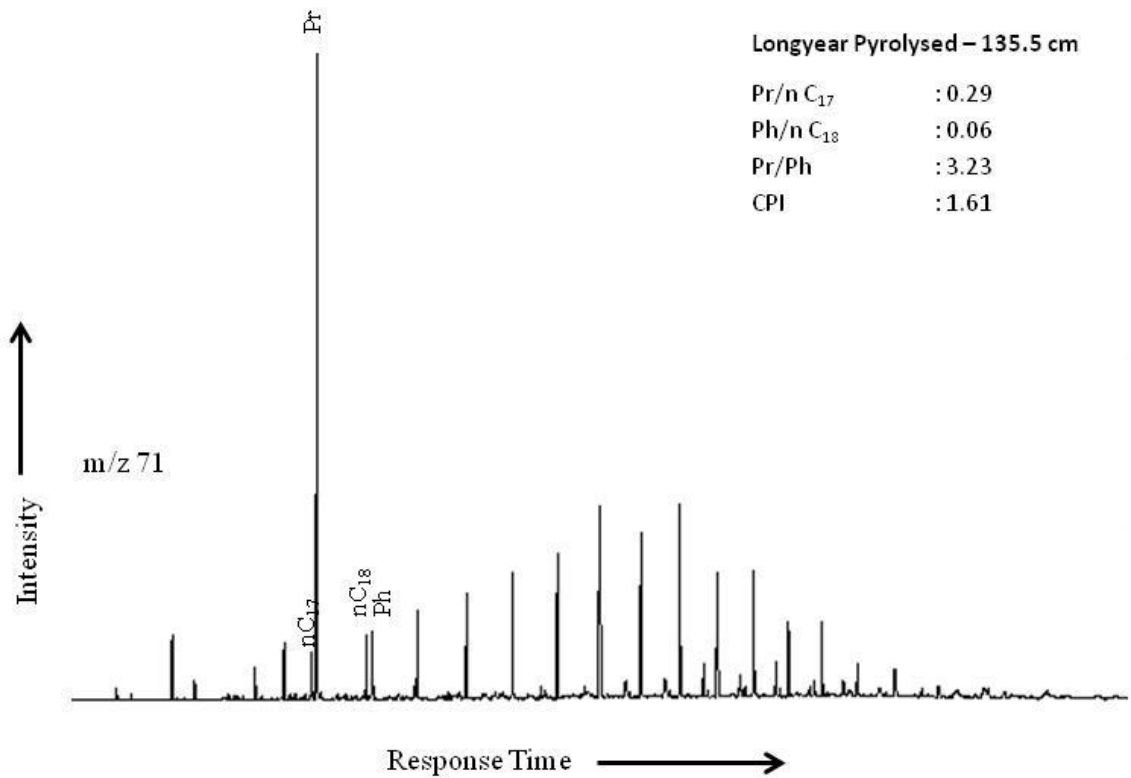
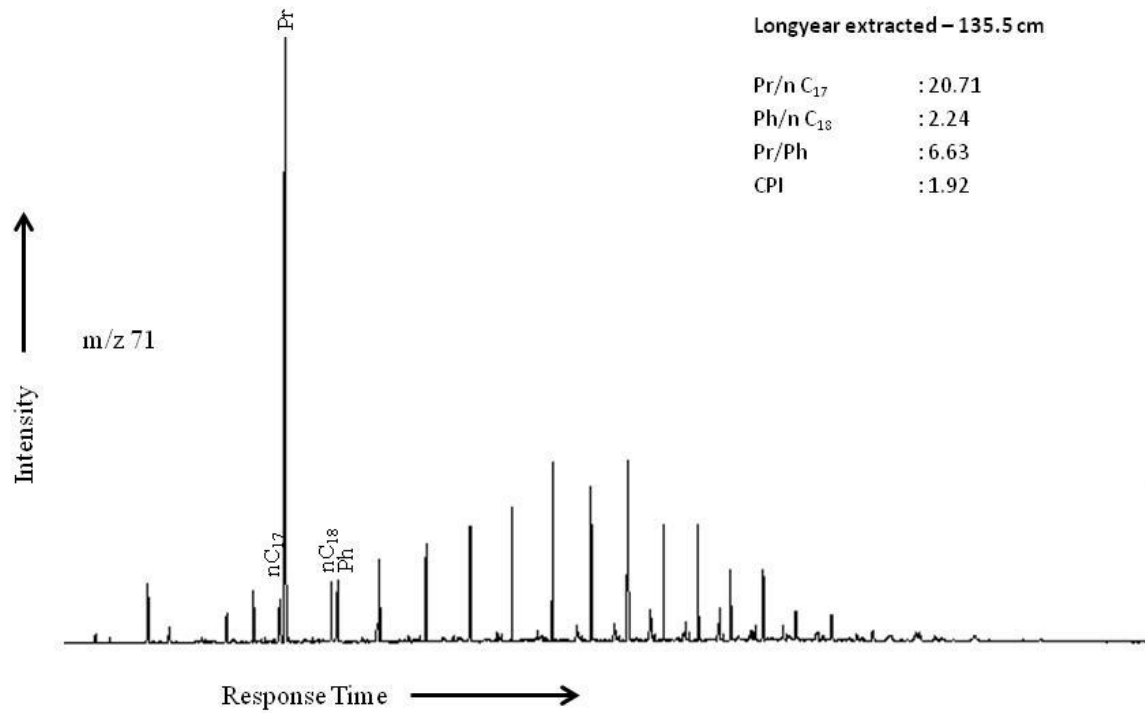
A12: Hopane chromatograms from the aliphatic composition of the Longyear seam at 66 cm.



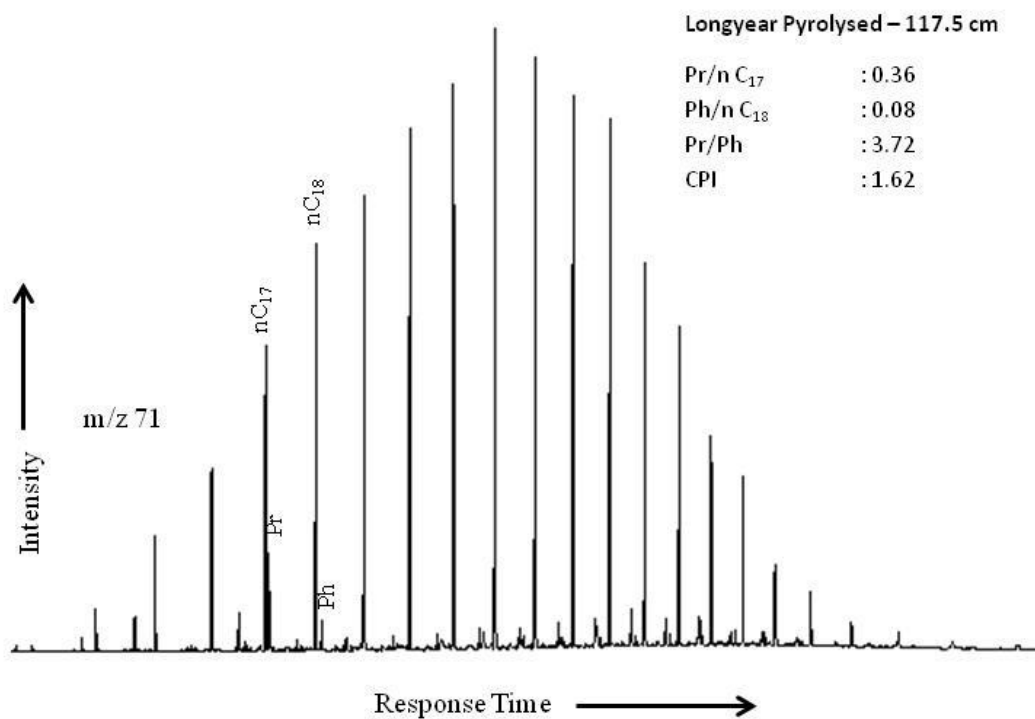
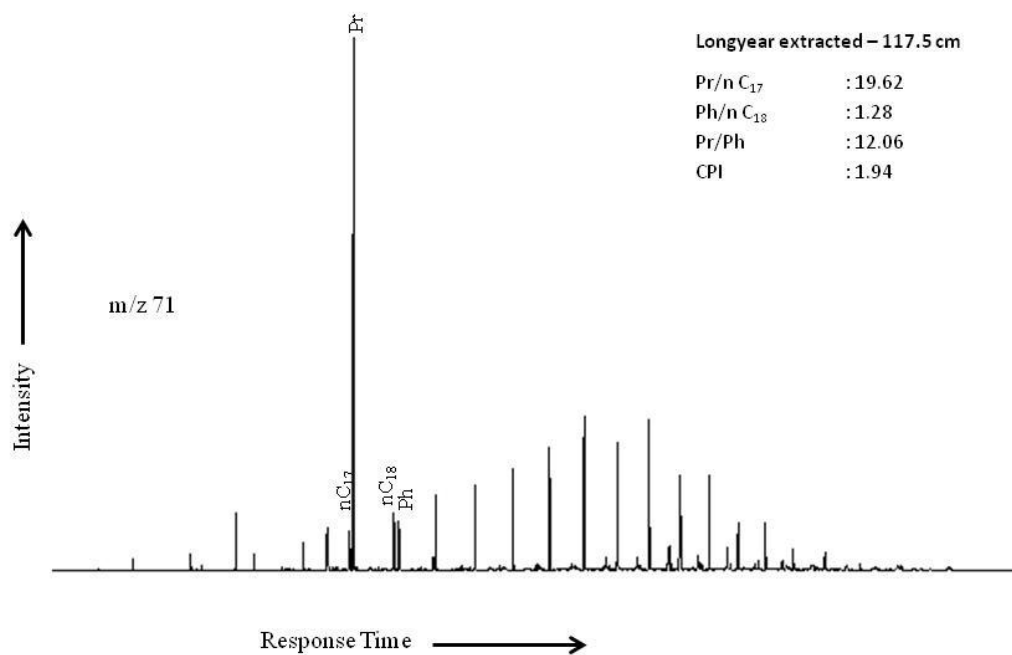
A13: Hopane chromatograms from the aliphatic composition of the Longyear seam at 29 cm.



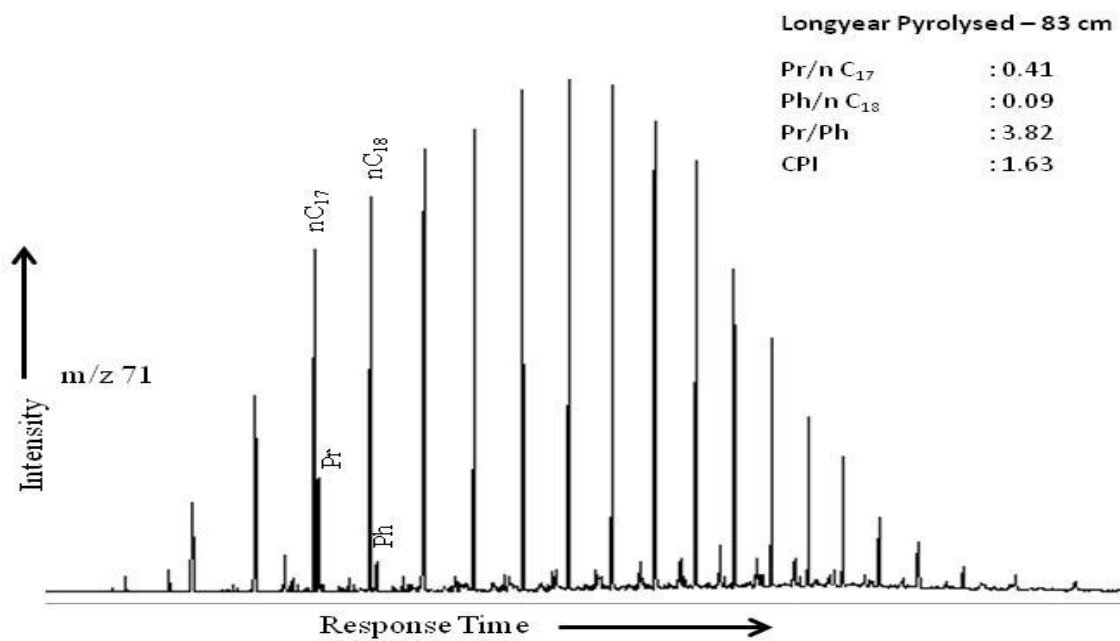
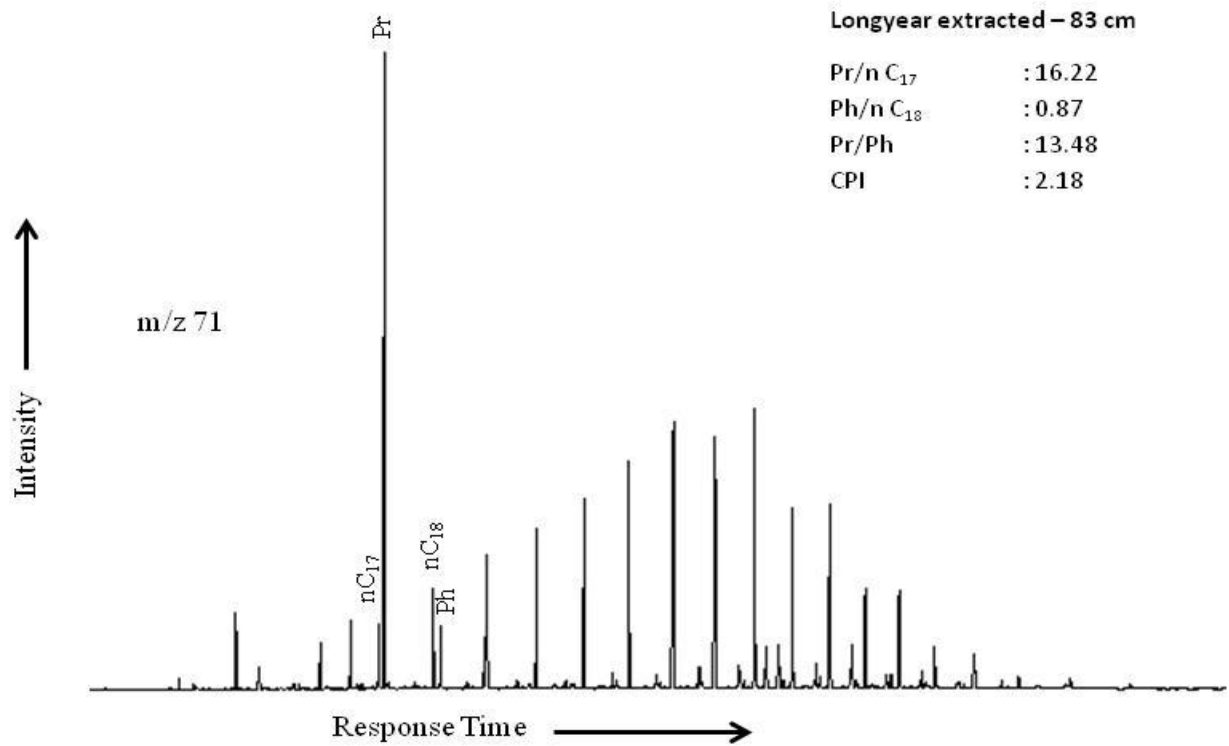
A14: Hopane chromatograms from the aliphatic composition of the Longyear seam at 5.5 cm.



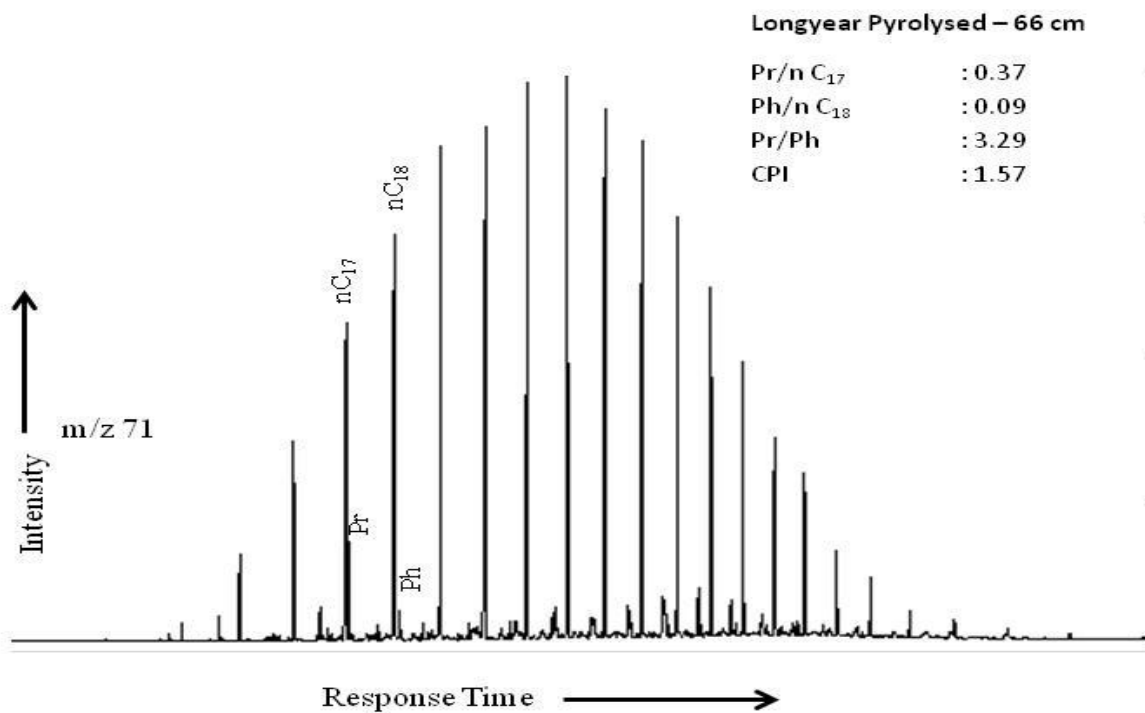
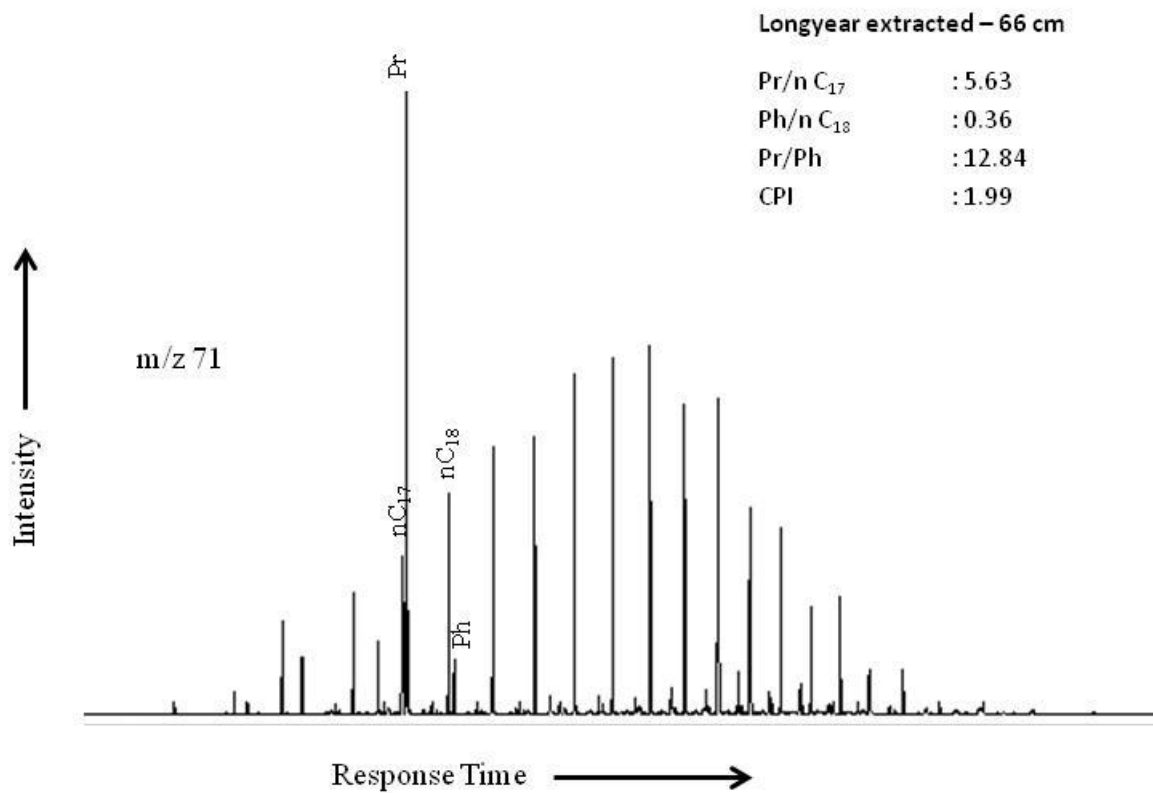
A15: Isoprenoid/n-alkane chromatograms from the aliphatic composition of the Longyear seam at 135.5 cm.



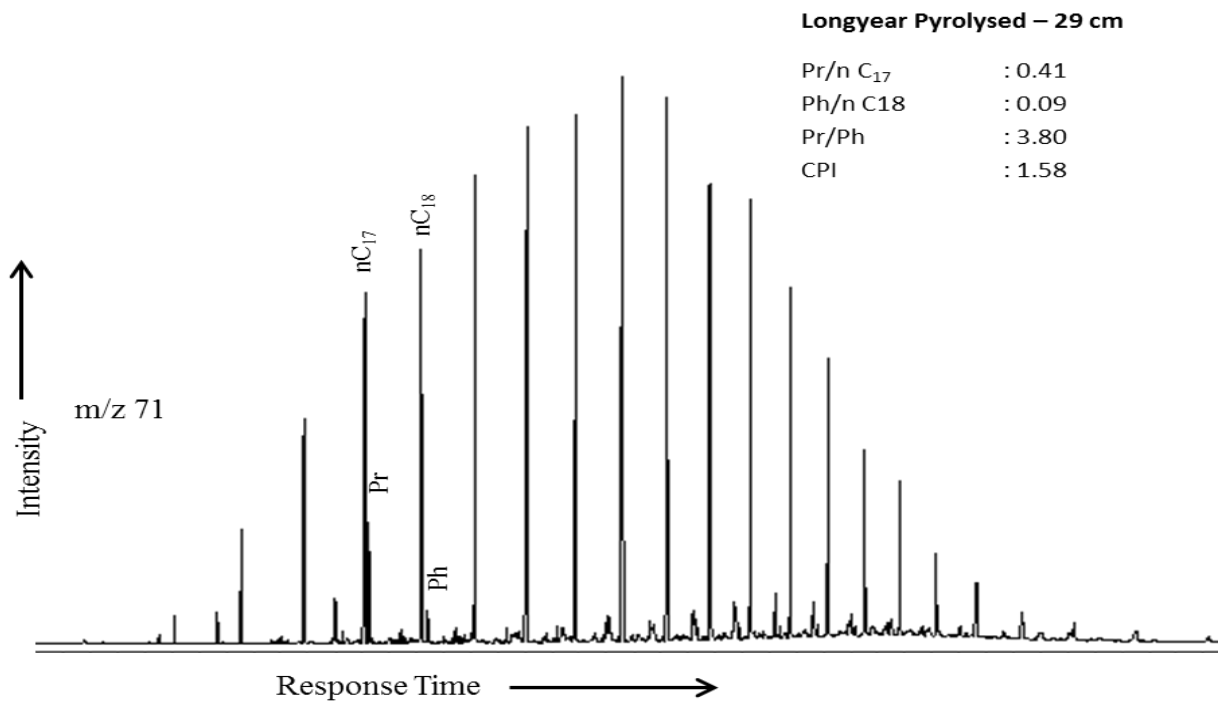
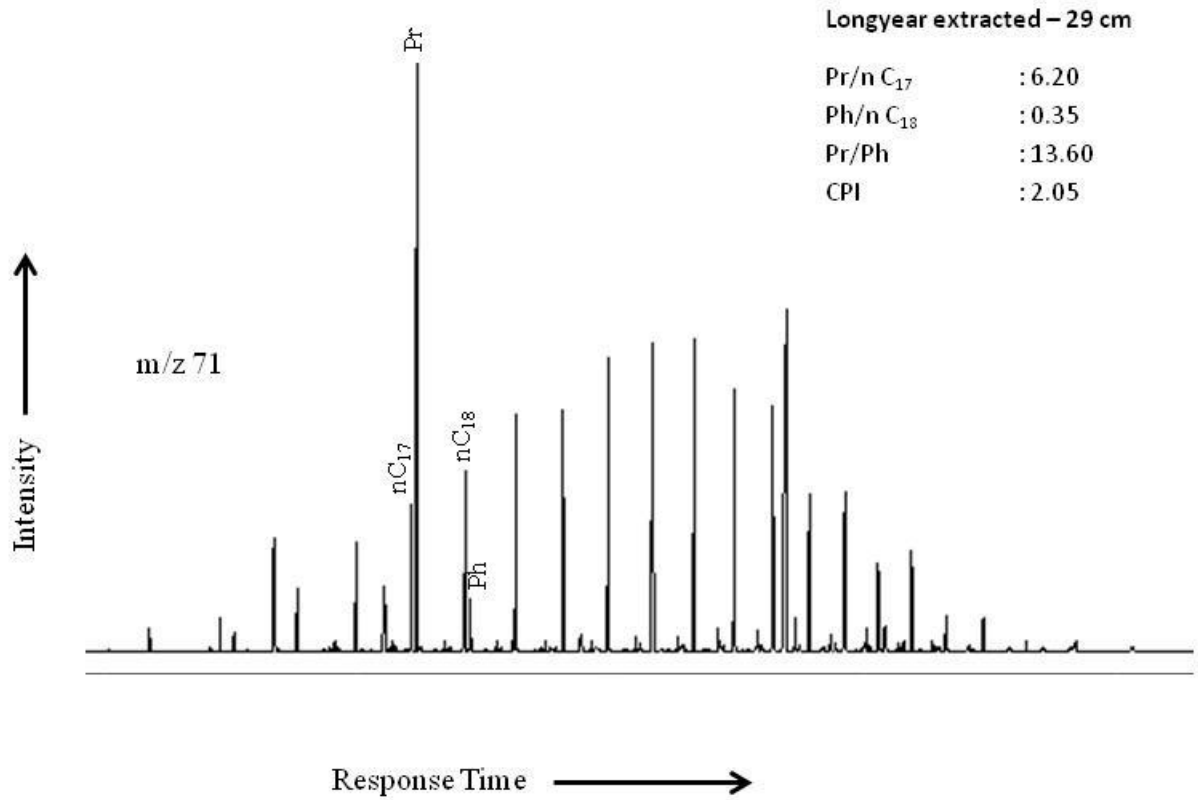
A16: Isoprenoid/n-alkane chromatograms from the aliphatic composition of the Longyear seam at 117.5 cm.



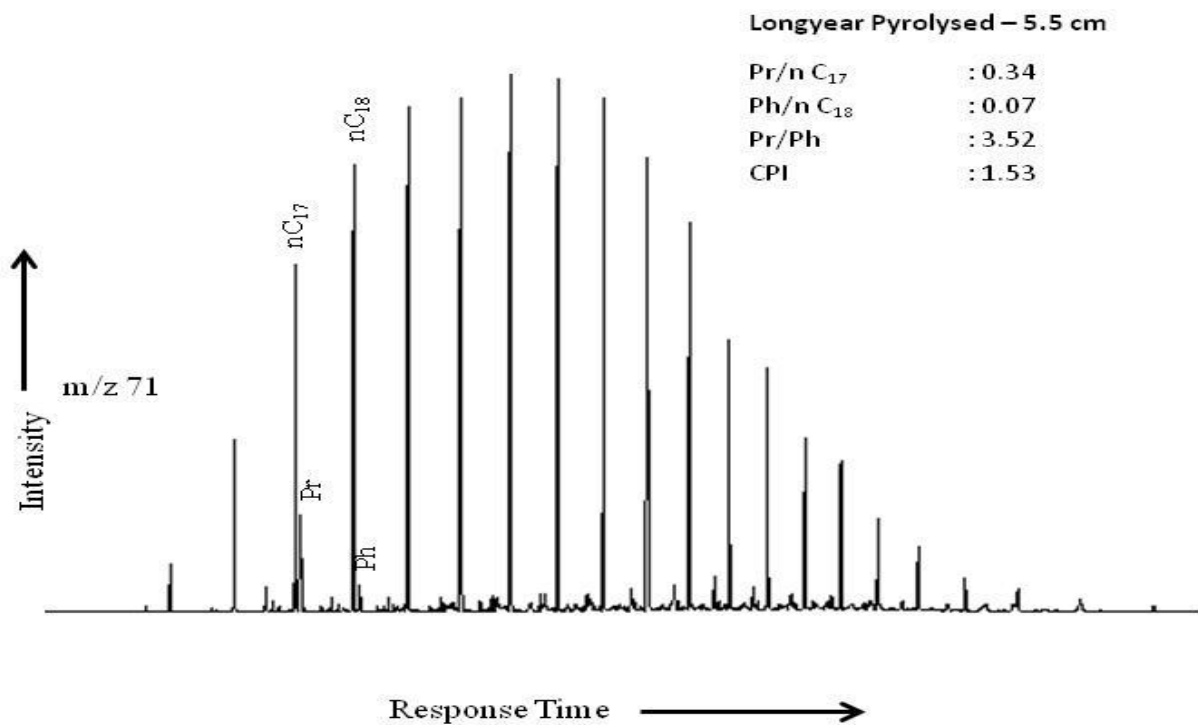
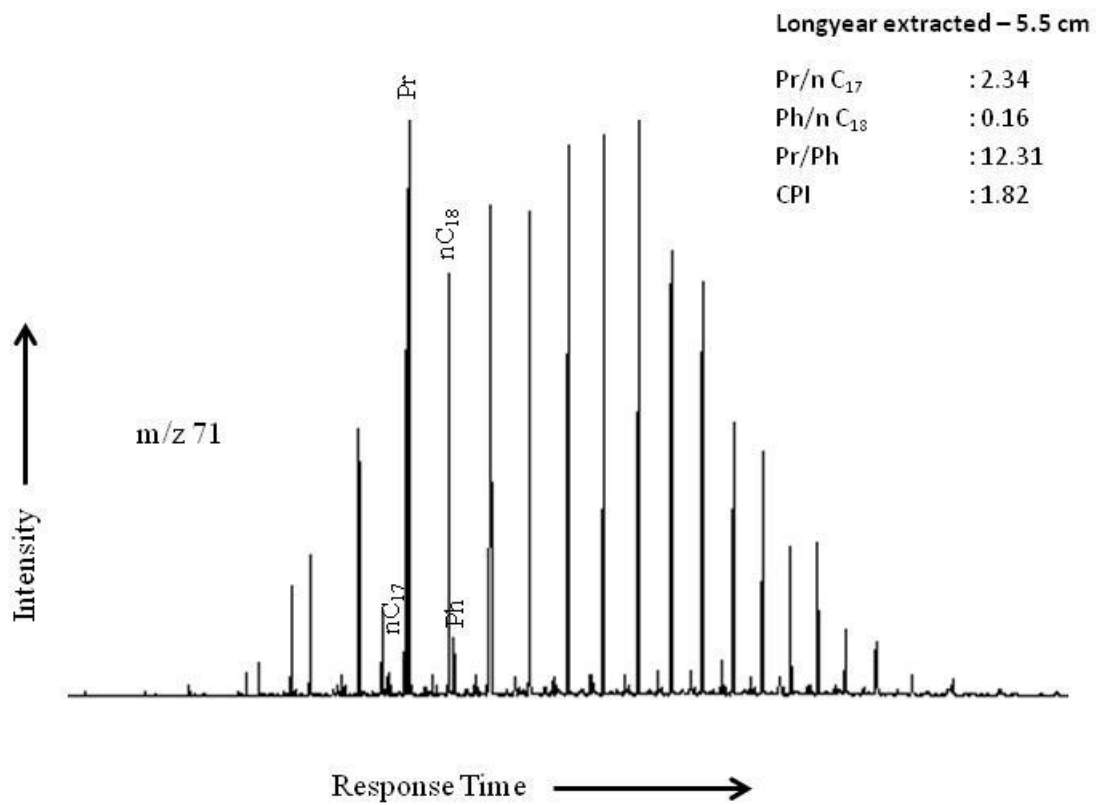
A17: Isoprenoid/n-alkane chromatograms from the aliphatic composition of the Longyear seam at 83 cm.



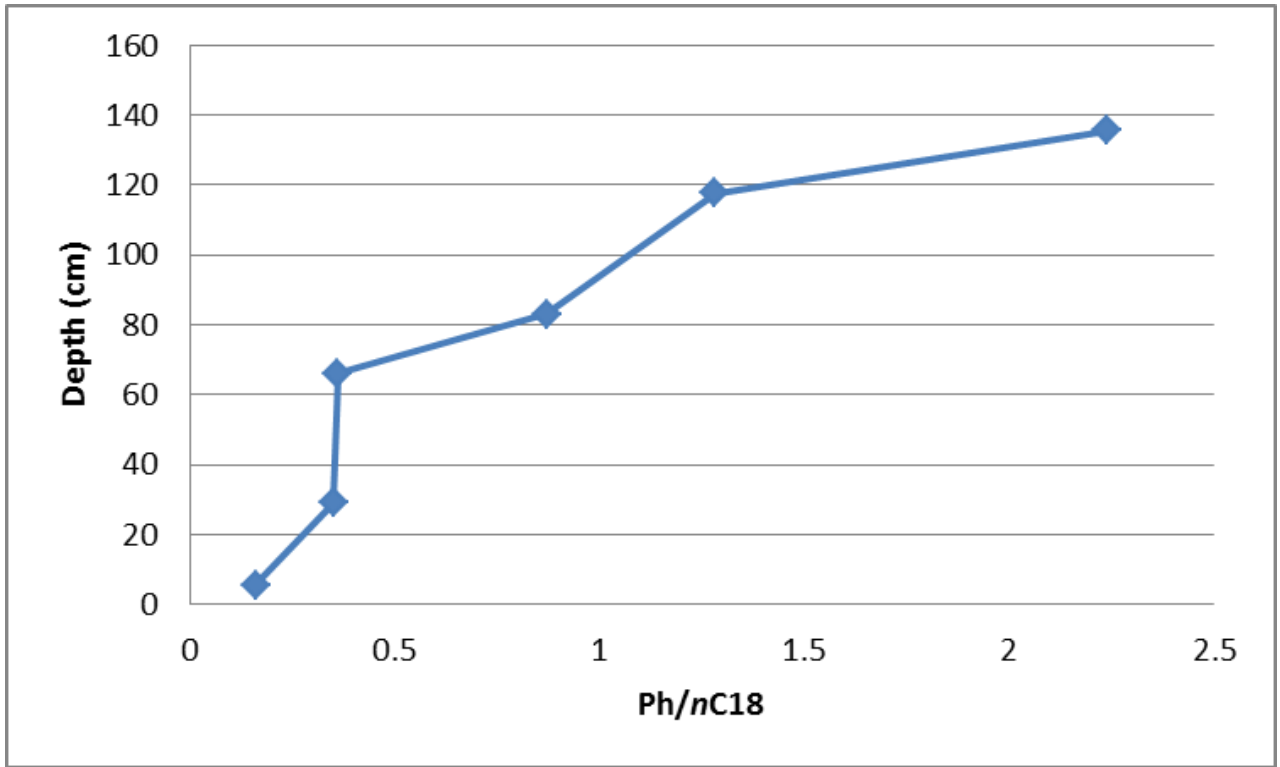
A18: Isoprenoid/n-alkane chromatograms from the aliphatic composition of the Longyear seam at 66 cm.



A19: Isoprenoid/n-alkane chromatograms from the aliphatic composition of the Longyear seam at 29 cm.



A20: Isoprenoid/n-alkane chromatograms from the aliphatic composition of the Longyear seam at 5.5 cm.



A20: Ph/nC₁₈ decrease with seam depth.

APPENDIX B-Calculations

Retorting implications

1 barrel of oil = 158.987 (L) liters of oil

Volume of oil generated = 404 mg/g (0.0404 kg)

1 ton of coal = 1000 kg of coal

If 1 g (0.001 kg) coal generated 404 mg oil, 1000 kg (1 ton) of coal will generate 404 kg of oil.

Assuming very heavy oil, the density of the oil is $\sim 1000 \text{ kg/m}^3$

Hence, 404 kg of oil is $\sim 0.404 \text{ m}^3$ of oil

0.404 m^3 of oil = 404 L (i.e. 1 ton of Longyear coal, produces 404 L of heavy oil)

404 L = 2.5 barrels

Hence, 1 ton of coal generates 2.5 barrels of petroleum.

1,000,000 tons = 2,500,000 barrels

Assuming cost of crude oil to be 100 US dollar (\$) per barrel, and a mining average of 1 million tons per year, these coals could generate \$ 250,000,000.00 (two hundred and fifty million US dollars).

Apparently, the Norwegian coal company (Store Norske) sold these coals at \$ 131 per ton in 2010 (Store Norske, 2010).

At 1,000,000 tons per year mining average, this would generate \$ 131,000,000 (one hundred and thirty one million US dollars).

However, the bitumen generated from the Longyear coals is dominated by the polar fraction and would need to be treated further to yield the more useful fractions. Such cost needs to be factored into the business decisions that need to be taken on the utilisation of these coals.